Faculdade de Engenharia da Universidade do Porto

In vivo mouse model to evaluate glycan-coated microparticles as *H. pylori* treatment

Lia M. R. Costa

MASTER THESIS

Integrated Masters in Bioengineering

Supervisor: Inês Gonçalves (PhD)

June 2015

Resumo

Helicobacter pylori (*H. pylori*) é uma bacteria espiralada que cresce e reveste o interior do estômago humano. A adesão desta bactéria ao epitélio gástrico facilita o processo inicial de colonização, a persistência da infecção e a libertação de factores de virulência para as células epiteliais hospedeiras. A infecção com *H. pylori* é comum nos humanos e, apesar de não causar enfermidades na maioria das pessoas afectadas, representa um grande factor de risco para o aparecimento de úlceras pépticas. Estudos nesta área têm provado que a colonização do estômago com *H. pylori* é uma importante causa de cancro gástrico, o qual corresponde à terceira maior causa de morte por cancro a nível mundial.

Apesar do uso de tratamentos com base em antibióticos para combater a infecção por *H. pylori*, a sua eficácia tem sofrido uma redução, dado o aumento de resistência da bactéria e estas substâncias. Por este motivo, tornar-se imperativo o desenvolvimento de novos estudos, na tentativa de combater este problema, usando métodos alternativos aos actualmente estabelecidos.

Uma vez que o processo de colonização de *H. pylori* está dependente da interacção de diferentes adesinas bacterianas com glicanos expressos pela mucosa gástrica, o estudo destas interacções demonstra grande interesse. Em particular, um grande número de estirpes adere à mucosa gástrica usando a blood group antigen-binding adhesin (*BabA*), que se liga especificamente a receptores *Lewis b* (Le^b).

Tendo isto em conta, o estudo proposto foi motivado por dois objectivos principais. Acima de tudo, esta investigação teve como objectivo determinar os parâmetros experimentais necessários para estabelecer um modelo de infecção por *H. pylori*, usando um modelo animal com expressão de Le^b e uma estirpe de bactéria *BabA* positiva. Em paralelo, o estudo de micropartículas de quitosano (Ch Mics) como um possível tratamento para a infecção foi também desenvolvido, avaliando a citotoxicidade destas partículas *in vitro* e testando *in vivo* a sua capacidade de erradicar a bactéria do estômago dos animais.

O modelo de infecção por *H. pylori* estabelecido, usando murganhos C57BL/6 demonstrou que a inoculação de $1x10^{10}$ CFU/mL (0.2mL; 3 inoculações numa semana) da estirpe *BabA* positiva *B128* em Brucella broth, isolada de um murganho infectado, foi capaz de infectar 5 de 6 animais com $1.55x10^4$ a $1.01x10^5$ CFU/estômago ($2.13x10^2$ CFU/g a $2.36x10^3$ CFU/g).

Relativamente ao tratamento da infecção por *H. pylori* (estirpe *SS1*), usando Ch Mics, a concentração de 10 000 Mics/animal (que revelou não ser citotóxica para células gástricas *MKN45*) não provou ser capaz de reduzir a infecção e, por este motivo, estudos adicionais devem ser realizados.

Abstract

Helicobacter pylori (*H. pylori*) is a spiral-shaped bacterium that grows and coats the inside of the human stomach. Adherence of this bacterium to the gastric epithelium facilitates initial colonization, persistence of infection and delivery of virulence factors to host epithelial cells. An infection with *H. pylori* is widely common in humans worldwide and, although most infected people do not develop disease, these bacteria mediate carcinogenesis and constitute a major risk factor for peptic ulcer disease. In fact, studies in this field have come to prove that colonization of the stomach with *H. pylori* is an important cause of gastric cancer, which corresponds to the third leading cause of cancer death worldwide.

Despite the use of standard antibiotic treatments to fight *H. pylori* infection, their efficacy is progressively being reduced, given the growing resistance of bacteria to these substances. Therefore, it becomes imperative to develop new studies to fight this problem, using different approaches.

Since the process of colonization of *H. pylori* relies on the interaction of different bacterial adhesins with glycans expressed by the gastric mucosa, the study of these interactions arouses potential means to find new treatments. Particularly, the blood group antigen-binding adhesin (*BabA*) and its specific binding to *Lewis b* (Le^b) blood group antigens, is of great interest, as adherence of most strains relies on this interaction.

Having this in mind, the proposed study was driven by two main goals. Most importantly, it was intended to determine the experimental parameters to establish an *H. pylori* infection model, using an animal model that expresses Le^b blood group antigens and a *BabA* positive *H. pylori* strain. In parallel, the study of chitosan microparticles (Ch Mics) as a treatment of *H. pylori* infection was developed, assessing their toxicity *in vitro* and evaluating *in vivo* their capacity to eradicate these bacteria from mice stomach, by oral administration of the particles.

The proposed study enabled the establishment of an *H. pylori* infection model, using C57BL/6 mice, and revealed that *B128* strain (*BabA* positive), isolated from an infected mouse and inoculated with $1x10^{10}$ CFU/mL (0.2mL; 3 inoculations in one week) to the animals, using Brucella broth as the administration vehicle, was able to successfully infect 5 out of 6 animals, with $1.55x10^4$ to $1.01x10^5$ CFU/stomach ($2.13x10^2$ to $2.36x10^3$ CFU/g).

Regarding the treatment of *H. pylori* infection (with *SS1 H. pylori* strain) using Ch Mics, a concentration of 10 000 Mics/mice (found non-cytotoxic to *MKN45* cells) did not prove to be able to reduce this infection and, so, further research needs to be performed on this topic.

Acknowledgements

A minha lista de agradecimentos poderia ser infindável. Tantas pessoas que se cruzaram comigo e que, de uma forma ou de outra, me viram crescer a todos os níveis. Agora, que termino esta fase tão importante, não posso deixar de fazer referência a algumas delas e de lhes retribuir um pouco da atenção e do carinho que fui recebendo.

Aos meus pais, que estão no topo desta lista e que merecem o meu maior agradecimento, estou-lhes verdadeiramente grata por me terem ensinado, entre milhares de outras coisas, as palavras garra e preserverança e por todos os dias terem, eles próprios, acreditado nestas palavras, mesmo quando separados por quilómetros de distância, para me darem o futuro que agora vêem a concretizar-se.

Ao Frederico Junqueira, o espírito mais positivo e sonhador que alguma vez encontrei e que tenho a sorte de ter a meu lado para me equilibrar em todos os momentos.

Ao grupo de melhores amigas com quem 5 anos de partilha e convivência se transformam agora em recordações que vou guardar sempre com muito carinho e que são a base de uma amizade que vai durar e perdurar. Espero que vejamos juntas os sucessos e os insucessos de cada uma e que todos os momentos sejam sempre um motivo para nos juntarmos.

Agradeço ainda o apoio da Doutora Inês Gonçalves por ter orientado e guiado o desenvolvimento do meu trabalho e, acima de tudo, por aquilo que me ensino ao longo deste tempo. Não posso deixar de agradecer também a toda a equipa na qual fui integrada (INEB), com um especial agradecimento à Catarina Seabra, Patrícia Henriques e Ricardo Carvalho. A ajuda e a disponibilidade da Doutora Ana Magalhães (IPATIMUP) e da Professora Doutora Fátima Gärtner (IPATIMUP/ICBAS) também merecem a minha atenção e gratitude.

Por último, mas não menos especial, não podia deixar de agradecer à Susana Neto. Não me vou esquecer de como tudo começou por uma mera ajuda ocasional e que agora acredito ter terminado com uma boa amizade.

"Success is not final, failure is not fatal: it is the courage to continue that counts."

Winston Churchill

Contents

Chapter 1 ..... **1**

Literature Review **1**

1.1. Anatomical and Physiological Considerations 1

1.2. *H. pylori* 3

1.3. Available treatments for *H. pylori* infection 7

1.4. *In vivo* models 9

1.4.1. *H. pylori* infection models 12

1.5. Chitosan as a biomaterial 20

1.5.1. Chemical structure 21

1.5.2. Properties 22

1.5.3. Chitosan microparticles 22

Chapter 2 ..... **25**

Motivation and Goals **25**

2.1. Motivation 25

2.2. Objectives 26

A. Establishment of a *BabA+ H. pylori* infection model 26

*BabA e*xpression in different *H. pylori* strains 26

H. pylori infection in C57BL/6 mice 26

B. Treatment of *H. pylori* infection using Ch Mics 27

Cytotoxicity of Chitosan Microparticles 27

In vivo mouse model – Eradication of *H. pylori* infection 27

Chapter 3 ..... **29**

Methodology **29**

3.1. *H. pylori* culture 29
3.2 Evaluation of *H. pylori* motility: liquid and solid media 30
3.A. Establishment of a *BabA+ H. pylori* infection model 31
3.A.1 *BabA e*xpression in different *H. pylori* strains 31
3.A.2 *H. pylori* infection in C57BL/6 mice 32
3.B. Treatment of *H. pylori* infection using Ch Mics 37
3.B.1 Chitosan Microparticles 37
3.B.2 Cytotoxicity of Chitosan Microparticles 37
3.B.3 *In vivo* mouse model - Eradication of *H. pylori* infection 38

Chapter 4 41

Results and Discussion 41
4.A. Establishment of a *BabA+ H. pylori* infection model 41
4.A.1 *BabA e*xpression in different *H. pylori* strains 41
4.A.2. *H. pylori* infection of C57BL/6 mice 42
4.B. Treatment of *H. pylori* infection using Ch Mics 62
4.B.1 Chitosan Microparticles 63
4.B.2 Cytotoxicity of Chitosan Microparticles 63
4.B.3 Treatment of *H. pylori* infection using Ch Mics – *In vivo* mouse model 66

Chapter 5 77

Conclusion 77
5.1. Future Perspectives 77

References 79

Appendix A 89

Appendix B 91

Appendix C 953

Appendix D 955

List of Figures

Figure 1. Gross and microscopic anatomy of the stomach 2

Figure 2. *H. pylori* crossing the mucus layer of the stomach 3

Figure 3. Schematic representation of disease outcomes in *H. pylori* infection 5

Figure 4. Mice: gross anatomy of the stomach. 11

Figure 5. Histomorphology of mice (left column) and human (right column) stomach. 12

Figure 6. Immunohistochemical staining of C57BL/6 mice gastric mucosa, using *Lewis b* recognizing antibodies (BG6). 19

Figure 7. Chemical structure of (A) chitosan and (B) protonated chitosan..... 21

Figure 8. Chitosan microparticles: Preparation methods 23

Figure 9. Schematic representation of GlyR immobilization on Ch microspheres..... 24

Figure 10. Experimental conditions, along with test groups' definition, and study protocol for the different experiments developed for the creation of an *H. pylori* infection model. 33

Figure 11. Schematic representation of the collection of mice stomach segments for analysis (histological analysis, cryopreservation and colonization) 35

Figure 12. Study protocol for *SS1 H. pylori* infection and treatment (with Ch Mics) of *C57BL/6* mice. 40

Figure 13. Western Blot analysis of *H. pylori* SS1, *B128* and *TN2GF4* strains, for the different passages (P2 Passage 2; P3 Passage 3) and culture media (S - solid; L - liquid) 42

Figure 14. *H. pylori* infection – Experiment I: C57BL/6 mice weight variations during the development of infection with *B128 H. pylori* strain 43

Figure 15. *H. pylori* infection – Experiment I: Colonization of *B128 H. pylori* strain in C57BL/6 mice (CFU/mice stomach and CFU/g) - Colony forming assay..... 44

Figure 16. Histomorphology of C57BL/6 mice (H&E staining). 45

Figure 17. *H. pylori* infection – Experiment I: Histological characterization (H&E staining) of C57BL/6 mice gastric mucosa infected with *H. pylori* (*B128* strain) 47

Figure 18. *H. pylori* infection – Experiment II: C57BL/6 mice weight variations during the development of infection with *B128 H. pylori* strain 48

Figure 19. *H. pylori* infection – Experiment II: Colonization of *B128 H. pylori* strain in C57BL/6 mice (CFU/mice stomach and CFU/g) - Colony forming assay 49

Figure 20. *H. pylori* infection – Experiment II: Histological characterization (H&E staining) of C57BL/6 mice gastric mucosa infected with *H. pylori* (*B128* strain) 52

Figure 21. *H. pylori* infection – Experiment II: C57BL/6 mice weight variations during the development of infection with *SS1, B128* and *TN2GF4 H. pylori* strains 53

Figure 22. *H. pylori* infection – Experiment III: Colonization of *SS1, B128* and *TN2GF4 H. pylori* strains in C57BL/6 mice (CFU/mice stomach and CFU/g) - Colony forming assay 55

Figure 23. *H. pylori* infection – Experiment III: Histological characterization (H&E staining) of C57BL/6 mice gastric mucosa infected with *H. pylori* (*SS1, B128* and *TN2GF4* strains) 60

Figure 24. *H. pylori* infection – Experiment III: Histological characterization (Modified Giemsa staining) of C57BL/6 mice gastric mucosa infected with *B128 H. pylori* strain. . 61

Figure 25. *H. pylori* infection – Experiment III: Histological characterization (H&E staining) of C57BL/6 mice liver 62

Figure 26. SEM images of Ch Mics 63

Figure 27. Optical microscopy images of a 24-well plate with increasing concentrations of Ch Mics. 64

Figure 28. Metabolic activity (%) of *MKN45* cells in the presence of increasing concentrations of Ch Mics 65

Figure 29. Immunofluorescence images of MKN45 gastric cells after 24h of incubation with increasing concentrations of Ch Mics. 66

Figure 30. Efficacy of treatment against *H. pylori* infection: C57BL/6 weight variations during the development of infection with *SS1 H. pylori* strain 67

Figure 31. Efficacy of treatment against *H. pylori* infection. Presence of *SS1* strain in C57BL/6 mice (CFU/mice stomach) 68

Figure 32. Efficacy of treatment against *H. pylori* infection: Histological characterization (H&E staining) of C57BL/6 mice gastric mucosa infected with *H. pylori* (*SS1* strain) 74

Figure 33. Efficacy of treatment against *H. pylori* infection: Histological characterization (H&E staining) of C57BL/6 mice liver 75

Figure A1. Preliminary results of Western Blot analysis of *H. pylori B128* strain. 89

Figure B1. BSA calibration curve for total protein quantification 91

Figure C1. Normal weight variation (g) curve as a function of the age (weeks) of *C56BL/6* mice. 93

Figure D1. Histological progression of *Helicobacter*-induced gastric cancer in a mouse model..... 95

Figure D2. Histological sections of mice liver 95

List of Tables

Table I. *H. pylori*: virulence factors and their effects. 6

Table II. Expression profiles of *BabA*, *CagA* and *VacA* activity in *H. pylori* strains found in humans. 7

Table III. Comparative anatomy and histology of mice and human stomach 10

Table IV. Main specific parameters reported to establish *H. pylori* infection in Mongolian gerbils. 14

Table V. Main specific parameters reported to establish *H. pylori* infection in BALB/c mice. 15

Table VI. Main specific parameters reported to establish *H. pylori* infection in C57BL/6 mice. 16

Table VII. Expression profiles of BabA, CagA and VacA in *H. pylori* strains found in Mongolian gerbils, BALB/c mice and C57BL/6 mice. 20

Table VIII. *H. pylori* infection model parameters. 20

Table IX. Experimental parameters for *H. pylori* infection with *SS1* strain. 39

Table X. Test groups in *H. pylori* infection experiment with *SS1* strain. 39

Table XI. Experimental parameters for Ch Mics treatment – *in vivo* mouse model. 39

Abbreviations and Acronyms

BabA	Blood group antigen-binding adhesin
BBL	Brucella broth
BHI	Brain heart infusion
CagA	Cytotoxin-associated gene A
CFU	Colony-forming units
Ch	Chitosan
Ch Mics	Chitosan microparticles
DA	Deacetylation degree
EDTA	Ethylenediaminetetraacetic acid
GlyR	Glycan receptor
HCl	Hydrochloric acid
H&E	Hematoxylin and eosin
H. pylori	*Helicobacter pylori*
LabA	LacdiNAc binding adhesin
Le^b	*Lewis b* blood group antigens
MALT	Mucosa-associated lymphoid tissue
Mics	Microparticles
NSAID	Nonsteroidal anti-inflammatory drug
OD	Optical density
PCR	Polymerase chain reaction
PMSF	Phenylmethylsulfonyl fluoride
PPI	Proton pump inhibitor
RIPA	Radioimmunoprecipitation assay buffer

RPMIc	RPMI complete
SabA	Sialic acid-binding adhesin
SAM	Self-assembled monolayer
SEM	Scanning electron microscopy
TPP	Tripolyphosphate
VacA	Vacuolating cytotoxin A
RT	Room Temperature

Chapter 1

Literature Review

In this chapter, some important concepts are explored to further understand the subject of this study and to consolidate some aspects concerning it.

First, the anatomical and physiological features of the stomach are considered, since this organ is the central point of this investigation.

To better understand the infection by *H. pylori* and the way this bacterium interacts with the stomach, the following sections include its description. Information about the available treatments nowadays and its benefits and drawbacks are also explored in this chapter. Furthermore, still taking into consideration the infection by *H. pylori*, *in vivo* models are established in order to carry out research studies and so, these are also regarded here, considering its evolution over the years and the differences between animals tested and humans. A summary of the most suitable parameters to establish an *H. pylori* infection model, with regard to the interaction between *BabA* adhesins and Le^b antigens is also presented.

Finally, the use of chitosan as a biomaterial is explored, with reference to its chemical structure, along with the most relevant properties for this work and, particularly, to its application as microparticles.

1.1. Anatomical and Physiological Considerations

The digestive system has a crucial role in providing nutrition to the cells that form the body, maintaining, along with the circulatory system, the supply of water, electrolytes and nutrients, indispensable to the survival of these fundamental biological units [1].

Essentially, two groups of organs form the digestive system: the gastrointestinal tract, also known as alimentary canal, and the accessory digestive organs. Particularly, the stomach belongs to the first mentioned group and its primary function is to store the food ingested during a meal, as well as to regulate its release into the duodenum (first section of the small intestine). It is a highly vascular distensible sac-like organ that holds food and starts to digest it by secreting gastric juice. Protein digestion is, therefore, initiated by this organ and is responsible for denaturing dietary proteins, a role played by digestive enzymes and, in particular, by hydrochloric acid (HCl), which, apart from maintaining the acid pH of the stomach (between 1 and 3), activates pepsin and lingual lipase, breaking up connective tissues and plant cell walls present in the food ingested. Both food and gastric juice are mixed with the help of peristaltic movements (performed by the muscle tissue present in this organ), producing a semifluid acid mass, known as chime [1-6].

Anatomically, the human stomach is located in the upper quadrant of the abdomen and can be divided into 4 distinct regions (Figure 1): cardia, fundus, corpus (body and antrum) and pyloric region. This latter includes the pyloric sphincter, responsible for regulating the passage of chime into the duodenum [6].

Regarding its microscopic anatomy (Figure 1), the stomach contains five wall layers, where the innermost, responsible for producing stomach acid and digestive enzymes, is called *mucosa* and is covered by simple columnar epithelial cells. The depressions in gastric *mucosa* are called gastric pits (also known as foveolae), which flatten when stomach is full, but form longitudinal wrinkles when empty. They are indentations in the stomach that denote entrances to the tubular shaped gastric glands, in charge of producing gastric juice. The subsequent layer is *submucosa* and, outside this, a thick layer of muscle is found (*muscularis propria*), allowing the stomach to move and mix its contents. Finally, the outermost layers are called *subserosa* and *serosa*, which wrap the stomach. [1, 3, 6].

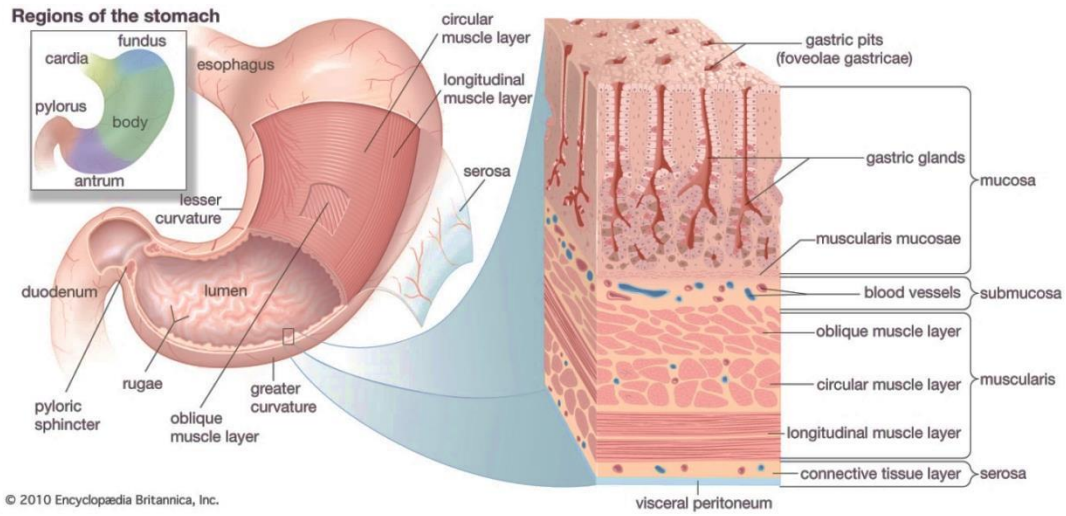

Figure 1. Gross and microscopic anatomy of the stomach. Retrieved from *Encyclopedia Britannica, Inc*. [7].

In particular, the mucous layer that protects the mucosa against acid, proteolytic enzymes and mechanical damage consists of a polymeric matrix formed by high-molecular mass oligomeric glycoproteins, called mucins. The most representative mucins present in the stomach are *MUC5AC* and *MUC6*, produced by the surface epithelium and the gastric glands, respectively. This mucin distribution determines the gastric glycosylation pattern since expression of *MUC5AC* is accompanied by similar distribution of fucosyltransferases, leading to co-expression of type 1 *Lewis a* and *Lewis b* blood group antigens, while MUC6 expression is associated with the type 2 *Lewis x* and *Lewis y* antigens [8, 9]. Particularly, *Lewis b* is naturally expressed in the human gastric surface mucosa in the majority of cases [10, 11].

Due to its intrinsic properties, the stomach is protected from the acidic and enzymatic environment it creates. As already mentioned, the presence of a thick, alkaline mucous is able to resist action of acid and enzymes. Besides, the fact that epithelial cells are separated from each other by tight junctions prevents gastric juice to pass between them and, thus, to destroy the connective tissue. Finally, the epithelial cells are constantly being replaced, living only 3 to 6 days. Failures in these protective measures can result in inflammation and peptic ulcer disease [6].

1.2. *H. pylori*

H. pylori is one of the most common bacterial pathogens of humans and it is mainly found in the *mucosa* layer, where it grows and coats the inside of the stomach. This Gram-negative spiral-shaped bacterium is 2-5 μm long and 0.5-1 μm wide and is microaerophilic, presenting high survival success in the stomach due to its adaptable mechanisms [12-17]. It is able to survive in the acidic conditions of this organ, secreting an enzyme (urease) that converts the chemical urea to ammonia, a substance responsible for neutralizing the acidic environment. This causes the mucin to liquefy, which, together with bacteria's helical shape and the presence of flagella movement, allows *H. pylori* to swim through it and burrow into the mucous layer (Figure 2), less acidic than the human stomach.

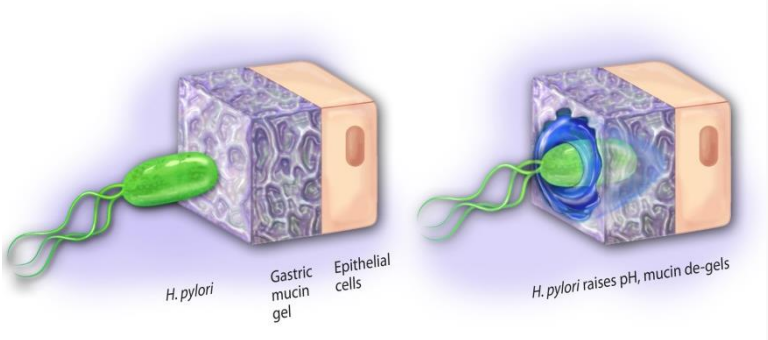

Figure 2. *H. pylori* crossing the mucus layer of the stomach. Adapted from Bansil, R. et. al. (Credits: Zina Deretsky) [18]

H. pylori is successful in persisting in this organ also because immune cells are unable to reach its lining, failing to recognize it and eliminate it. Adherence of *H. pylori* to the gastric epithelium facilitates, thus, initial colonization, persistence of infection and delivery of virulence factors to host epithelial cells [13-16, 19]. The colonizing *H. pylori* adhere to gastric epithelium by different bacterial adhesins and bind to glycans (fucosylated ABO blood group antigens, glycans with charged modifications such as sialic acid and sulfate, and also unsubstituted core chain glycans), present in the stomach, as receptors [20]. In other words, the adaptation of *H. pylori* to the gastric environment relies on the binding to glycoconjugates that work as receptors or binding epitopes for establishing the infection [10]. Overall, mucosal adherence of this bacterium is dependent on a different range of attachment proteins, known as adhesins. The best characterized interaction is between the blood group antigen-binding adhesin (*BabA*; protein of 78kDa, encoded by *babA*2 gene [21]) and the ABO blood group and Le^b antigens [20, 22-25]. In addition, the sialic acid-binding adhesin (*SabA*) mediates the adherence of *H. pylori* to inflamed gastric mucosa by binding sialylated carbohydrate structures such as sialyl-*Lewis* x and sialyl-*Lewis* a. *LabA* (LacdiNAc binding adhesin), in turn, binds LacdiNAc motifs [10]. Localization of this *LabA* target, restricted to the gastric mucosa, suggests a plausible explanation for the tissue tropism of *H. pylori* [26]. Moreover, bacterial virulence factors such as the cytotoxin-associated gene A (*CagA*) pathogenicity island-encoded protein and the vacuolating cytotoxin A (*VacA*), present in some *H. pylori* strains, are also reported to help in the colonization of the gastric mucosa and to modulate the immune response of the host [19].

The process of colonization induces chronic gastric inflammation, due to a high production of urease that increases the pH and activates host immune response, which can progress to a variety of diseases, ranging in severity, from superficial gastritis and peptic ulcer to gastric cancer and mucosa-associated lymphoid tissue (MALT) lymphoma (Figure 3)[12, 27].

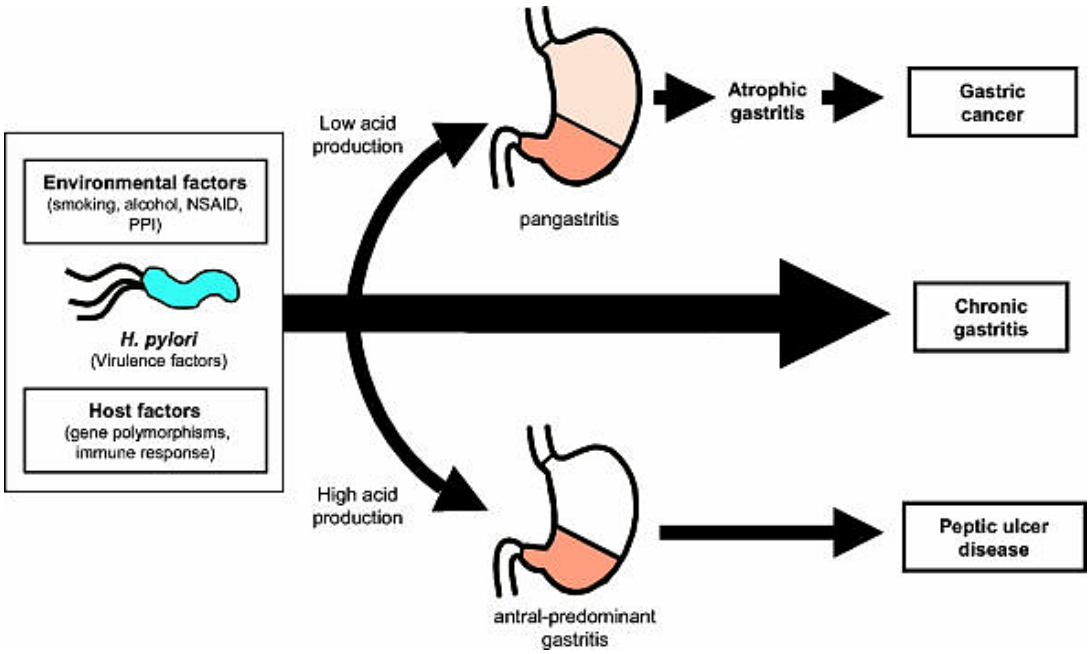

Figure 3. Schematic representation of disease outcomes in *H. pylori* infection. NSAID – nonsteroidal anti-inflammatory drug; PPI - Proton pump inhibitor. Retrieved from *Kusters, J. G., et al.* [19].

Furthermore, the virulence factors of *H. pylori* and the effects that these trigger are presented in Table I, to better understand its action in the human body.

Unlike other bacterial pathogens, *H. pylori* is genetically heterogeneous, suggesting low clonality. This implies that different *H. pylori*-positive subjects may carry distinct strains of this bacterium. Thus, clinical *H. pylori* strains are highly diverse both in their genetic information and potential to induce pathogenicity [28]. This diversity might be associated with *H. pylori's* adaptation mechanisms to the gastric conditions and the patterns of the host-mediated immune response [19].

Changes in the conformation of *H. pylori* from a spiral shape to a coccoid form are reported to be caused by aging or exposure to unfavorable conditions (nutrient starvation or media containing growth inhibitors) and so, this might be an indication that bacteria are either deceased or in a dormant state [29-31]. Thus, during infection, mostly spiral-shaped *H. pylori* bacilli are found in the gastric mucosa of the hosts, despite the presence of some coccoid forms [30].

Table I. *H. pylori*: virulence factors and their effects. Adapted from Wang, X. [12].

Bacterial properties	Virulence factors	Effects/properties
Colonizing	Flagella	Active movements through mucin
	Urease	Neutralization of gastric acid
	Adhesins	Anchoring *H. pylori* to the epithelium
Tissue damaging	Proteolytic enzymes	Glucosulfatase degrades mucin
	120-kDa Cytotoxin-associated gene A (*CagA*)	Related to ulcer and severe gastritis
	Vacuolating cytotoxin A (*VacA*)	Damage of the epithelium
	Urease	Toxic effect on epithelial cells, disrupting cell tight junctions
	Neutrophil activating protein	Lead to neutrophil-mediated mucosal injury
	Phospholipase A	Digest phospholipids in cell membranes
	Alcohol dehydrogenase	Gastric mucosal injury
Survival	Intracellular surveillance	Prevent killing in phagocytes
	Superoxide dismutase	Prevent phagocytosis and killing
	Catalase	Prevent phagocytosis and killing
	Coccoid forms	Dormant form
	Heat shock proteins	Sheathing antigen
	Urease	Prevent phagocytosis
Other	Lipopolysaccharide	Low biological activity
	Lewis x/y blood group homology	Autoimmunity

Isolated *H. pylori* strains have been classified as type I strains (highly virulent), intermediate strains or type II strains (reduced virulence) [32]. Particularly, some studies reveal that patients infected with *H. pylori* strains expressing *BabA* are more likely to present severe gastric diseases such as peptic ulcer and gastric adenocarcinoma, especially if they also present the *VacA* s1/m1 genotype and the cytotoxin-associated antigen (*CagA*) [22, 33-36]. Thus, apart from bacterial toxins, the adherence factors of each strain also contribute to the pathogenicity of *H. pylori* [37]. The expression of *CagA*, *VacA* and *BabA* in different *H. pylori* strains that infect humans is presented in Table II.

With this in mind, when developing an animal model to study infection by this bacterium, it is important to choose the adequate strain, as the capacity of *H. pylori* strains to colonize different animals is both bacterial strain and host dependent [12].

Table II. Expression profiles of *BabA*, *CagA* and *VacA* activity in *H. pylori* strains found in humans. Adapted from Tummuru et al., Henning et al., McClain et al. and *Magalhães et al.* [38-41].

H. pylori strain	*BabA*	*CagA*	*VacA*[a,b]
J99	+	+	s1b/m1
J87; J116; J123; J133; J258	+	+	NA
J104; J128; J166; J178; J223	-	+	NA
J63; J154; J195	-	-	NA
J190; J262	+	-	NA
86-313; 86-338	-	-	-
87-33; 87-29; 87-81; 87-91; 87-199	+	+	+
87-203	+	-	-
87-75; 87-230	-	-	-
92-18; 92-25; 92-26; 92-27	+	+	+
92-19; 92-21	-	+	+
92-20; 92-23; 92-28	-	-	-
92-29	-	+	NA
26695	-	+	s1a/m1
60190	-	+	+
Tx30a	-	-	-
17875/Le[b]	+	NA	NA
17875*babA1A2*	-	NA	NA

[a] *vacA* gene is present in all strains, however, the secretion of *VacA* does not always occur, this being dependent on the *vacA* genotype (signal region alleles: *s1a*, *s1b* and *s1c* or *s2*; middle region alleles: *m1* or *m2*) [36, 42].

[b] (+) and (-) symbols were attributed to the bacteria strain, when vacuolating-cytotoxin activity was reported to be present or absent, respectively, but no information about *vacA* genotype was found.

NA Information not available.

1.3. Available treatments for *H. pylori* infection

The treatment of *H. pylori* is subject of great attention, given the constant need to eliminate these bacteria from the human stomach and to prevent potentially severe consequences of its expansion in this organ. Taking this into consideration, different perspectives to eradicate this pathogen have been considered and implemented in clinical practice over the years.

The first applied treatments were based on monotherapies using, thus, an unique compound to fight *H. pylori* infection, with *clarithromycin* being the most effective single drug. However, despite allowing an eradication rate close to 40%, this was still considered a low efficacy treatment, which led to the emergence of dual therapies. These, in turn, corresponded to the administration of a proton pump inhibitor (PPI) combined with *amoxicillin*. This second approach is still in practice in some countries, but it has mainly been replaced by triple therapies, a combination of two antibiotics and a PPI or a *bismuth* compound. Overall, the main drugs used in these therapies include *tetracycline*, *amoxicillin*, *imidazoles* (predominantly *metronidazole* and *tinidazole*) and *macrolides* (in particular *clarithromycin*) [19].

Nowadays, PPI-based triple therapy is considered the first-line treatment for *H. pylori* infection, being the standard approach a combination of PPI, *amoxicillin* and *clarithromycin* or *metronidazole*, accordingly to the *Maastricht Consensus Report IV* [43]. However, since first-line therapy fails in approximately 20% of patients, there is the need for second-line and even third-line approaches that imply the use of regimens with an improved performance against antibiotic-resistant *H. pylori* strains [43-47].

Although the knowledge of the pathogenesis of gastric neoplasms is increasing and new approaches to the prevention of gastric cancer by eradication of *H. pylori* infection are being investigated, this disease is still the third leading cause of cancer death in both genders worldwide (723,000 deaths, 8.8% of the total) [48], with antibiotic resistance being a growing problem. This might be associated with the antibiotic degradation in the acidic environment of the gastric lumen or to its poor penetration that leads to sub-bactericidal concentration of antibiotics in infection site, unable to successfully eliminate this pathogen [49].

In regards to future therapies, as an attempt to overcome this problem, efforts towards the elucidation of the molecular and genomic structure of *H. pylori* will help to identify specific molecules that represent potential targets for developing new antibiotics [44, 50]. Vaccination is another valuable approach that is gradually being considered a mean to control *H. pylori* and its associated morbidity [44, 47, 51]. However, further research needs to be performed before this can become an option in clinical practice [44, 49]. Moreover, the use of Ch nano and microparticles is increasingly being sought as an innovative approach to deliver the necessary compounds for the elimination of *H. pylori* from infected patients, by encapsulation of several antibiotics [49]. This provides, thus, local and controlled delivery at the infection site by encapsulation of conventional antibiotics, protecting them from enzymatic and acidic degradation [49]. Besides, the use of these microparticles as binding agents of *H. pylori* urease, flagella, adhesins, etc., is also revealing their ability to inhibit, kill or remove this bacterium from the stomach, particularly if target molecules towards *H.* pylori, such as fucose or carbohydrates (namely, Le^b or sialyl-*Lewis* x), are incorporated [10, 49, 52]. This strategy has been

pursued by our group [10] and involved the development of Ch microparticles, chemically modified with glycans (GlyRs, also known as glycan receptors) (*Lewis b* and sialyl-*Lewis x*) [52, 53]. In the referred study, the specificity of the referred adhesin-glycan interactions was evaluated both *in vitro* (using Le^b positive gastric mucosa sections from human and mice) and *ex vivo* (resorting to mice fresh stomach samples), revealing that the immobilization of Le^b increases the affinity of *H. pylori* towards the microparticles, replacing gastric mucosa with similar carbohydrates [10]. Previously, *Parreira et al.* [54] have already proven that these same immobilized GlyRs (Le^b and *Lewis x*) onto bioengineered surfaces (self-assembled monolayers - SAMs) were able to specifically interact with the correspondent adhesins present in *H. pylori*, revealing, once again, the specificity of the interaction between Le^b receptors and *BabA* adhesins.

As studies in the field of biomedical engineering and pharmacogenomics evolve, new approaches are being discovered, always with the concern of guarantying complete therapeutic efficacy in the process of eradication of *H. pylori*. Markedly, the above mentioned Ch microparticles with glycan receptors constitute a promising approach to study *H. pylori* infection. Therefore, further research concerning this strategy should be followed, with the establishment of infection models to better understand the underlying mechanisms that contribute to the survival of this bacterium in the stomach.

1.4. *In vivo* models

Understanding the factors involved in *H. pylori* infection is crucial for the recognition of the role of these bacteria in the etiology of upper gastrointestinal pathology [19]. With this in mind, *H. pylori* infection models have long been established and different animals have been challenged to try to mimic this process seemingly with what happens in humans, always with the goal of finding new strategies to eradicate these bacteria from the stomach.

The first attempts in this area were performed in laboratory animals, such as mice, rats and rabbits, but rather unsuccessfully, due to limitations in technological advances by that time. Therefore, alternatively, models using naturally infected animals (ferrets and non-human primates) or also gnotobiotic dogs and piglets were used [12, 55].

With the increasing knowledge and experience in this area, experiments with Mongolian gerbils, guinea pigs, cats and macaque monkeys have also been performed. Particularly, the longer life span of gerbils, when compared to mice and the larger amount of gastric tissue available for histologic examination represents important advantages [56]. However, on the basis of cost and availability of immunological reagents and genome information, mouse is, nowadays, considered to be the most convenient and appropriate animal model to use [12, 55].

It is crucial, though, to keep in mind that, despite the undeniable value of using animals as *H. pylori* infection models, the results obtained in these experiments cannot be fully extrapolated to humans. Despite the basic structural similarities, the gross morphology of the mammalian stomach presents some differences across species. In fact, the stomach morphology is greatly influenced by adaptation mechanisms, frequency and type of food ingested, animal size, among various other aspects [19, 57].

Particularly, comparing the anatomy and histology of mice and human stomach, some differences can be found and these are described in Table III.

Table III. Comparative anatomy and histology of mice and human stomach. *Retrieved from Treuting, P. M. et al.* [58]

	Feature	Mouse	Human
Gross	Forestomach	Yes; keratinized squamous epithelium; thin-walled right half	No
	Glandular stomach	Left half of stomach; thick mucosa; cardiac, fundus, pyloric regions	Yes; cardiac, fundus, corpus, antrum
	Rugal folds	Not as prominent	Prominent when stomach empty; most prominent in corpus and fundus
	Areae gastricae	Not described	Mucosal shallow grooves that do not flatten with distention
	Limiting ridge/margo plicatus	Present projection between glandular and nonglandular stomach mucosa	No
Tissue	Mucosa	Keratinized squamous or glandular; simple compact straight glands; cell composition varies with region	Simple columnar epithelium
	Lamina propria	Yes	Same
	Submucosa	Yes	Same
	Muscularis mucosae	Yes	Same
	Muscular tunics	Inner oblique; middle circular; outer longitudinal	Same
	Serosa	Yes	Yes
	Squamous epithelium	Amount of keratin is diet- and fasting-dependent; increased keratin with decreased food; can see adherent bacterial colonies	No
Cells	Foveolar (cardiac) cells	Simple columnar; mucus-secreting; line top portion of mucosa	Same
	Parietal cells	Eosinophilic; acid-secreting; midportion of glands	Same
	Chief cells	Basophilic; zymogen-secreting; near base of glands	Same
	Cardiac glands	Mucous glands near limiting ridge; smallest portion	Same
	Fundic glands	Parietal and chief cells; top portion lined with foveolar cells	Same
	Pyloric glands	Near duodenum; mucous cells only	Parietal cells; chief cells absent
	Enterochromaffin	Between basement membrane and chief cells	Diffusely scattered in epithelium

As illustrated in Figure 4, the stomach of mice is divided into two distinct regions, the non-glandular forestomach and the glandular stomach, separated by a limiting ridge. The demarcation between the two areas is easily identified, as the non-glandular area has keratinized epithelium, similarly to the esophagus [59]. For most investigators, the region of interest is precisely the corpus and the adjacent segments, as it presents more similarities with the human stomach [19, 60].

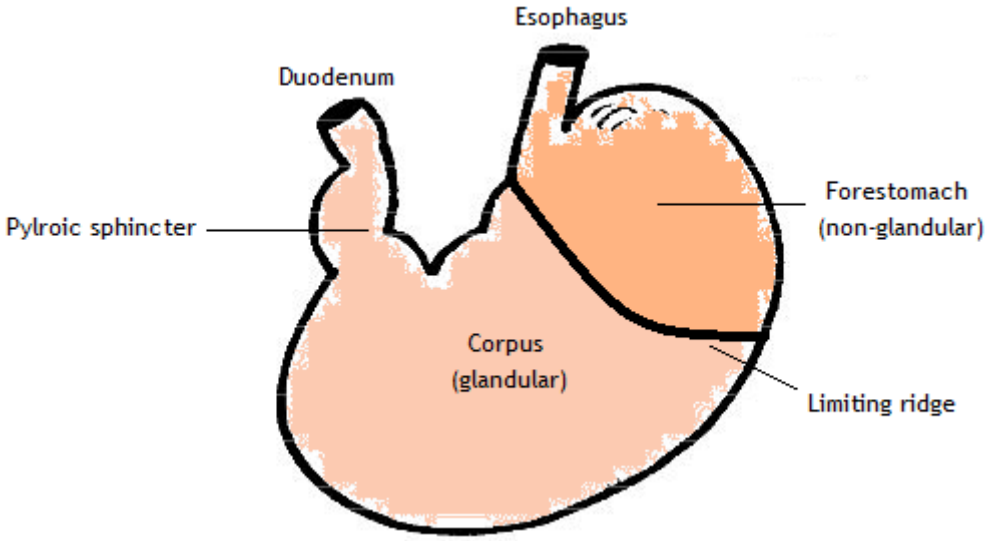

Figure 4. Mice: gross anatomy of the stomach.

Histologically, differences between mice and human's stomach can also be denoted (Figure 5.). Once again, whereas mice have a limiting ridge (Figure 5 (I)), humans have the esophageal Z-line (Figure 5 (II)) that links the esophagus with the cardiac region of the stomach. The fundic region, on the other hand, is similar to both, with the presence of gastric pits, parietal and chief cells. Particularly, in mice, their fundic region is the largest portion of the glandular stomach and cardiac region (Figure 5 (V)) is the smallest. In this latter region often mild inflammation can be found, which can be aggravated by the presence of certain diseases and as animals age [58].

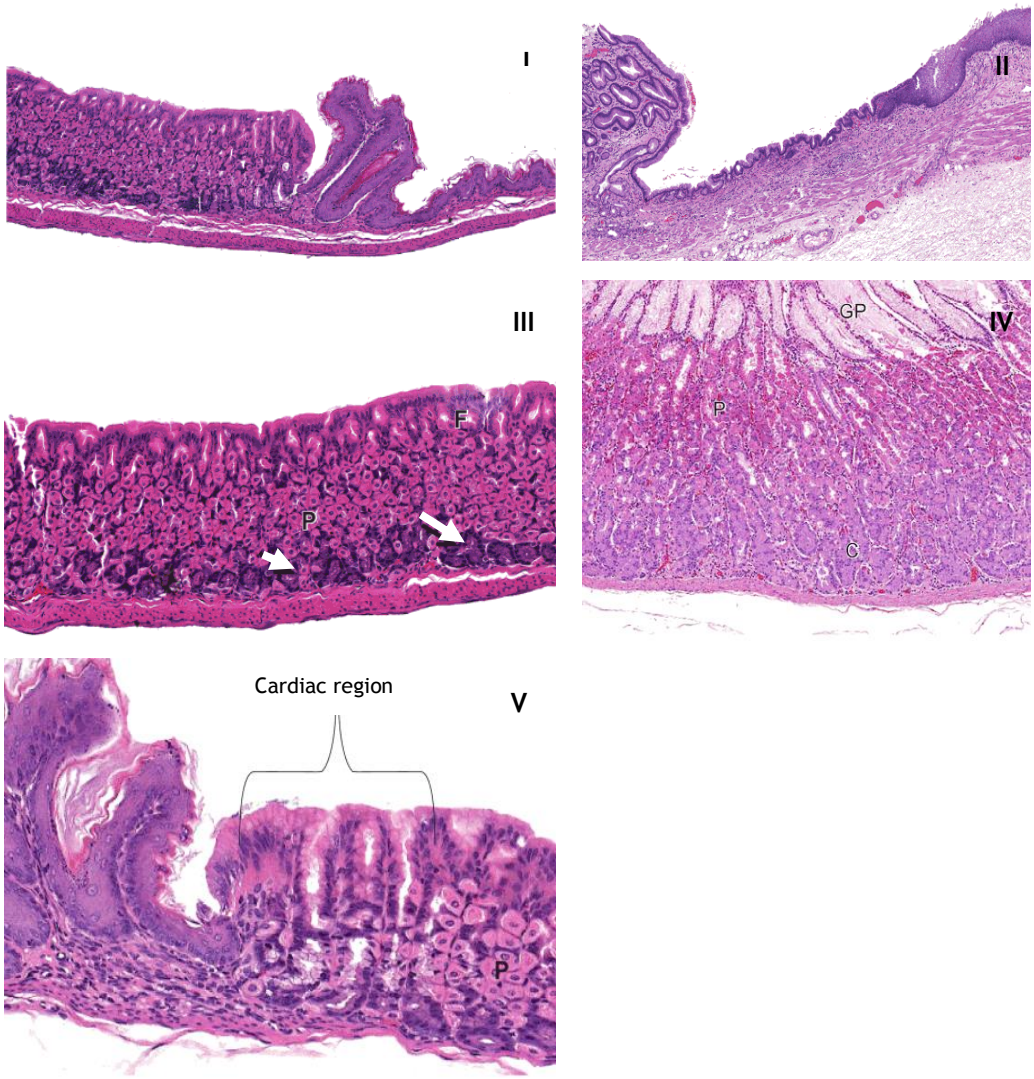

Figure 5. Histomorphology of mice (left column) and human (right column) stomach. (I) Mouse gastric limiting ridge (margo plicatus); (II) Human Z-line line (junction of the esophagus with the cardia of the stomach); (III) Mouse fundic mucosa; (IV) Human fundic mucosa; (V) Mouse cardia. **F** Foveolar columnar mucus-secreting cells, **P** Parietal cells, **GP** Gastric pits, **C** Chief cells. Arrows point to chief cells. *Adapted from Treuting, P. M. et al.* [58].

Notwithstanding, the use of *in vivo* animal models to study human diseases has greatly contributed to improvements in medicine and it is an important first step before moving to human trials and to clinical practice.

1.4.1. *H. pylori* infection models

When using animal models, it is crucial to determine specific parameters to establish *H. pylori* infection. First of all, it is necessary to choose an adequate bacterial strain for the inoculation, in order to meet the requirements of the investigation. Hereupon growth

conditions used for the preparation of inoculum should be set, ensuring that the majority of bacteria are motile and spiral-shaped, prior to inoculation.

Since *H. pylori* is microaerophilic, these have to be grown in jars (with gas-generation kits or a standard microaerobic atmosphere), CO_2 incubators or anaerobic chambers with a microaerobic atmosphere [21]. Regarding the culture media, bacteria can be grown either in liquid or on solid media [61, 62], but it is reported that these grow slowly in liquid environment, with formation of a high number of coccoid forms [21]. For that reason, generally, solid medium is preferred. Particularly, *H. pylori* seems to grow more and with larger colonies on solid media containing blood or blood products, such as 10% horse blood agar plates and 7% lysed horse blood agar plates [21]. Columbia agar, *Brucella* agar and brain heart infusion agar are also commonly used solid media [31, 63]. Notwithstanding, *H. pylori* is also described to be grown in brain heart infusion, *Brucella* broth (BBL), Mueller-Hinton broth or tryptone soya broth, all liquid media [63].

Regarding the choice of animal model to establish *H. pylori* infection an extensive number of studies involving *H. pylori* culture have already been reported as an attempt to establish *in vivo* infection models. The most widely used animals are mice, namely BALB/c and C57BC/6 strains, and also Mongolian gerbils (*Meriones unguiculatus*) [35, 56, 61, 64-70]. Apart from the animals referred, studies on DBA/2, CH3, SJL and NMRI mice have also been reported, but with rather unsuccessful level of colonization in most regions of the stomach. Furthermore, *FVB/N* Le^b-expressing transgenic mice are also reported as potential models for studying *H. pylori* infection, given the production of Le^b antigens found in the gastric pits and surface mucous cells [71, 72]. However, studies using this animal focus specifically on the establishment of adhesion models [72, 73] and so, further research needs to be performed before *FVB/N* Le^b-expressing transgenic mice can become an *H. pylori* infection model [74].

To develop *H. pylori* infection, the number and size of the inoculum doses should also be set. For mouse-adapted *H. pylori* strains, as it is the case of *SS1* strain, one inoculation (10^6 - 10^8 CFU/mouse) is generally sufficient, while other strains may require more inoculations (up to three) [62, 75]. The choice of the animal species and strain is equally important for the course of the investigation. In the particular case of mice, it is reported that C57BL/6 are more susceptible to infection than BALB/c animals. The remaining aspects include the determination of the vehicle for the inoculation of the bacteria, the euthanasia time-point to establish infection and the methods for the detection of *H. pylori* infection [19, 61, 62]. For most studies, the presence of *H. pylori* is best detected 1 month after inoculations [62].

An overview of the conditions established on some of these studies, with regards to the most common tested animals mentioned, namely Mongolian gerbils, BALB/c mice and C57BL/6 mice is presented in Tables IV, V and VI, respectively.

Table IV. Main specific parameters reported to establish *H. pylori* infection in **Mongolian gerbils**.

Bacteria strain	**B127, B129**[a] [56]	**B128**[a] [56, 64]	**SW18, *B102*, B108, B120**[b] [56]	***TN2GF4*** [70]
Bacterial concentration (CFU/mL)	10^9 - 10^{10}		10^9 - 10^{10}	10^8
Vehicle	BBL		BBL	BBL supplemented with 2.5% heat-inactivated FBS
Nº inoculations	3x (days 0, 2, 4)		3x (days 0, 2, 4)	1x
Inoculations volume (mL)	0.8 - 1.0		0.8 - 1.0	1.0
Time to develop infection (weeks)	2 - 4		NA	6
Infection efficiency	HA: 93% - 100% animals infected		HA: 23% animals infected	CFU's counting (CFU/stomach): 10^5

[a] cagA+ strains
[b] cagA- strains
NA Information not available.
HA Histological analysis; **CFU** Colony-forming units; **BBL** Brucella broth; **FBS** Fetal Bovine Serum.

Table V. Main specific parameters reported to establish *H. pylori* infection in **BALB/c mice**.

Bacteria strain	***Human sample*[a]**			***Human sample*[b] [35]**	***SS1***	
	[65]	[76]	[77]		[61]	[77]
Bacterial concentration (CFU/mL)	10^8	10^9		0.8×10^9	10^9	
Vehicle	BBL			BBL supplemented with 2% FBS	BHI	Peptone water
Nº inoculations	2x (consecutive days)	3x (2 day interval)		3x (consecutive days)	3x (5 day period)	1x
Inoculations volume (mL)	1.0	0.1		0.8	0.1	
Time to develop infection (weeks)	2 – 3	NA	4	≈ 8	NA	4
Infection efficiency	HA: 18%-30% infected animals	NA		HA: 81,3% infected animals	CFU's counting (CFU/g tissue):	
					10^3 – 10^6	10^4 - 10^6

[a] Clinical isolate of *H. pylori* obtained from a patient with several gastric ulcers.
[b] Clinical isolate of *H. pylori* obtained from a patient with several duodenal ulcers.
NA Information not available.
HA Histological analysis; **CFU** Colony-forming units; **BBL** Brucella broth; **FBS** Fetal Bovine Serum; **BHI** Brain Heart Infusion broth.

Table VI. Main specific parameters reported to establish *H. pylori* infection in **C57BL/6 mice**.

Bacteria strain	***SS1***						***Human sample*** [a]	***B128***		
	[61]	[66]	[68]	[77]	[75]	[78]	[76]	[79]	[80]	[81]
Bacterial concentration (CFU/mL)	10^9	10^7	10^8	10^9	10^8	10^8	10^9	10^9	3 x 10^8 [c]	2 x 10^8 [c]
Vehicle	BHI[b]		BBL	Peptone water		BBL	NA	Isosensitest broth	NA	NA
N° inoculations	3x (3 day period)	3x (5 day period)	1x			3x (1 day interval)	3x (2 days interval)	3x (1 day interval)	2x (2 days interval)	NA
Inoculations volume (mL)	0.1		1.0	0.1		0.2	0.1	0.1	NA	NA
Time to develop infection (weeks)	NA		4		NA	NA	2 - 4	3	3	2
Infection efficiency	CFU's counting (CFU/g tissue):									CFU's counting (CFU/stomach):
	10^3 – 10^6	NA	5 x 10^5	10^4 - 10^6	NA	NA	NA	10^5 – 4 x 10^5	10^4	10^4 - 10^5

[a] Clinical isolate of *H. pylori* obtained from a patient with several gastric ulcers.
[b] In some cases [66] supplemented with 10% sheep blood, 5% horse serum, and Skirrow's supplement.
[c] Bacterial concentration in *H. pylori* cells/mice, instead of CFU/mL.
NA – information not available.
HA Histological analysis; **CFU** Colony-forming units; **BBL** Brucella broth; **BHI** Brain Heart Infusion.

Regarding the choice of the bacteria strain for inoculation, this is highly variable, but it is verified a preference for *SS1* strain in murine infection models, regarding its adaptation features to these animals [61, 66, 68, 75, 77, 82, 83]. *B128* strain, in turn, is widely applied on gerbils [56, 64], although studies with C57BL/6 refer its use [79-81]. Studies with C3H [84] and 129/SvJ mice [85] are also reported for infection development using *B128 H. pylori* strain.

The commonly used method for inoculation of *H. pylori* in infection models is oral gavage, also known as orogastric inoculation [35, 56, 61, 64-70]. This corresponds to the administration of the bacteria suspension directly into the lower esophagus, introducing a feeding needle into the mouth [86]. Animals chosen for these studies are, generally, aged between 6 to 8 weeks old for both, mice and gerbils. In fact, the sexual maturity of mice is attained between these ages, while gerbils reach puberty at an earlier age (around 70–84 days old). This suggests that, preferentially, young adults are chosen as infection models [87, 88].

Regarding the administration of bacterial suspensions to the animals, its concentrations range between 10^7 and 10^9 CFU/mL for mice (C57BL/6 and BALB/c) and are, generally, higher for gerbils (10^9 - 10^{10} CFU/mL). The administration pattern varies between one and three inoculations, with volumes ranging from 0.1mL to 1.0mL. The solutions normally selected for the bacterial suspension (inoculation vehicle) are BBL, brain heart infusion (BHI) and peptone water, in some cases supplemented with fetal bovine serum. Finally, considering the time to develop infection, studies suggest that two to four weeks is sufficient to find colonizing units of *H. pylori* in gerbils and C57BL/6 mice, and two to eight weeks in BALB/c mice [35, 56, 61, 64-70]. Specifically for C57BL/6 mouse strain, several authors indicate that 1 month after infection, animals have a concentration of approximately 10^3 to 10^6 CFU/g tissue of *H. pylori,* if infected with the *SS1* strain [61, 68, 77, 82].

The application of the infection models is widely variable. Comparisons between different strains, specially, *cagA*-positive (*B127*, *B128*, *B129* strains, etc.) and *cagA-negative* (*B102*, *B108*, *B120* strains, etc.) are a common approach to study *H. pylori* infection, indicating that this virulence factor might be associated with a higher pathogenicity of the bacteria. Similarly, studies analysing the role of *VacA* cytotoxin during colonization of *H. pylori* are also reported, suggesting that *H. pylori* strains expressing active alleles of *vacA* may be better adapted for host-to-host transmission [68]. In particular, severe pathology in mice is associated with the expression of this cytotoxin, along with CagA expression [77]. Furthermore, gastric pathology, including gastric cancer, is analyzed in the different animal models and comparisons across animal species and strains are regarded, with the goal of mimicking, as closely as possible, the infection by *H. pylori* in humans [62].

Generally, the common practice to analyze and interpret results from these animal tests includes the performance of histological analysis and CFU countings of the stomach to examine, qualitatively and quantitatively, the extend of *H. pylori* colonization and infection. Histology of the liver, kidney and spleen are also investigated to better understand the effects of *H. pylori* infection in animals [89]. With that purpose, hematoxylin and eosin (H&E) staining, Giemsa staining and Warthin-Silver staining are, generally, employed on sections of the organs under analysis. Hematoxylin is able to stain nucleic acids and, thus, the nuclei region, in a blue/purple color, whereas eosin's pink color stains proteins non-specifically, revealing the cytoplasm and the extracellular matrix of the cells. Therefore, this technique allows the identification of different cell types and morphologies, including cancer-type specific patterns. Giemsa staining is characterized by colouring bacteria in blue/grey, with a background pink/pale blue. Nuclei are also coloured in blue [90]. The silver staining, in turn, deposits silver granules on some types of bacteria (comprising *H. pylori*), making them larger and more pronounced, which enhances its detection. It stains organisms in brown/black, giving the background a golden shade [91]. Apart from these, immunohistochemical staining (in this case, anti-*H. pylori* antibody immunostain) is also applied in most cases, relying on antibody-antigen interactions that may be valuable for the detection of certain cells expressing specific proteins of interest and, particularly, abnormal cells that might be associated with cancerous tumors [92, 93]. Furthermore, to confirm the presence of *H. pylori*, since urease, catalase and oxidase are produced by this bacterium, tests can also be performed to confirm their presence, based on these products [12, 19, 94]. Polymerase chain reaction (PCR) is, generally, used to characterize isolates of this bacterium and, so, to detect the genetic status of *H. pylori* [35, 61, 94].

Reviewing the many studies developed in this area, it is possible to summarize the most adequate parameters to establish *H. pylori* infection for the study of the interactions between *BabA* adhesins and Le^b receptors. This takes into consideration the ultimate goal of this investigation which consists in evaluating the efficiency of Le^b-decorated microparticles in the eradication of *H. pylori* from the stomach.

C57BL/6 mice seem to be more suitable *H. pylori* animal models, presenting higher colonization rates and similar pathological results as in human gastric experiments, if compared to BALB/c mice and Mongolian gerbils [66, 76, 77]. Furthermore, compared to other animals, it is known their advantages concerning costs, availability of immunological reagents and genome information, small size and reproducibility [95]. Most importantly, regarding the most widely studied animals for *H. pylori* infection (Mongolian gerbils, BALB/c and C57BL/6), this mouse strain has Le^b receptors (Figure 6), which are absent from the gastric mucosa of gerbils [96]. Regarding BALB/c mice, no information referring to the presence of these antigens was found. Nevertheless, reports suggest that BALB/c

animals are less susceptible to infection than C57BL/6 mice, which, once again, makes the use of these latter a more interesting approach.

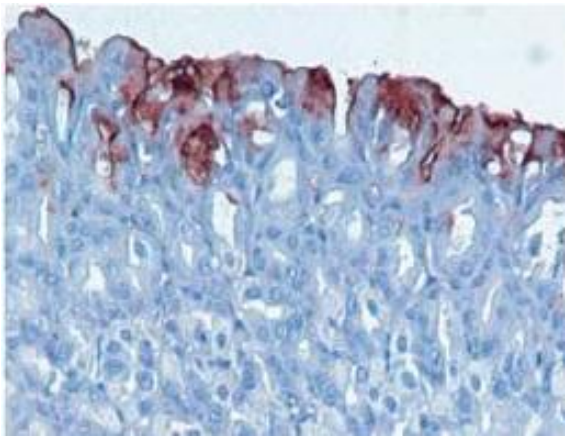

Figure 6. Immunohistochemical staining of C57BL/6 mice gastric mucosa, using *Lewis b* recognizing antibodies (BG6). Magnification 200×. Adapted from Magalhães, et al. [40].

The choice of the bacteria strain should guarantee the expression of *BabA* adhesin. Focusing on this condition and according to Table II, there is a wide range of options available. However, the referred bacteria strains infect humans and, thus, adaptation to these animal models could be difficult. For that reason and assuming the choice of C57BL/6 mice, it is known that *SS1* strain is adapted to these animals. However, this strain lacks the expression of *BabA* adhesin (unpublished work by our group), essential to the conduction of the investigation proposed. Hereupon, an analysis of the expression profiles of *BabA*, *CagA* and *VacA* of the different strains reported to infect Mongolian gerbils, BALB/c and C57BL/6 is presented in Table VII. Two of the strains revised were found to express *BabA* adhesin (*B128* and *TN2GF4*) and so, either of them could be chosen to proceed the study. Particularly, *TN2GF4* strain carries *s1/m1 vacA* genotype, which is associated with higher levels of pathogenicity [36].

Table VII. Expression profiles of BabA, CagA and VacA in *H. pylori* strains found in Mongolian gerbils, BALB/c mice and C57BL/6 mice.

Bacteria strain	*BabA*	*CagA*	*VacA*
***B102* [56]**	NA	-	NA
***B108* [56]**	NA	-	NA
B120 [56]	NA	-	NA
B127 [56]	NA	+	NA
B128	+ [unpublished work, Appendix A, Figure A1]	+ [97]	s1a/m1 [97]
***B129* [56]**	NA	+	NA
TN2GF4	+ [96]	+ [96]	s1/m1 [98]
SS1 [99, 100]	- [unpublished work]	- [99]	s2/m2 [100]

NA – information not available.

Once these two parameters are defined, the conditions to establish the infection can be analyzed. Generally, for a mouse-adapted strain, concentrations ranging from 10^7 to 10^9 CFU/mL are able to establish infection in C57BL/6 mice after two to four weeks. The number of inoculations is reported to vary from one to three inoculations, with volumes that range from 0.1mL to 1.0mL. Notwithstanding, using *B128* or *TN2GF4* (not adapted to mice) might require some adaptations. Typically, *H. pylori* is administered in BBL, BHI or peptone water. A summary of the parameters selected can be found in Table VIII.

The optimization of these conditions for the animal model and bacteria strain chosen may, eventually, enable the establishment of these infection model and constitute a valuable strategy to further explore the potential of Le^b-decorated Ch microparticles to eradicate *H. pylori* from human's stomach.

Table VIII. *H. pylori* infection model parameters.

Animal model	C57BL/6 mice
Bacteria strain	*B128* or *TN2GF4*
Bacterial concentration (CFU/mL)	10^7 to 10^9 CFU/mL
Vehicle	BBL, BHI or peptone water
Number of inoculations	1x – 3x
Inoculations volume (mL)	0.1mL to 1.0mL
Euthanasia time-point (weeks)	2 - 4

1.5. Chitosan as a biomaterial

Chitosan is an unique polymer with valuable physico-chemical properties allied to the ability to establish interactions with proteins, cells and living organisms [101]. In addition,

Ch can have a wide variety of shapes and structures with controlled composition, function and morphology, which reveals its versatility and great value, especially in biomedical and pharmaceutical formulations [102]. In these areas, the main chitosan-based biomaterial types include hydrogels, sponges, films, porous membranes and nano/microparticles. The application of these materials is mostly addressed to tissue replacements, drug delivery systems and wound dressing skin substitutes [101].

1.5.1. Chemical structure

Chitosan results from the deacetylation of chitin, the primary structural polymer in the exoskeleton of crustaceans. This polymer is a linear, semi-crystalline polysaccharide, composed of repeating units of *N*-acetyl-*D*-glucosamine and *D*-glucosamine (Figure 7 (A)). The deacetylation degree (DA) of Ch indicates the number of amino groups present in the chain, corresponding to the ratio of *D*-glucosamines. Actually, if chitosan DA increases, the number of positive charges also increases [101]. This feature influences greatly the physical, chemical and biological properties of this polymer [101, 103, 104].

Chitosan is soluble in dilute acidic conditions, where its molecular chains become protonated (soluble form: R-NH_3) through the amino groups (Figure 7 (B)). Both the DA and the degree of protonation influence the antibacterial properties of Ch, particularly in acidic environment with a pH inferior to 6 [101, 102].

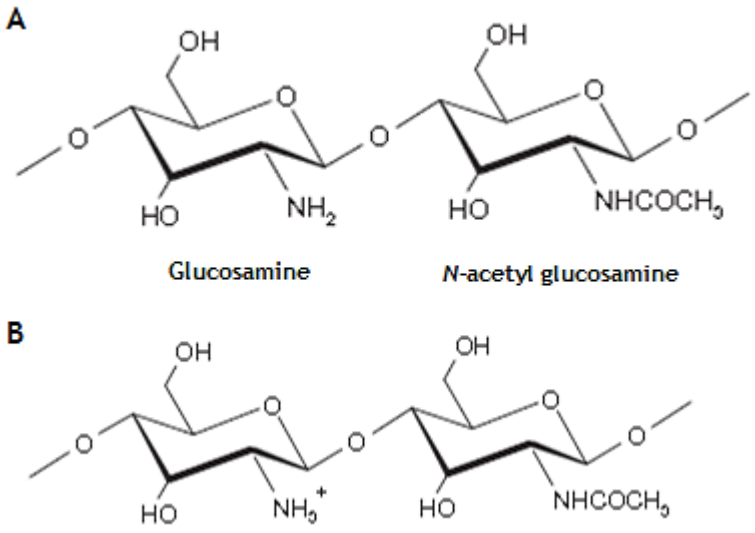

Figure 7. Chemical structure of (A) chitosan and (B) protonated chitosan. Adapted from *Jiang, T., et al.* [103].

1.5.2. Properties

Ch is a polymer with several peculiar and interesting properties, which include its non-toxicity, biodegradability and biocompatibility [49, 101, 103, 104]. In fact, the degradation of Ch results in the formation of non-toxic oligosaccharides that can be incorporated in metabolic pathways or further eliminated from the body. The degradation rate is dependent on the DA of chitosan [101].

Most importantly, regarding the focus of this study, this polymer has been widely investigated in the treatment of *H. pylori* infection, being used for drug encapsulation systems and for bacterial binding, which results from its mucoadhesive and antimicrobial/binding properties, respectively [49]. The mucoadhesion of Ch is due to the interaction between chitosan's positively charged amino groups and negatively charged gastric mucins [52, 105]. The presence of strong hydrogen bonding groups (-OH and -COOH), the flexibility of the chain and the surface energy properties that favor spreading into the mucus are also reported to influence the mucoadhesive properties of chitosan [105]. In turn, its antibacterial properties result from the electrostatic interactions between the cationic Ch amino groups and the anions from the bacterial wall, being responsible for its intrinsic antibacterial activity and inhibiting proliferation of bacteria [53].

Overall, chitosan derives from an abundant naturally occurring polymer, the chitin, gathering singular and valuable properties, with great pertinence in the field of biomedical engineering and health sciences.

1.5.3. Chitosan microparticles

In particular, the use of chitosan microparticles (Ch Mics) has been widely explored for pharmaceutical applications, being highly regarded as a drug delivery system. Its main function in these systems is to encapsulate drugs and allow its release into the stomach, increasing gastric retention time of the dosage forms and, therefore, allowing greater therapeutic benefits of the drugs. Allied to these, possible reduction of the frequency of administration and dose sizes may also be among the many advantages of using these particles. Most importantly, the versatility of microparticles takes advantage of its mucoadhesive properties, enabling the adhesion to multiple mucosal tissues, as it is the case of those found in the stomach [106]. Using innovative microencapsulation techniques, microparticles can be tailored into optimal drug delivery systems, with the desired release profile, by variation of copolymer ratio, molecular weight, as well as the DA of chitosan and the degree of crosslinking [52, 102].

More recently, another application of Ch Mics is under investigation, relying on the creation of an *H. pylori* binding system for the capture and removal of this bacterium from

the stomach. This might constitute a complement or even an alternative for standard therapy [52].

To produce these microparticles, different methodologies can be applied and these are schematized in Figure 8. Among them, ionic/ionotropic gelation using tripolyphosphate (TPP) for ionic-crosslinking and genipin for covalent crosslinking, are the most common approaches. Regarding the high solubility of Ch in acidic conditions, crosslinking is crucial to maintain the three dimensional structure of the microparticles in gastric fluids, mainly when developing binding systems with this polymer [49]. Particularly, TPP allows ionic interaction between its negatively charged counterion and the amino groups of Ch. This interaction is dependent on the charge density of both TPP and Ch [107, 108]. Complexation between oppositely charged species results in precipitation of Ch in the form of particles, approximately spherical [49]. Genipin, in turn, is a naturally occurring crosslinking agent, commonly used for biomedical applications, given its ability to form stable and biocompatible crosslinked products. Genipin reacts with compounds containing primary amine groups to form covalently crosslinked networks that are significantly less cytotoxic than those crosslinked by glutaraldehyde (a commonly used synthetic crosslinking inductor). In the case of Ch, genipin reacts with the free primary amines present in the glucosamine units, conferring stability to the microparticles, if crosslinked in the optimal proportion [52, 109, 110]. Production of these three-dimensional polymeric structures using the referred methods provides controlled size of the particles by variation of the compressed air pressure or spray-nozzle diameter.

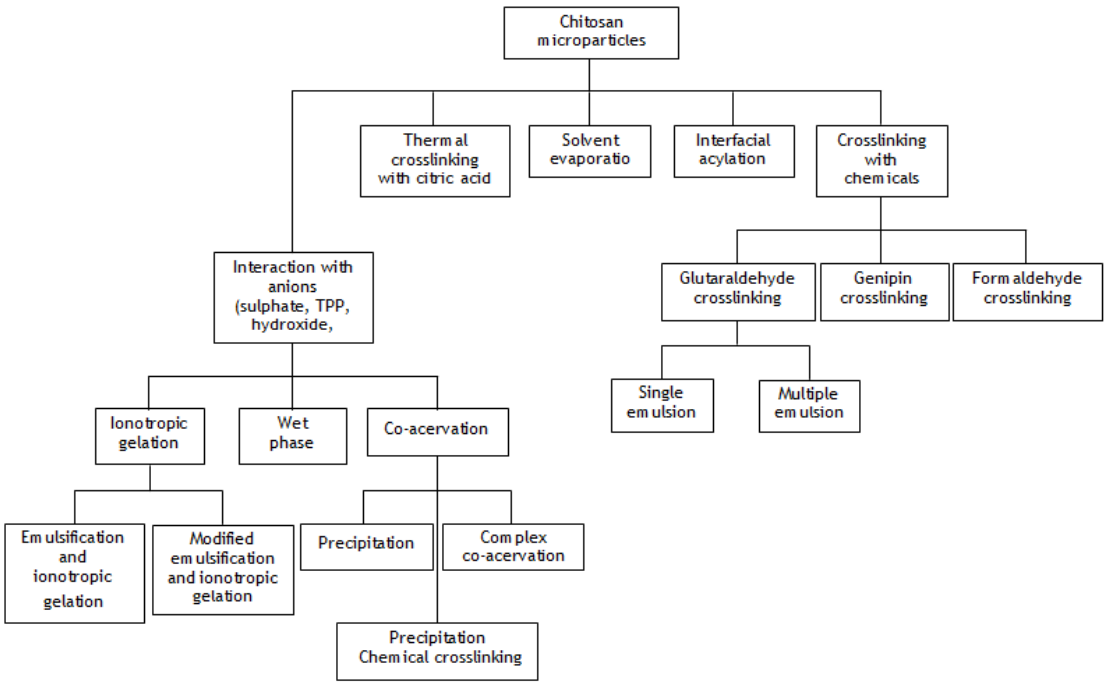

Figure 8. Chitosan microparticles: Preparation methods. Adapted from Sinha, V. R., et al. [102]

Given the purpose of this investigation, *Gonçalves et al.* [53] have produced 170µm microparticles (DA of 15%) using TPP and genipin for ionic and covalent crosslinking, respectively. Authors have demonstrated that these particles, although unspecifically, are able to bind different strains of *H. pylori* (namely, *J99*, *17875/Leb*, *17875babA1A2* and *097UK*), decreasing *H. pylori* adhesion to *MKN45* gastric cells and revealing no cytotoxicity (*in vitro* studies) [53]. Moreover, two preliminary *in vivo* studies using *C57BL/6* mice, revealed that these Ch Mics were able to reduce the infection with *SS1 H. pylori* in approximately 63% (unpublished data), despite no significant differences were found due to variability of infection, suggesting, however, the potential utility of these particles.

As an effort to improve the removal of *H. pylori* from the stomach, Ch microparticles can be additionally decorated with GlyRs (namely, Le^b glycans) on its surface, as already demonstrated by *Gonçalves et al.* (*ex vivo* studies using sections of the gastric mucosa) [10]. To immobilize GlyRs onto microparticles' surface, authors have reported the use of azide-alkyne coupling ("click chemistry") (Figure 9), which maintained their morphology, size and stability in simulated gastric fluid. The application of this strategy involved the use of primary alcohol groups of Ch, alternatively to primary amines, since these latter contribute to the maintenance of chitosan's mucoadhesiveness [111].

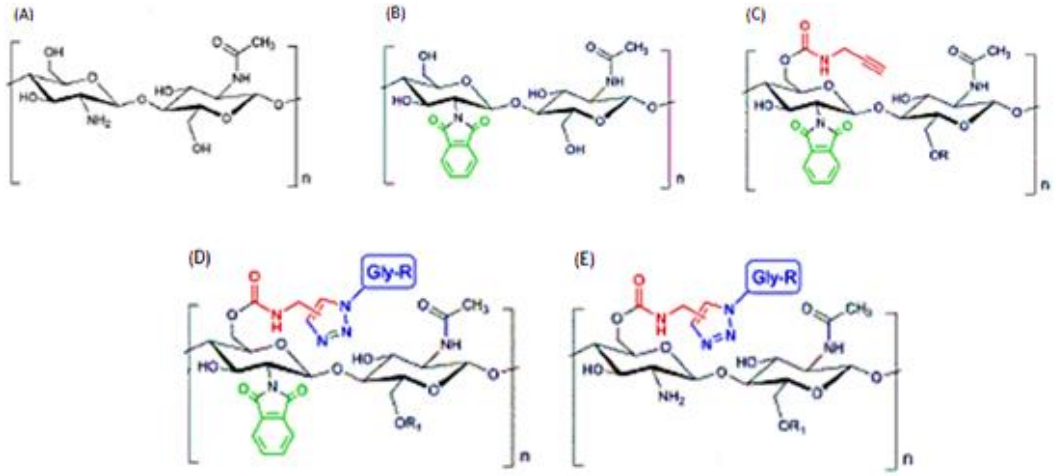

Figure 9. Schematic representation of GlyR immobilization on Ch microspheres. (A) Chitosan, (B) Protection of chitosan reactive primary amine groups with phthalic anhydride , (C) Chitosan *O*-alkynylation, (D) Immobilization of N3-GlyR using the azide-alkyne "click" coupling, (E) Deprotection of chitosan primary amine groups to produce the target GlyR-decorated chitosan microspheres. Adapted from *Gonçalves et al.* [111].

Recently, our group has also focused on the reduction of Ch Mics' size and increase of charge, with diameters close to 30µm, using Ch with a DA of 6%, to explore the idea that smaller microparticles can penetrate to more internal regions of the gastric foveolae (gastric invaginations), where *H. pylori* is also present and, thus, improve the removal of this bacteria. Furthermore, by producing Ch Mics with a lower DA, increases the number of amines, which become protonated in the acid gastric pH and can, possibly, enhance the binding of *H. pylori* by electrostatic interactions.

Chapter 2

Motivation and Goals

2.1. Motivation

Helicobacter pylori (*H. pylori*) is among the most common human infections worldwide: it colonizes over 50% of the world's population [25] and 80% to 90% of the Portuguese [112]. Although disease is not developed in most infected people, it is a major risk factor responsible for the prevalence of various gastrointestinal diseases that range from gastritis, to peptic ulcer disease and gastric cancer, among other problems [14, 15]. Therefore, the eradication of *H. pylori* infection becomes crucial for the management of these health problems [44, 45].

The reduced efficacy of the available treatments to fight *H. pylori* infection is a consequence of the growing resistance of the bacteria to these substances [44, 49], thus, it is imperative to develop new studies to fight this infection, using different approaches.

Recently, the use of chitosan microparticles (Ch Mics) has been given a different perspective. A strategy has been described to bind *H. pylori*, impairing its adhesion to host cells and, ultimately, eliminating it from the stomach [53]. The use of these structures as binding systems may include chemical modification of microparticles with urease, flagella, adhesins and other components as targeting compounds, which may enhance their properties and improve their efficacy [49]. In particular, our group has demonstrated the possibility of decorating Ch Mics with glycan receptors (GlyRs), namely, *Lewis b* (Le^b), on its surface to increase the removal of *H. pylori* from the stomach [10], taking advantage of the specific interactions between Le^b receptors and *BabA* adhesins present in bacteria [10, 54]. However, despite the potential utility of the proposed treatment, this lacks proper *in vivo* validation and, therefore, it becomes imperative to establish an *in vivo* model of *H.*

pylori infection for the consequent study of the efficacy of these particles. In parallel, cytotoxicity of Ch Mics without surface modifications also needs to be assessed *in vitro* before moving to *in vivo* tests, where their capacity to adhere and remove *H. pylori* from the stomach should be evaluated.

Regarding the importance and pertinence of this subject, this new approach reveals great interest in the field of biomedical engineering and can, potentially, correspond to an innovative solution if further explored.

2.2. Objectives

Motivated by the urge of a new treatment for *H. pylori* infection, the development of this investigation was driven by two main goals. Most importantly, this study was intended to determine the experimental parameters to establish an *H. pylori* infection model, using an animal model that expresses Le^b blood group antigens (as it is the case of *C57BL/6* mice) and a *BabA* positive bacteria strain of *H. pylori*.

In parallel, the study of chitosan microparticles as a treatment of *H. pylori* infection was developed, assessing their toxicity (*in vitro*) and evaluating (*in vivo*) their capacity to eradicate these bacteria from the stomach, by oral administration of the particles and removal trough the gastrointestinal tract.

A detailed explanation of the objectives of this study is described below.

A. Establishment of a *BabA+ H. pylori* infection model

***BabA* expression in different *H. pylori* strains**

The main focus of this study was to find a strategy to establish *H. pylori* infection in *C57BL/6* mice (known to express Le^b receptors), using a *BabA* positive strain.

Therefore, and once *H. pylori* culture conditions were defined (comparing its motility in solid and liquid media), *TN2GF4*, *B128* and *SS1* strains were tested for the presence of *BabA* using the Western Blot technique, as an attempt to confirm the expression of this adhesin. Again, bacteria were cultured in liquid and solid media to understand if these conditions would alter the expression profile of *BabA*. Extracts from different passages were also tested to guarantee that *BabA*'s expression was not affected overtime.

***H. pylori* infection in C57BL/6 mice**

Upon confirmation of *BabA* expression in *B128* and *TN2GF4* strains, *in vivo* experiments to infect *C57BL/6* mice with *H. pylori* were carried out, with variation of some parameters (namely, administration vehicle, number and volume of inoculum and time to develop infection), as an attempt to optimize the development of infection and,

thus, to establish an adequate model that could be used in the future to validate the efficiency of Leb-coated chitosan microparticles.

B. Treatment of *H. pylori* infection using Ch Mics

Cytotoxicity of Chitosan Microparticles

Focusing now on the treatment of *H. pylori* infection, this study suggests the employment of Ch Mics (previously characterized by scanning electron microscopy) as a binding system for the capture and removal of this bacterium from the stomach. Therefore, primarily, the potential cytotoxicity of different amounts of Ch Mics was evaluated *in vitro*, using *MKN45* cells, a human gastric carcinoma-derived cell line.

***In vivo* mouse model – Eradication of *H. pylori* infection**

Once tested the cytotoxicity of Ch Mics *in vitro*, these particles were administered to *H. pylori* infected C57BL/6 mice, in the adequate concentration, to evaluate its efficiency in the treatment of *H. pylori* infection. The bacteria strain chosen to infect the animals was the mouse-adapted *SS1*, as it is an already well-established model, guaranteeing development of infection and allowing the study of the suggested treatment.

Results obtained in this study can be an important guide to further research in this area and will enable *in vivo* evaluation of Le^b-decorated microparticles to target and bind specifically *H. pylori*. This may be transposed to human clinical trials and constitute, eventually, a new solution to eradicate the most successful pathogen from the human stomach.

Chapter 3

Methodology

This chapter describes the methodology applied to develop the proposed study. It is important to mention that, since this work involved *in vivo* procedures with mice handling, an introductory course in Laboratory Animal Science was attended. The course included lectures on rodents, rabbits and fish specific contents, and also practical sessions to learn basic procedures, from rodents (mice and rats) handling, to administration of substances (using different routes) and euthanasia techniques. In addition, this also included a tutorial training at the animal facility to deepen the previously acquired knowledge. The course was validated with an appropriate certification at IBMC Training Center (FELASA, Category B).

3.1. *H. pylori* culture

Preparation of blood agar plates

The development of this study included the preparation of agar plates to grow *H. pylori in vitro*. With this purpose, Blood Agar base 2 (approximately 44.4 mg/mL; *OXOID,* Hampshire, UK) was weighed and added to ultrapure water (90% v/v of the desired volume of medium). After autoclaving (20min, 115ºC), defibrinated horse blood was added (10% v/v final, *Probiológica*, Lisbon, Portugal), together with antibiotics (0.2% v/v final; conserved at 4ºC and protected from light). This antibiotic cocktail was prepared with polymixine B (0.115 mg/mL; *Sigma-Aldrich,* Missouri, USA), vancomycin (6.25 mg/mL; *Sigma-Aldrich*), amphotericine B (1.25 mg/mL; *Sigma-Aldrich*), triméthroprime (3.125 mg/mL; *Sigma-Aldrich*) and DMSO (2.5% v/v, *Sigma-Aldrich*), for the desired volume of ultrapure water. About 18-20mL of medium were added to each plate and, after agar solidification, these were kept at 4ºC until use.

Preparation of BBL

Brucella broth (BBL) was used in this study as a vehicle for the administration *H. pylori* to mice and also to grow these bacteria in liquid media. With this purpose, 28mg/mL of *brucella broth base* (*Sigma-Aldrich*) were dissolved in ultrapure water, autoclaved for 15min, at 121℃, and stored at 4℃.

Preparation of Peptone water

The preparation of peptone water consisted in weighing peptone (20 mg/mL, *Sigma-Aldrich*) and sodium chloride (5 mg/mL, *VWR Chemicals*, Radnor, Pennsylvania) to the desired volume of ultrapure water. The pH was, then, adjusted to 7.4 and the solution was autoclaved (20min, 115℃).

***H. pylori* strains**

Three *H. pylori* strains were investigated in this study, namely, *SS1, B128* and *TN2GF4*. The first two were obtained from the Unité de Pathogenése de Helicobacter, Institut Pasteur (France) and *TN2GF4* strain was obtained from the Department of Medical Biochemistry and Biophysics, Umea University (Sweden).

Growth and collection of *H. pylori*

H. pylori aliquots of the different strains cultured (*SS1, B128* and *TN2GF4*) (frozen at -80℃) were grown (in spots of 20µL each) in blood agar plates, for 32h-48h (37℃, microaerophilic conditions). After this time, bacteria were spread and left to grow for another 32h-48h in the same conditions. These timepoints established to grow *H. pylori* (32h-48h in each passage) correspond to the exponential growth phase of bacteria, as suggested by *Parreira, et al.* [113]. Bacteria were, then, collected in the adequate administration vehicle (peptone water or BBL, depending on the experiment) and centrifuged at 3660, for 5min. The supernatant was discarded and the pellet was ressuspended in this same vehicle. A sample (diluted 1:100) was used to read the optical density at 600nm (OD600) in a spectrophotometer to obtain the concentration of *H. pylori*.

3.2 Evaluation of *H. pylori* motility: liquid and solid media

To compare the motility of different *H. pylori* strains in liquid and solid media (blood agar plates and BBL, respectively), *SS1* and *B128* strains were grown according to the methodology described in *section 3.1.*. Similarly, bacteria grown in the same conditions were passaged to liquid media (20 ml of *Brucella Broth* with 10% heat-inactivated FBS), after spotting and spreading growth. Bacteria in liquid media were collected and, after centrifuging the suspension (3660, for 5min), the pellet was ressuspended in BBL.

H. pylori grown in liquid and solid media were analyzed under the optical microscope to assess their motility. For that, 10µL of bacterial suspension from each condition were placed between two glass coverslips (24x50mm coverslip topped by a 18x18mm coversplip).

3.A. Establishment of a *BabA+ H. pylori* infection model

3.A.1 *BabA e*xpression in different *H. pylori* strains

Collection of the different passages

H. pylori was grown under the conditions described in *section 3.1.* Bacteria at passage 2[1] were collected after 32h with 1mL PBS. The sample was centrifuged at 5856 rpm, for 5min. Once this time was over, the supernatant was discarded and lysing buffer, freshly prepared, was added. This consisted of 1mL of RIPA 4ºC (50 mL 1M Tris-Cl 7.4 (50mM); 37.5 mL 4M NaCl (150mM); 4 mL 0.5M EDTA (2mM); 10 mL NP-40 1%; 10 mL 10% SDS (0.1%)), 10µL of PMSF 100mM (*Sigma-Aldrich*), 10µL of sodium orthovanadate 100mM (*Sigma-Aldrich*) and 40µL of Complete 25% (protease inhibitor cocktail, *Roche*, Basel, Switzerland). The collected bacteria were incubated in this buffer for 15min in ice and, then, centrifuged at 3000rpm, for 5min (4ºC). Finally, the supernatant, containing the protein extract, was stored at -20ºC until use.

Bacteria grown in the same conditions (*section 3.1.*) were re-spread onto new blood agar plates or cultured in liquid media (20 ml of *Brucella Broth* with 10% heat-inactivated FBS). Both cultures (passage 3, solid media and passage 3, liquid media) were left to grow for another 32h and collected after this period, following the methodology already explained for protein extraction.

Protein Quantification

To quantify the amount of protein present in the samples collected, a BSA calibration curve was constructed. With that purpose, eight different concentrations of BSA were prepared: 2000µg/mL, 1500µg/mL, 1000µg/mL, 750µg/mL, 500µg/mL, 250µg/mL, 125µg/mL, 50µg/mL. 5µL of each solution were plated in a 96-well plate in triplicates, along with a blank (ultrapure water; also in triplicates). The calibration curve obtained allowed the quantification of total protein present in the samples.

The protein extracts of passage 2 and passage 3 (solid and liquid) of *SS1*, *B128* and *TN2GF4 H. pylori* strains were diluted 1:5 and 1:25 and plated in the 96-well plate (5µL

[1] For *H. pylori* culture, passage 1 was considered the spot phase. Passage 2 corresponds to the first spread after bacteria were grown for 32h in spots. Passage 3, in turn, corresponds to a re-spread onto liquid or solid media.

per well, in triplicates). To determine the protein concentration, the *Bio-Rad DC Protein* assay was used. Absorbance was read in a spectrophotometer at 750nm.

Western Blot

Once determined the total protein concentration of each sample (Figure B1, *Appendix B*), it was possible to normalize the amount to load the lanes. Solutions of each sample were prepared with the same amount of protein (25µg) on a total volume of 25µL. Likewise, aliquots from *17875/Leb* and *17876 babA1A2* (positive and negative control, respectively) were also prepared. For each solution, 6.25µL of sample buffer (Laemmli 4x - 277.8 mM Tris-HCl pH 6.8; 44.4% (v/v) glycerol; 4.4 % LDS - e Bromophenol Blue 0.02%), together with 10% (v/v) 2-mercaptoethanol, were added. Solutions were heated at 100°C for protein denaturation, for 10min, and separated by 10% Tris-Glycine SDS PAGE, for 1h (150V). Transference was performed by electrophoresis onto a Nitrocellulose Blotting Membrane 0.45µm (*GE Healthcare Life Science*, Little Chalfont, UK), for 1h30, 60V. Once this process was over, the membrane was blocked with 5% skim milk in PBST (containing 0.05% Tween 20) for 1h. After washing the membrane (3x) with PBST, AK277 antibody (primary antibody), diluted 1:10000 in 5% skim milk in PBST, was added (1mL of antibody solution per cm^3) and incubated for 2h at RT, under continuous agitation (35 rpm). The bound antibodies were detected by horseradish peroxidase-conjugated anti-rabbit Ig secondary antibody, followed by ECL detection system, from *Amersham (TM) ECL (TM) Western Blotting Detection Reagents (GE Healthcare)*. For the development process of the films different exposure times were tested (5s, 10s and 30s).

3.A.2 *H. pylori* infection in C57BL/6 mice

H. pylori infection in C57BL/6 mice included three different studies, with alterations in the experimental conditions, as an attempt to establish an infection model for a *H. pylori BabA* positive strain. The study protocol and the experimental parameters used in each experiment are described in Figure 10. In Experiment I *H. pylori* culture and mice infection were performed with the parameters already established in our lab, accordingly to *Correia et al.* [75]. Experiment II was performed as an attempt to improve the efficacy of the infection, with the alteration of some conditions (Figure 10, Experiment II), namely, the administration vehicle (changed to BBL), the number (increased to 3 times) and volume of inoculations (doubled) and, finally, the time to develop infection was tested for 3 and 4 weeks. The last experiment (Experiment III) maintained most of the conditions, but *H. pylori* infection was evaluated only at the end of the 4 weeks timepoint for 3 different *H. pylori* strains: *SS1*, *B128* and *TN2GF4*.

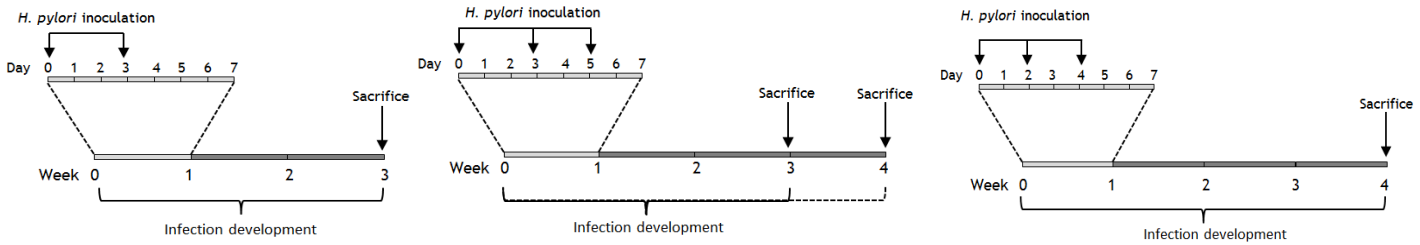

Experimental parameters	Experiment I		Experiment II		Experiment III	
Animal model	C57BL/6 mice		C57BL/6 mice		C57BL/6 mice	
Age (weeks)	7		7		7	
Number of animals	8 male mice		14 male mice		15 male mice	
***H. pylori* strain**	*B128*		*B128*		*SS1, B128*[b]*, TN2GF4*	
Bacterial concentration (CFU/mL)	10^{10}		10^{10}		10^{10}	
Vehicle	Peptone Water		BBL		BBL	
Number of inoculations	2x		3x		3x	
Inoculations volume (mL)	0.1		0.2		0.2	
Time to develop infection (weeks)	3		3 and 4 [a]		4	
Test Groups	**Name**	**n**	**Name**	**n**	**Name**	**n**
	Hp-	2	Hp- 3w[c]	1	Hp-	1
	Hp+	6	Hp- 4w[c]	1	Hp+SS1	2
			Hp+ 3w[c]	6	Hp+B128	6
			Hp+ 4w[c]	6	Hp+TN2GF4	6

[a] From the 12 infected animals, 6 were sacrificed 3weeks post infection (along with one control animal) and the remaining were euthanized one week after (i.e. 4 weeks post infection).

[b] In this case, *B128* bacteria were collected from a subculture of this strain, obtained from *H. pylori* positive cultures of mice stomach (from experiment II).

[c] Time to develop infection. **3w -** 3 weeks; **4w -** 4 weeks.

n number of animals; **BBL** Brucella broth; **Hp-** Non-infected animals; **Hp+** Infected animals

Figure 10. Experimental conditions, along with test groups' definition, and study protocol for the different experiments developed for the creation of an *H. pylori* infection model.

***H. pylori* culture**

The culture of *H. pylori* for infection comprised the steps described in *section 3.1*. After this period, on the infection day, bacteria were collected with peptone water or BBL (according to the parameters defined for each experiment) to a falcon and kept in suspension in the corresponding vehicle.

In order to adjust the bacterial concentration to $1x10^{10}$ CFU/mL for the inoculation, a spectrophotometer was used to measure the optical density (OD), where it was considered a correspondence of OD600=1 to $5x10^{8}$CFU/mL. Apart from preparing the bacterial suspension for mice infection, serial dilutions were performed and dilutions of 10^{5}, 10^{6}, 10^{7} and 10^{8} were spotted (10µL/drop) in blood agar plates for CFU counting (4-6 days after) to confirm its concentration. The number of CFU/mL present was calculated based on equation 1,

$$CFU/mL = \frac{CFU \times DF}{V_{drop}} \quad (1),$$

where CFU corresponds to the number of colony forming units found in the defined volume of the spot (V_{drop}) and DF is the dilution factor.

Infection of C57BL/6 mice with *H. pylori*

Infection with *H. pylori* was performed in C57BL/6 mice (7-8 weeks old, specific-pathogen-free), from *Charles River's* company (Massachussetts, USA). During their stay at the animal facility, mice were housed, inside ventilated cages, in an ABSL2 room, with a 12h light/12h dark cycle. Animals were fed with commercial pellet diets and water *ad libitum* and fasted 24h before inoculation (being transferred to clean cages without corn cob or food, but with proper enrichment material to guarantee animals' welfare). Water was removed 3h before administration of the bacterial suspension and food/water access was re-established 1h to 2h after infection.

The bacterial suspension ($1x10^{10}$ CFU/mL) was administered to the animals by oral gavage (B.Braun 20G cannula 1.1x32mm, Hesse, Germany), with the correspondent number of inoculations of each experiment (with 2 or 3 days interval). Additionally, control mice were given the same amount of peptone water or BBL (correspondent to the vehicle used to administer bacteria in test groups).

Animals' sacrifice

The animals' physical appearance was observed twice a week and their weight variations were inspected weekly, until sacrifice. Mice (previously fasted for 24h) were euthanized by cervical dislocation, with previous anaesthesia (50-75 mg/kg Ketamine and 0.5-1 mg/kg Medetomidine) through intraperitoneal injection (B. Braun 20G cannula 0.45x12mm).

The blood of anaesthetized animals was collected by cardiac puncture into gel-cot activator tubes, which were centrifuged (3500 rpm, 2min) and each supernatant was added to an *eppendorf* and frozen at -20ºC.

After sacrifice, mice stomachs were rinsed in NaCl (to remove food) and cut accordingly to the scheme presented in Figure 11. This organ divided into 4 parts (each half of the stomach was divided into parts A and B). One portion was collected for cryopreservation (cryo vials were placed in a container with liquid nitrogen and then stored at -80ºC), another for histological analysis and the remaining half (parts A and B) were cultured in blood agar plates for CFU's counting.

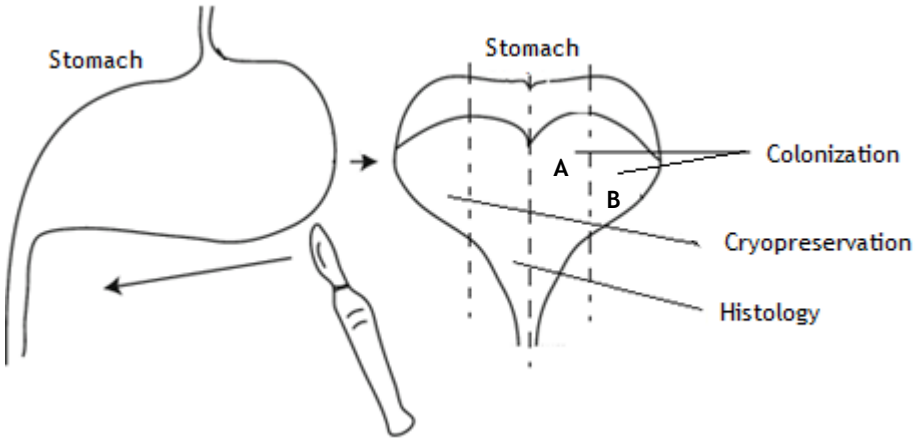

Figure 11. Schematic representation of the collection of mice stomach segments for analysis (histological analysis, cryopreservation and colonization). Adapted from *Roberts, A. B.* .

Two portions (from different lobes) of mice liver were also collected for cryopreservation and histological analysis.

Histological analysis

To prepare the samples for histological analysis, each portion of the stomach and liver was placed in a cassette and immersed in 10% formalin (*Atom Scientific*, Manchester, UK) for 24h. Particularly, to guarantee that gastric sections were well stretched, these were placed between two sponges in the cassettes.

After this period, cassettes were inserted in a tissue processor, where tissues were immersed in solutions of: 70% ethanol, 80% ethanol, 90% ethanol, 2x in 100% ethanol, 3x in Clear Rite for 1h each and in 2x Paraffin for 1h and 20 min each). Tissues were, finally, embedded in paraffin wax for later analysis of histological sections.

To analyze the morphology of stomach and liver, 3µm tissue sections from all animals were obtained using the microtome. For histological analysis sections were stained with Hematoxylin and Eosin (H&E). For that, samples were deparaffinated with xylene (10min in xylene and another 5min in a new solution of xylene) and subsequently hydrated with ethanol (5min in 100% ethanol, 5min in 96% ethanol, 5min in 70% ethanol) and, then, with running water (5min). Samples were stained with Hematoxylin for 2min and, again, rinsed

with running water. After being placed in ethanol solutions (2min in 70% ethanol and 2min in 96% ethanol), samples were stained with Alcoholic Eosin and, then, dehydrated with ethanol (quick passages in 100% ethanol). The last process was the diaphanization with xylene (10min in xylene and another 10min in a new solution of xylene).

Regarding Experiment III (described in *section 3.A.1.*), modified Giemsa staining was also performed to analyze tissue sections, as an attempt to find bacteria in animals' stomach. With this purpose, similarly, samples were deparaffinated with xylene (5min in xylene and another 5min in a new solution of xylene) and hydrated in ethanol (quick passages in 70% ethanol, 95% ethanol and 100% ethanol), followed by a wash in running water (5min). Samples were, then, stained with 2% Giemsa solution for 30min. At the end of this period, tissue sections were washed, once again, in running water (5min), passaged in ethanol (100% ethanol) and diaphanized with xylene (quick passages).

After both stainings, samples were mounted with entellan, between each slide (76X26mm) and the coverslip (18x18mm), and analyzed under the optical microscope.

Colonization - Colony-forming Assay

H. pylori infection levels with mice stomach tissue were quantified by colony-forming assay. The culture of stomach sections involved the use of blood agar plates, prepared as previously described in *section 3.1.*, but supplemented with 50mg/ml Bacitracin (*Sigma-Aldrich*) and 20mg/ml Nalidixic Acid (*Sigma-Aldrich*). Each stomach portion (Parts A and B) was collected to an *eppendorf* with 400μL of peptone water, weighed and smashed with a tissue homogeneizer using sterile pistons. Dilutions of 10^1, 10^2 and 10^3 were, then, made and spread with the correspondent non-diluted solution (10μL of each solution) for CFU's counting. After 7-15 days culture as above, colonies were counted, and the number of colony forming units per mice stomach and per g were calculated, according to equations 2 and 3, respectively.

$$CFU/mice\ stomach = (CFU/mL_{Part\ A} + CFU/mL_{Part\ B}) \times V_{sol} \times 2 \quad (2)$$

$$CFU/g = \frac{CFU/mL_{\ Part\ A} \times V_{sol}}{m_{stomach\ Part\ A}} + \frac{CFU/mL_{\ Part\ B} \times V_{sol}}{m_{stomach\ Part\ B}} \quad (3)$$

where CFU/mL can be calculated by equation 1, $m_{stomach}$ is the weight of the gastric portion and V_{sol} is the volume in which each part was ressuspended (400μL).

Statistical Analysis

To analyze weight variations between the different groups independent samples t-test was applied. Whenever possible, results from CFUs countings were also compared to look for significant differences, using, once again, the independent samples t-test. Results were considered significant for $p < \alpha$ (considering $\alpha = 0.05$).

3.B. Treatment of *H. pylori* infection using Ch Mics

3.B.1 Chitosan Microparticles

Chitosan microparticles' production

The Ch Mics used in this study have been previously produced in the lab by ionotropic gelation into a sodium tripolyphosphate solution, using an aerodynamically assisted spraying system. These microparticles were prepared with chitosan with a DA of 6% and were crosslinked with 10mM genipin for 45min to prevent dissolution in gastric acidic pH. Microparticles were, then lyophilized at –80ºC and stored at 4ºC in ethanol, until use.

Chitosan microparticles morphology - SEM analysis

For morphology analysis of Ch Mics using SEM, a sample of lyophilized particles was placed on the top of a carbon tape, attached to a sample holder. Ch Mics were analyzed using a *TM3030(Plus)* microscope from *Hitachi* (Tokyo, Japan).

3.B.2 Cytotoxicity of Chitosan Microparticles

Gastric cell line *MKN45* culture

Chitosan microparticles' cytotoxicity was evaluated *in vitro*, using the gastric carcinoma cell line *MKN45*. *MKN45* gastric cell line, from passage 3, was maintained in culture in RPMI 1640 with glutamax and HEPES (*Gibco, Life Technologies*, California, USA), supplemented with 10% heat-inactivated (30min, 56ºC) fetal bovine serum and 1% penicillin/streptomycin (RPMIc), at 37ºC, in a humidified 5% CO_2 atmosphere. Culture medium was exchanged every 2 days. After expanding the cells in 75cm^3 T-flasks these were seeded in 24-well plates, with 1mL of cell suspension per plate (at a density of 5x10^{4}cells/mL), under the conditions above mentioned.

Direct contact assay

The cytotoxicity of Ch Mics was evaluated by direct contact assay, according to ISO international standard 10993-5 [114]. With this in mind, increasing concentrations of Ch Mics in RPMIc were prepared to obtain a final concentration in the wells of 1000 Mics/well, 10 000 Mics/well, 50 000 Mics/well and 100 000 Mics/well. For that, Ch Mics from the

stock solution (suspended in ethanol) were centrifuged (5000 rpm, 8min), the ethanol was discarded and microparticles were re-suspended in RPMIc, followed by another centrifugation (5000 rpm, 8min), and adjusted to the different concentrations.

Ch Mics were added to the wells with adherent cells (6 replicates per concentration). Cells with TCPS microspheres (~270µm in diameter, 75mg/mL) were used as positive control of cell metabolic activity to guarantee that cells were not affected if completely covered by particles (this guarantees that any change in metabolic activity is caused by direct contact with Ch Mics and not because cells are prevented from their normal atmosphere) and cells with 10% hydrogen peroxide in RPMIc were used as positive control. Cells in RPMIc, RPMIc alone, Ch Mics in RPMIc and TCPS Mics in RPMIc also served as a control to determine cells metabolic activity when cultured alone and to guarantee that culture media or culture media with Ch Mics would not influence the results from the metabolic activity.

Metabolic activity - Resazurin Assay

Metabolic activity of *MKN45* cells was measured using the resazurin assay, to evaluate the cytotoxicity of Ch Mics. With this in mind, 20% resazurin in RPMIc was added to the wells and incubated for 4h. Once this incubation period was over, 200µL of supernatant were added to a 96-well black plate to measure its fluorescence (λ_{ex} = 530nm and λ_{em} = 590nm), using a microplate fluorometer (Spectra Max GeminiXS, Molecular Devices). Blanks for fluorescence emission subtraction were performed with RPMIc, Ch Mics in RPMIc or TCPS microspheres in RPMIc. Cell viability was determined based on the percentage of metabolic activity of *MKN45* cells.

Immunocytochemistry

After fixation of cells with 4% PFA (15min), cells were permeabilized with 0.1% Triton X-10 for 5min, at 4℃. Wells were, then, rinsed with PBS and phalloidin (Alexa Fluor 488; excitation/emission: 499/520 nm), diluted 1:100 in PBS, was added (30 min, protected from light). Afterwards, wells were rinsed with PBS to add DAPI 3µg/mL (DAPI; excitation/emission: 359/457 nm) (15min protected from light). Finally, cells were analyzed under inverted fluorescence microscope.

Statistical Analysis

Variations in cellular metabolic activity for the different conditions were analyzed using one-way ANOVA. Results were considered significant for $p < \alpha$ (considering $\alpha = 0.05$).

3.B.3 *In vivo* mouse model - Eradication of *H. pylori* infection

Infection of C57BL/6 mice with *H. pylori*

Infection with *H. pylori* was performed in 20 C57BL/6 mice (7-8 weeks old, specific-pathogen-free), in accordance with the parameters described in Tables IX and X.

Table IX. Experimental parameters for *H. pylori* infection with *SS1* strain.

Animal model	C57BL/6 mice
Age (weeks)	7
Number of animals	20 male mice
Bacteria strain	*SS1*
Bacterial concentration (CFU/mL)	10^{10}
Vehicle	Peptone water
Number of inoculations	3x
Inoculations volume (mL)	0.1mL
Time to establish infection (weeks)	3

Table X. Test groups in *H. pylori* infection experiment with *SS1* strain.

Name	n
Hp-Mic-	2
Hp-Mic+	2
Hp+Mic-	8
Hp+Mic+	8

n number of animals; **Hp-** Non-infected animals; **Hp+** infected animals; **Mic-** Non-treated animals; **Mic+** Treated animals.

***H. pylori* culture**

SS1 H. pylori strain was grown in accordance with the methodology described in *section 3.1* and the preparation of bacteria to infect the animals followed the steps presented in *section 3.A.1.*.

Treatment of *H. pylori* infection using Ch Mics

Three weeks after infection, the treatment plan was applied to the animals, during a period of 14 days. This involved the daily administration (1 dose/day) of 10 000 Mics in 100µL of phosphate-citrate buffer pH6, by oral gavage (B. Braun 20G cannula 1.1x32mm). A summary of the experimental parameters used in this treatment is presented in Table XI. In addition, a study protocol of inoculation, infection and treatment processes is described in

Figure 12.

Table XI. Experimental parameters for Ch Mics treatment – *in vivo* mouse model.

Treatment duration (days)	14

Number of doses	14 (1 dose/day)
Dosage (Mics/mL)	$1x10^5$
Volume (mL)	0.1
Vehicle	phosphate-citrate buffer pH6

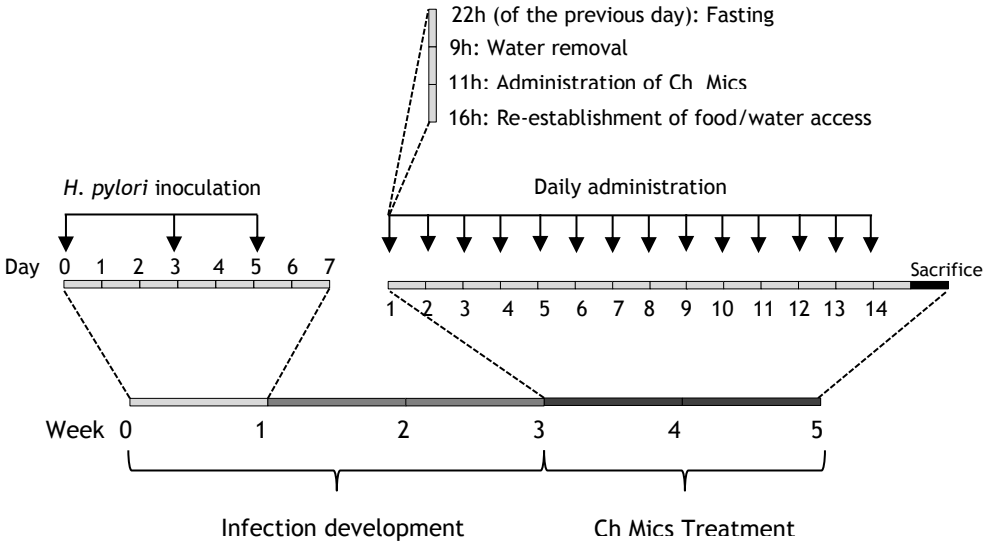

Figure 12. Study protocol for *SS1 H. pylori* infection and treatment (with Ch Mics) of *C57BL/6* mice.

From the four control animals (not infected with *H. pylori*), two were given phosphate-citrate buffer alone, whereas the remaining were given Mics. The sixteen infected animals were, in turn, divided into two groups of eight animals each: one received phosphate-citrate buffer and Mics were administered to the other group.

Animals' sacrifice

Animals were sacrificed the day after the end of the treatment plan, accordingly to the procedure presented in *section 3.A.2.*.

Statistical Analysis

To test the null hypothesis between the groups (animals' infected, but without Mics treatment, and animals infected and treated), *Kruskal-Wallis* non-parametric test was applied. Results were considered significant for $p < \alpha$ (considering $\alpha = 0.05$).

Chapter 4

Results and Discussion

In this chapter the results obtained from the methodology applied are presented and evaluated, as an attempt to give an answer to the proposed goals.

4.A. Establishment of a *BabA+ H. pylori* infection model

First of all, to evaluate and compare the motility of different *H. pylori* strains (*SS1* and *B128*), bacteria were grown in solid and liquid media (blood agar plates and BBL, respectively), since these are among the most common culture media reported (as described in *section 1.4.1.*). Bacteria were visualized by optical microscopy (bright field), right after collecting them from culture. Comparing solid with liquid media, both strains were found to be motile, and mainly in rod morphology, with no apparent differences observed between them. For this reason the use of blood agar plates (solid media) was adopted in the subsequent experiments to grow *H. pylori*, since it was already a common practice in the lab.

4.A.1 *BabA e*xpression in different *H. pylori* strains

To determine the expression of *BabA* adhesin in *TN2GF4*, *B128* and *SS1* strains, a Western Blot was performed. With this purpose, protein from these samples was extracted and a calibration curve of BSA was used to determine the protein concentration of each sample (described in *Appendix B*). Based on this curve, it was possible to normalize the amount of protein to load in each lane (for electrophoresis).

The detection of *BabA* adhesin from bacteria grown in solid and liquid media (blood agar plates and BBL, respectively) and from different passages was evaluated, using the

AK277 primary antibody. Results obtained (Figure 13) confirmed that *B128* and *TN2GF4* strains show a band just above the 75kDa ladder mark. This suggests the expression of *BabA* adhesin, known to have a molecular weight of around 78kDa [31], and is supported by the presence of this same band in the positive control strain (*17875/Leb*), which also expresses this protein, in agreement with the previously described [40]. Therefore, this confirms the results found in our preliminary work for *B128* strain (Appendix A, Figure A1) and found in the literature for *TN2GF4* strain [96]. Moreover, the culture media and the different passages do not seem to affect the expression of *BabA* adhesin. Nevertheless, in lanes correspondent to *B128* strain culture in solid media (for passages 2 and 3) a second band, less pronounced, can be found. A strategy to find the reason underlying these results was not pursued, but an incomplete denaturation of proteins could be hypothesized as an explanation.

Concerning the *SS1* strain loaded lanes, results showed a band close to 75kDa ladder mark. Further research should be performed on these results but a previous study (performed by our group collaborators at IPATIMUP, Glycobiology in Cancer Group) already pointed to the absence of *BabA* in this strain (unpublished work) and, in fact, a weaker signal, compared with the remaining samples, is found in this case.

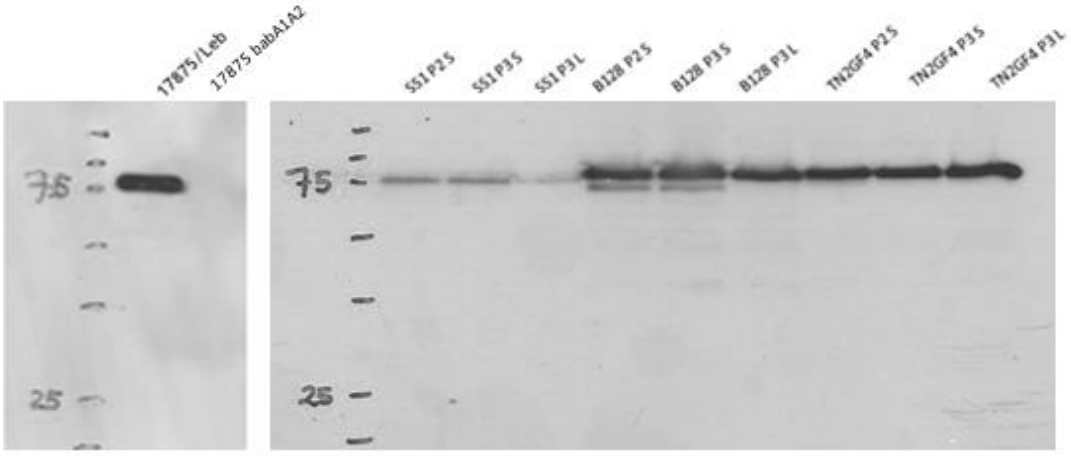

Figure 13. Western Blot analysis of *H. pylori* SS1, *B128* and *TN2GF4* strains, for the different passages (**P2** Passage 2; **P3** Passage 3) and culture media (**S -** solid; **L -** liquid). *17875/Leb* and *17875 babA1A2* served, respectively, as positive and negative controls. Amount of protein: 25µg; Exposure time: 10s.

4.A.2. *H. pylori* infection of C57BL/6 mice

Once defined the conditions to culture *H. pylori* and upon confirmation of *BabA* adhesin expression in *B128* and *TN2GF4* strains, the development of infection in *C57BL/6* mice with these strains was assessed. With this in mind, different experiments were

developed, varying some parameters (described in *section 3.A.2.*) to establish the adequate infection model.

The first experiment was intended to evaluate the applicability of a well-established (also in our lab) animal model for *SS1 H. pylori* strain, but using the *BabA* positive *H. pylori* strain *B128*. In other words, the aim of this study was to determine the effectiveness of pre-defined conditions (bacterial concentration, number of inoculations and time to establish infection) in the establishment of *H. pylori* infection (presented in Figure 10, *section 3.A.2.*), using *B128* strain, by verifying the presence of this bacterium in the stomach of C57BL/6 mice.

After growing *H. pylori* in blood agar plates, bacteria were inoculated to mice and results revealed a bacterial concentration of $1.03x10^{10}$ and $1.53x10^{10}$ CFU/mL (for each of the 2 inoculations, respectively), which was close to the desired value ($1x10^{10}$ CFU/mL).

During the development of infection, to assure animals' welfare, besides inspecting their physical appearance, weight variations were registered weekly for each animal, until sacrifice, and results are presented in Figure 14 as an average within each group.

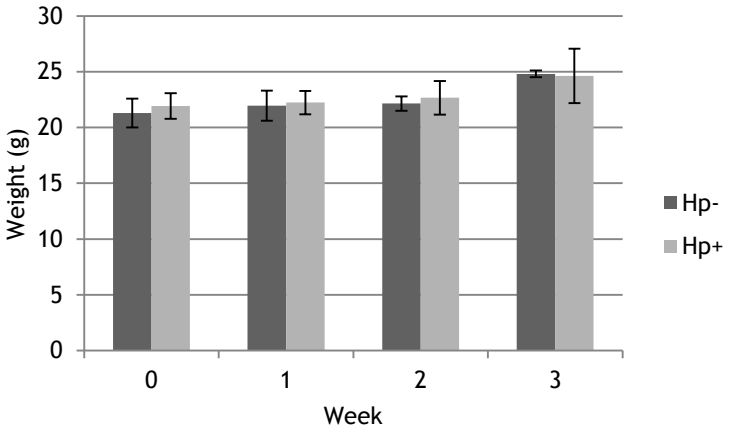

Figure 14. *H. pylori* infection – Experiment I: C57BL/6 mice weight variations during the development of infection with *B128 H. pylori* strain. Groups: **Hp-** Non-infected animals; **Hp+** Infected animals. Values from week 0 correspond to the pre-infection weighing (the day before the first *H. pylori* inoculation), whereas values from weeks 1, 2 and 3 relate to post-infection weighings. No significant differences were found between groups for each timepoint (Independent samples t-test).

Results obtained revealed no significant differences between control and test groups and a progressive weight increase was verified over the course of weeks. To understand if animals' weight was in accordance with their normal growth curve, the technical file of C57BL/6 mice (from Charles River, their source place) was analysed and their theoretical

weight variation curve is presented in Figure C1 *Appendix C*. At week 0, animals were 7 weeks old and their weight was around 20g for both groups, which is in accordance with the theoretical value described for males. Animals increased their weight over the weeks and, at the end of the 3 weeks timepoint, their weights were close to 25g, which, once again, corresponds to a normal value for 10 weeks old male mice.

Despite presenting the results in terms of average weight per group, mice weight evolution was also evaluated individually (data not shown). Each animal increased weight over time and all mice maintained good physical appearance throughout the experiment.

Regarding the development of infection in mice, this was assessed by plating the animals' stomach in blood agar and counting the CFUs present (as explained in *section 3.A.2.*). Histological analysis of stomach sections was also performed to look for morphological changes that could indicate presence of infection.

Results of the CFUs found in mice stomachs (Figure 15) confirmed that, as expected, non-infected animals were *H. pylori* negative. However, these also revealed that only 1 out of the 6 infected animals gave positive results for *H. pylori* culture, with a concentration of $5.3x10^3$ CFU/stomach ($7.8x10^4$ CFU/g). This suggests that, possibly, the conditions applied, already established for infection with *SS1* strain, are not adequate for the development of *B128 H. pylori* infection in mice. In fact, for *SS1 H. pylori* strain, studies reveal the presence of 10^3-10^6 CFU/g in C57BL/6 mice, 4 weeks post-infection [68, 77]. And, although the CFUs found in the animal infected were within this range, only one animal was infected.

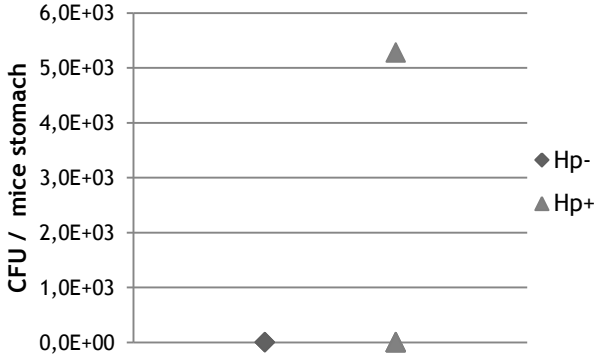

Group	Animal	CFU/mice stomach	CFU/g
Hp-	1	0	0
	2	0	0
Hp+	1	0	0
	2	0	0
	3	0	0
	4	0	0
	5	0	0
	6	$5.3x10^3$	$7.8x10^4$

Figure 15. *H. pylori* infection – Experiment I: Colonization of *B128 H. pylori* strain in C57BL/6 mice (CFU/mice stomach and CFU/g) - Colony forming assay. Groups: **Hp-** Non-infected animals; **Hp+** Infected animals.

Regarding the histological analysis of mice stomach sections it was possible to find in all animals a well demarked transition between the non-glandular forestomach and the glandular stomach, as identified in Figure 16 (margo plicatus). Further analysis of the histological sections was compared with images found in the literature (illustrated in Figure D1, *Appendix D*).

Figure 16. Histomorphology of C57BL/6 mice (H&E staining). Group Hp- Animal 1. The region marked with an arrow corresponds to margo plicatus. Scalebar: 500µm.

Analyzing in more detail gastric sections of the different animals (Figure 17), it is possible to observe that control mice (Group *Hp-*) presented no alterations in their gastric morphology. In what concerns infected animals (Group *Hp+*), a large inflammatory infiltrate can be found in animal *Hp+ 3*. However, this mouse was not *H. pylori* positive in the colony forming assay. For this reason, these events might not be associated. Regarding the only animal found with CFUs in this experiment (animal *Hp+ 6*), no significant changes in the gastric histomorphology could be denoted, suggesting that bacteria did not trigger an inflammatory response from this animal's immune system, for the period defined to develop infection (3 weeks).

Overall, results suggest that the administration of *B128* strain to C57BL/6 mice, with the parameters applied in this experiment, were not able to develop infection consistently and in a reproducible manner.

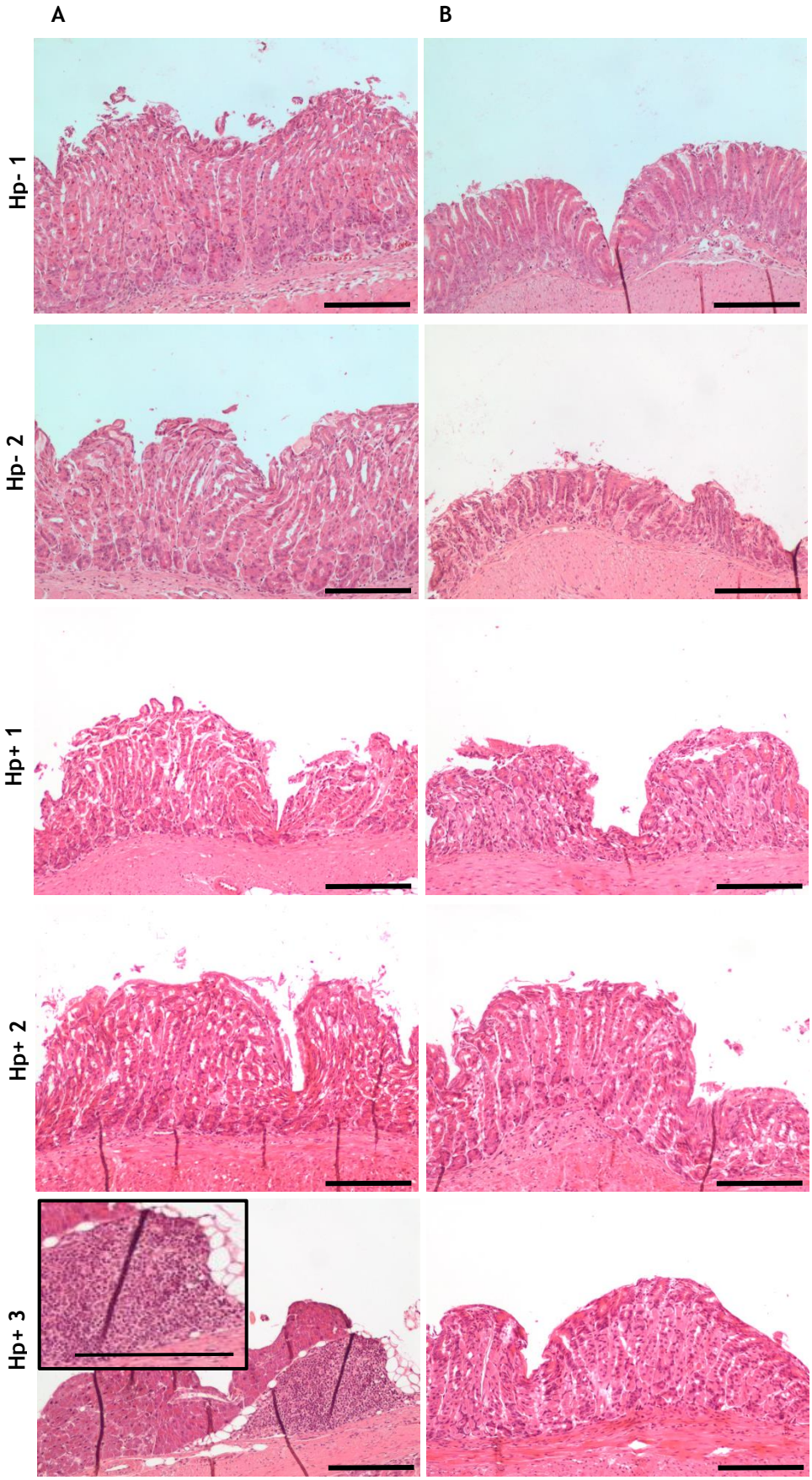
A
B
Hp- 1
Hp- 2
Hp+ 1
Hp+ 2
Hp+ 3

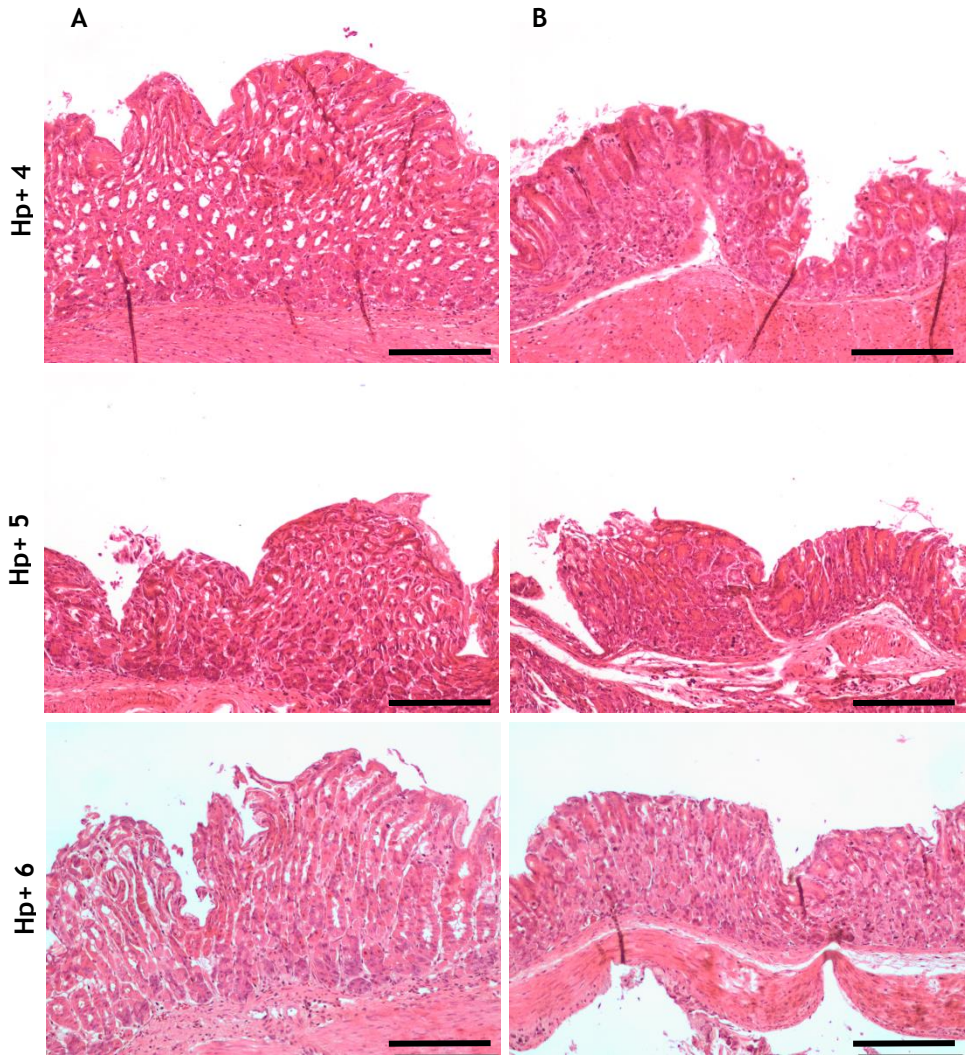

Figure 17. *H. pylori* infection - Experiment I: Histological characterization (H&E staining) of C57BL/6 mice gastric mucosa infected with *H. pylori* (*B128* strain). Groups: **Hp-** Non-infected animals; **Hp+** Infected animals. Column A – proximal portion of glandular stomach. Column B –distal portion of glandular stomach. Scalebar: 200µm.

Since the conditions previously applied were not successful in the establishment of an *H. pylori* infection model, a second experiment was carried out, again using the *B128* strain. Yet, some parameters were altered as described in Figure 10 (*section 3.A.2.*). The number of administrations was increased from two to three times and the volume of inoculum was doubled (200µL). The bacterial concentration was maintained, accordingly to the values suggested in the literature [56, 64, 79]. In this experiment, BBL was used as the administration vehicle, instead of peptone water, since its use is most described on the literature (see Tables IV, V and VI). In addition, concerning the time to develop infection, besides maintaining the 3 weeks timepoint, a group of animals was sacrificed after 4 weeks to understand the influence of this parameter. The timepoints were chosen

in accordance with the periods suggested to develop infection in C57BL/6 mice in other published studies (see Table VI). Furthermore, in this particular case, and although the defined concentration of bacterial suspension was $1x10^{10}$ CFU/mL, the density of the inoculum administered to mice was $6x10^{9}$ CFU/mL, $3.67x10^{9}$ CFU/mL and $4x10^{9}$ CFU/mL (for the 3 inoculations, respectively), given the lack of bacteria obtained.

Mice weight variations are presented in Figure 18. Similarly and as expected, mice varied their weight from approximately 20g at 7 weeks old and were close to 25g after 3 and 4 weeks. This suggests that the experimental procedures did not affect the normal growth of the animals involved. Individually, animals showed good physical appearance in the course of the experiment and gradually increased their weight (data not shown).

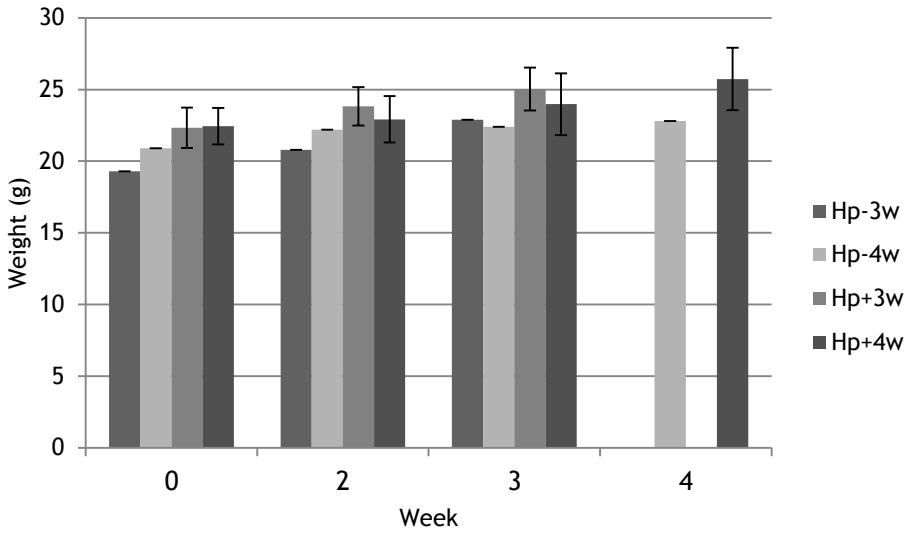

Figure 18. *H. pylori* infection – Experiment II: C57BL/6 mice weight variations during the development of infection with *B128 H. pylori* strain. Groups: **Hp-3w** Non-infected animals sacrificed 3 weeks post-infection; **Hp-4w** Non-infected animals sacrificed 3 weeks post-infection; **Hp+3w** Infected animals sacrificed 3 weeks post-infection; **Hp+4w** Infected animals sacrificed 4 weeks post-infection. Values from week 0 correspond to the pre-infection weighing (the day before *H. pylori* inoculation), whereas values from weeks 2, 3 and 4 relate to post-infection weighings. Week 1 is absent as no weighing was performed at this time-point. No significant differences were found between groups for each timepoint (Independent samples t-test).

Results from CFU's countings are presented in Figure 19. Once again plates of control mice stomachs were absent from *H. pylori* colonies. From the infected animals, none of the mice sacrificed after 3 weeks (Group Hp+3w) were positive for *H. pylori* culture and only 1 out of 6 animals from the 4 weeks group (Group Hp+4w) was infected, with a concentration of $3.2x10^{2}$ CFU/stomach (5.8 CFU/g).

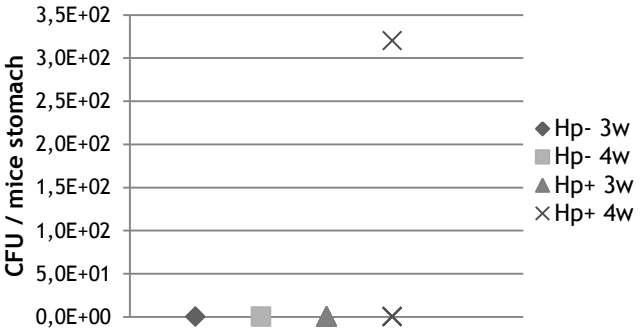

Group	Animal	CFU/mice stomach	CFU/g
Hp-3w	1	0	0
Hp+3w	1	0	0
	2	0	0
	3	0	0
	4	0	0
	5	0	0
	6	0	0
Hp-4w	1	0	0
Hp+4w	1	0	0
	2	0	0
	3	$3.2x10^2$	5.8
	4	0	0
	5	0	0
	6	0	0

Figure 19. *H. pylori* infection – Experiment II: Colonization of *B128 H. pylori* strain in C57BL/6 mice (CFU/mice stomach and CFU/g) - Colony forming assay. Groups: **Hp-3w** Non-infected animals sacrificed 3 weeks post-infection; **Hp-4w** Non-infected animals sacrificed 3 weeks post-infection; **Hp+3w** Infected animals sacrificed 3 weeks post-infection; **Hp+4w** Infected animals sacrificed 4 weeks post-infection.

A recent study from *Cook, K. et. al.* [79] has proven the ability to infect C57BL/6 mice, with a colonization density ranging from $0.625x10^5$ CFU/g to $3.88x10^5$ CFU/g, using approximately the same bacterial concentration (10^9 CFU/mL, 10^8 CFU/mice) as in this experiment. The only apparent difference seems to be the use of isosensitest broth (see Table VI in *section 1.4.1.*), instead of BBL as inoculation vehicle and, yet, this revealed a much higher efficiency in the development of infection. Likewise, studies from *Wang, G. et al.* [80] and *Cullen, T. et al.* [81] also showed the ability to infect C57BL/6 mice with 10^4 CFU/g and 10^4 to 10^5 CFU/stomach, respectively. Therefore, although experimental conditions were altered to what is reported to be favourable for the growth of *H. pylori* and for the success of the infection, the low amounts of this bacterium, found in only one of the animals infected, and the absence of colonies in animals from the 3 weeks timepoint might indicate that the development of infection with *B128* strain is highly variable.

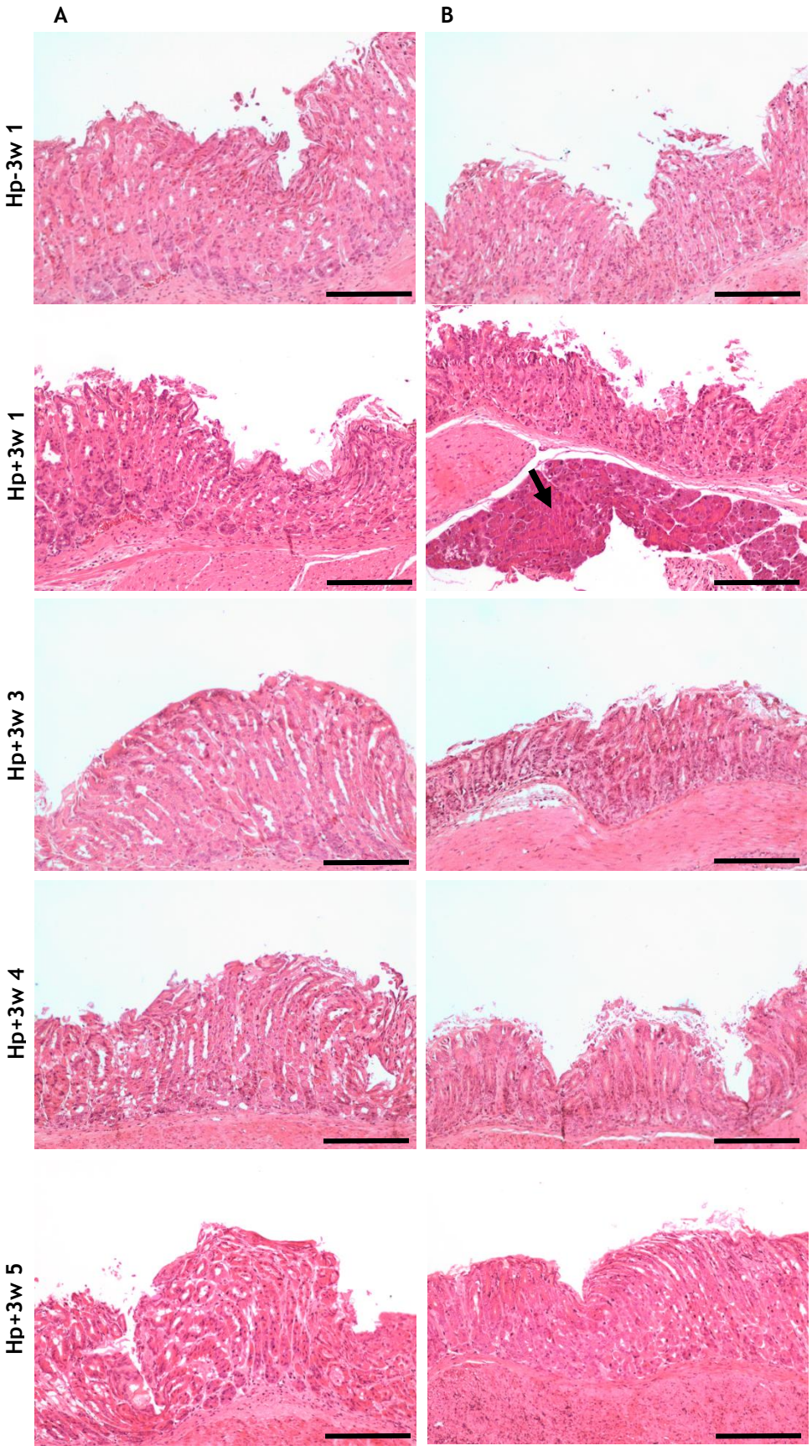
A
B
Hp-3w 1
Hp+3w 1
Hp+3w 3
Hp+3w 4
Hp+3w 5

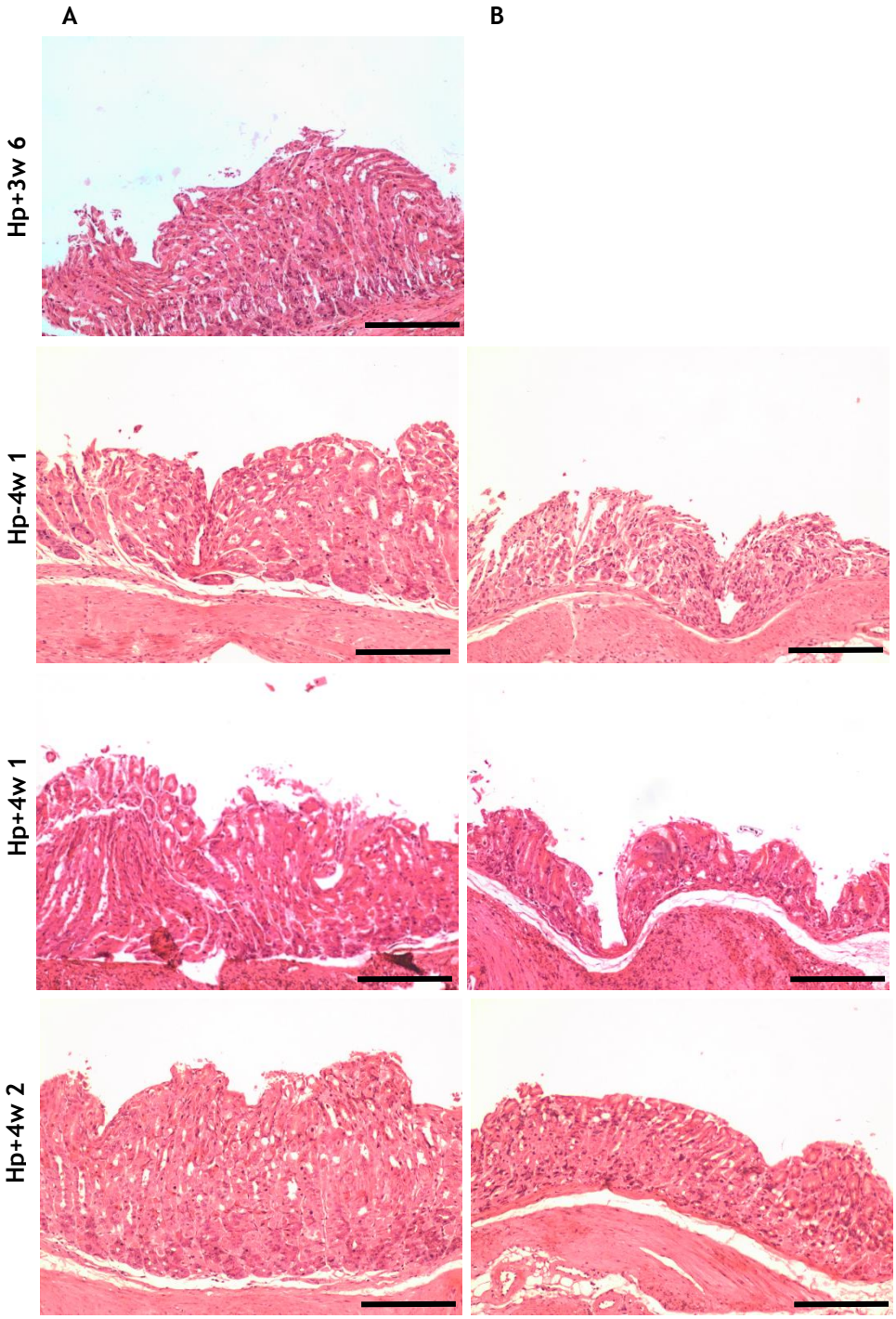
A
B
Hp+3w 6
Hp-4w 1
Hp+4w 1
Hp+4w 2

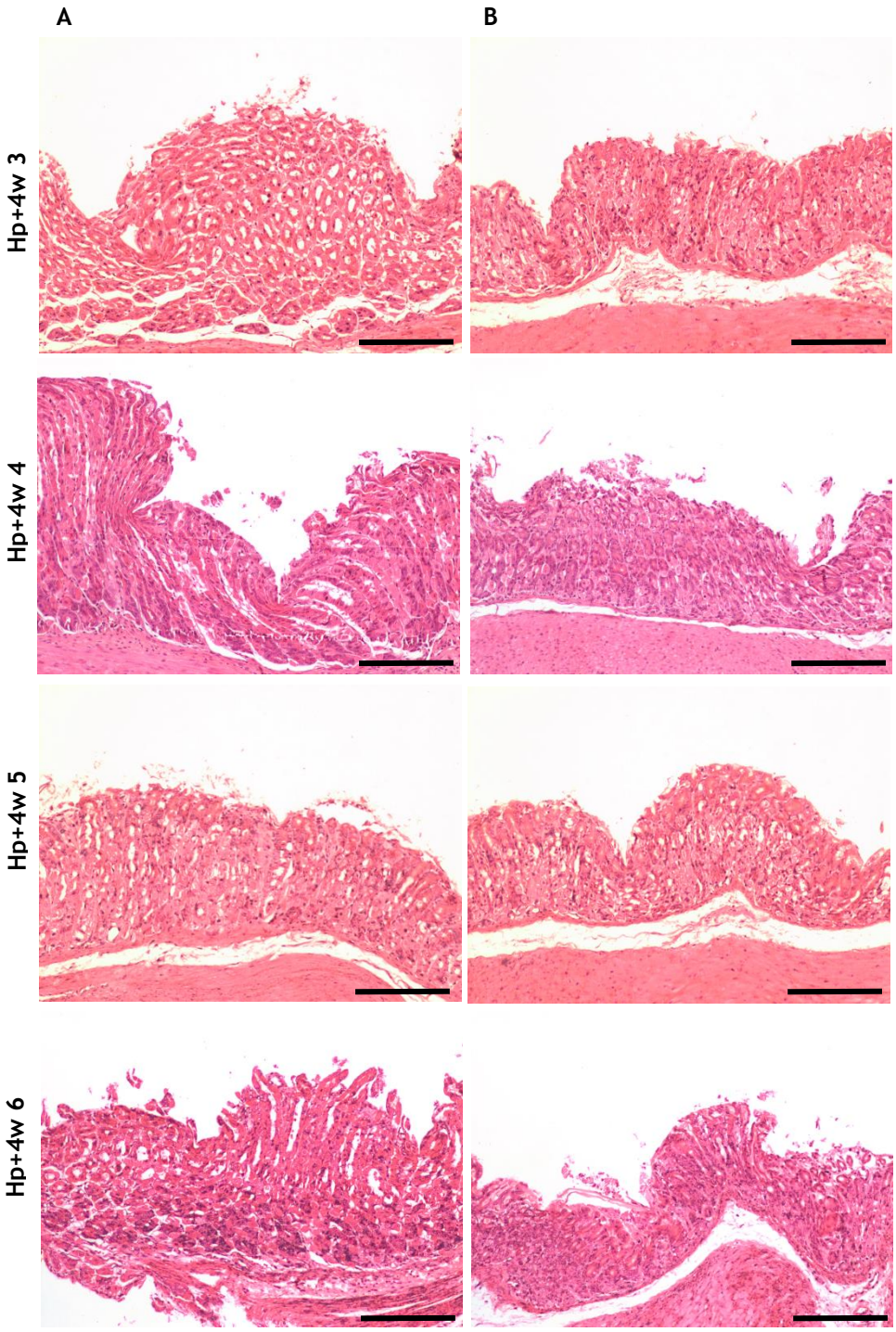

Figure 20. *H. pylori* infection - Experiment II: Histological characterization (H&E staining) of C57BL/6 mice gastric mucosa infected with *H. pylori* (*B128* strain). Groups: **Hp-3w** Non-infected animals sacrificed 3 weeks post-infection; **Hp-4w** Non-infected animals sacrificed 3 weeks post-infection; **Hp+3w** Infected animals sacrificed 3 weeks post-infection; **Hp+4w** Infected animals sacrificed 4 weeks post-infection. Column A – proximal portion of glandular stomach. Column B –distal portion of glandular stomach. The region identified with an arrow (Hp+3w 1) corresponds to a portion of mice pancreas. Images from animal Hp+3w 2 were not obtained, as well as from the distal portion of Hp+3w 6. Scalebar: 200µm.

From histological analysis of stomach sections (Figure 20), no apparent differences between infected (*Hp+3w* and *Hp+4w*) and non-infected animals (Hp-3w and Hp-4w) can be observed. In fact, animals do not seem to change their gastric epithelial morphology, even in the animal with positive culture of *H. pylori* (animal *Hp+4w 3*).

Taking this into consideration, a new experiment was performed using *TN2GF4 H. pylori*. *C57BL/6* mice were, thus, infected with this strain and, simultaneously, two other groups of animals were tested for the same conditions, using *SS1* and *B128* strains to compare the efficiency of different strains in the establishment of *H. pylori* infection. *SS1* was used as the positive control, since it is known its ability to infect C57BL/6 for the defined conditions. *B128* strain was collected from a subculture of these bacteria found in mice stomach after colonization in blood agar plates, from the previous *in vivo* experiment (Experiment II, Group *Hp+4w* 6). Since these bacteria have proven to infect mice, these might be able to develop infection more efficiently. The parameters considered in the study are presented in Figure 10.

The weight variations of the animals, displayed in Figure 21, show a progressive increase in mice's weights for the different groups, with no significant differences between them, for each timepoint. Additionally, results are in accordance with the values suggested in Figure C1 *Appendix C*, revealing, once again, that animals' normal growth was not affected. All animals were followed individually, having increased their weight progressively and maintaining good physical appearance throughout the experiment.

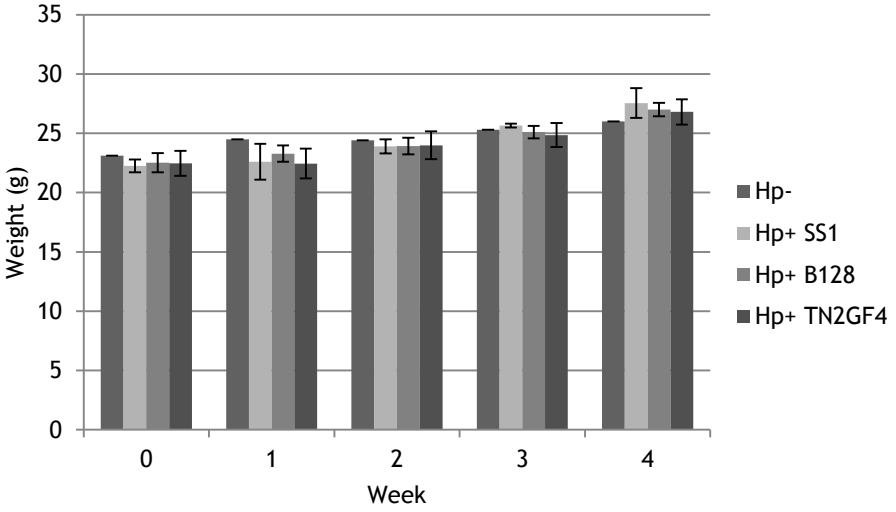

Figure 21. *H. pylori* infection – Experiment II: C57BL/6 mice weight variations during the development of infection with *SS1, B128* and *TN2GF4 H. pylori* strains. Groups: **Hp-** Non-infected animals; **Hp+SS1** Animals infected with *SS1 H. pylori* strain; **Hp+B128** Animals infected with *B128 H. pylori* strain; **Hp+TN2GF4** Animals infected with *TN2GF4 H. pylori* strain. Values from week 0 correspond to the pre-infection weighing (the day before *H. pylori* inoculation), whereas values from weeks 1, 2, 3 and 4 relate to post-infection weighings. No significant differences were found between groups for each timepoint (Independent samples t-test).

Results from CFU's countings are presented in

Figure 22. As expected, the control animal (*Hp-1*) was found to be *H. pylori* negative. On the other hand, both animals infected with the mouse-adapted strain *SS1* (*Hp+SS1*) revealed the presence of these bacteria, with a concentration of $1.24x10^6$ CFU/stomach and $4.44x10^4$ CFU/stomach (corresponding to $2.23x10^4$ CFU/g and $7.68x10^2$ CFU/g, respectively), in accordance with results found in the literature 4 weeks post-infection [68, 77]. In what concerns animals infected with *B128* strain (*Hp+B128*), 5 out of 6 were *H. pylori* positive, with concentrations ranging from $1.55x10^4$ to $1.01x10^5$ CFU/stomach ($2.13x10^2$ to $2.36x10^3$ CFU/g). Finally, the *TN2GF4* strain (*Hp+TN2GF4*) did not reveal the capacity to infect C57BL/6 animals, with no animal presenting positive results for the culture of *H. pylori*.

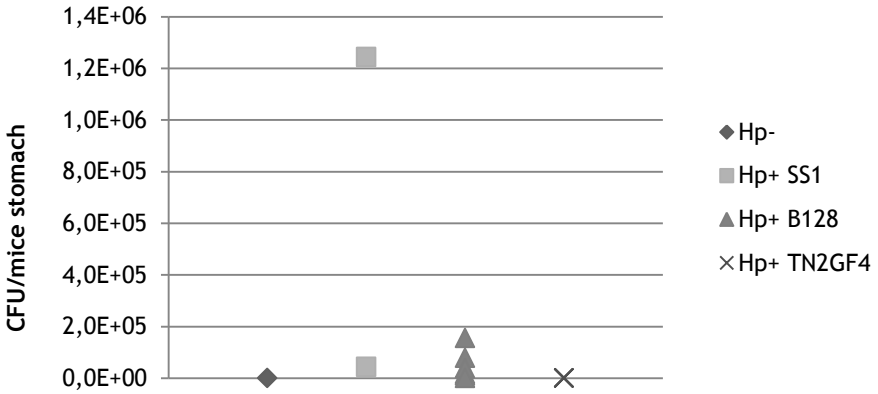

Group	Animal	CFU/mice stomach	CFU/g
Hp-	1	0	0
Hp+SS1	1	$1.24x10^6$	$2.23x10^4$
	2	$4.44x10^4$	$7.68x10^2$
Hp+B128	1	$1.55x10^5$	$2.36x10^3$
	2	$1.01x10^4$	$2.13x10^2$
	3	$1.63x10^4$	$2.28x10^2$
	4	$7.88x10^4$	$1.58x10^3$
	5	$3.76x10^4$	$7.04x10^2$
	6	0	0
Hp+TN2GF4	1	0	0
	2	0	0
	3	0	0
	4	0	0
	5	0	0
	6	0	0

Figure 22. *H. pylori* infection – Experiment III: Colonization of *SS1, B128* and *TN2GF4 H. pylori* strains in C57BL/6 mice (CFU/mice stomach and CFU/g) - Colony forming assay. Groups: **Hp-** Non-infected animals; **Hp+SS1** Animals infected with *SS1 H. pylori* strain; **Hp+B128** Animals infected with *B128 H. pylori* strain; **Hp+TN2GF4** Animals infected with *TN2GF4 H. pylori* strain. No significant differences were found between groups (Independent samples t-test).

The results from histological analysis (presented in Figure 23) revealed some minor inflammatory infiltrates in *Hp-1* animal, which is reported to be a common feature inherent to these animals [58]. The same can be found for animals infected with *SS1* strain (*Hp+SS1*), suggesting that, even though these were found positive for the culture of *H. pylori*, an inflammatory response was not triggered by the presence of bacteria.

Nevertheless, it is visible the presence of atrophy in the distal portion of their stomachs, as opposed to non-infected mice, which might indicate the presence of infection.

Animals infected with *B128* strain (*Hp+B128*), on the other hand, revealed more evidenced inflammatory infiltrates (infiltration of mucosal and submucosal lymphocytes), especially in animals *Hp+B128 3, Hp+B128 4* and *Hp+B128 5* spread throughout the entire stomach sections. In addition to this, it is visible in all infected animals that the distal portion of the stomach (Figure 23, Column B) has suffered an atrophy in comparison with the control animal and with normal gastric architecture (Figure D1, *Appendix D*), which, once again, might indicate that *B128* was able to successfully infect C57BL/6 mice, leading to inflammatory response. Animals infected with *TN2GF4 H. pylori* strain, besides presenting negative cultures of bacteria, also showed no morphological changes and no inflammatory response, revealing, once again, the inability of this strain to infect C57BL/6 mice.

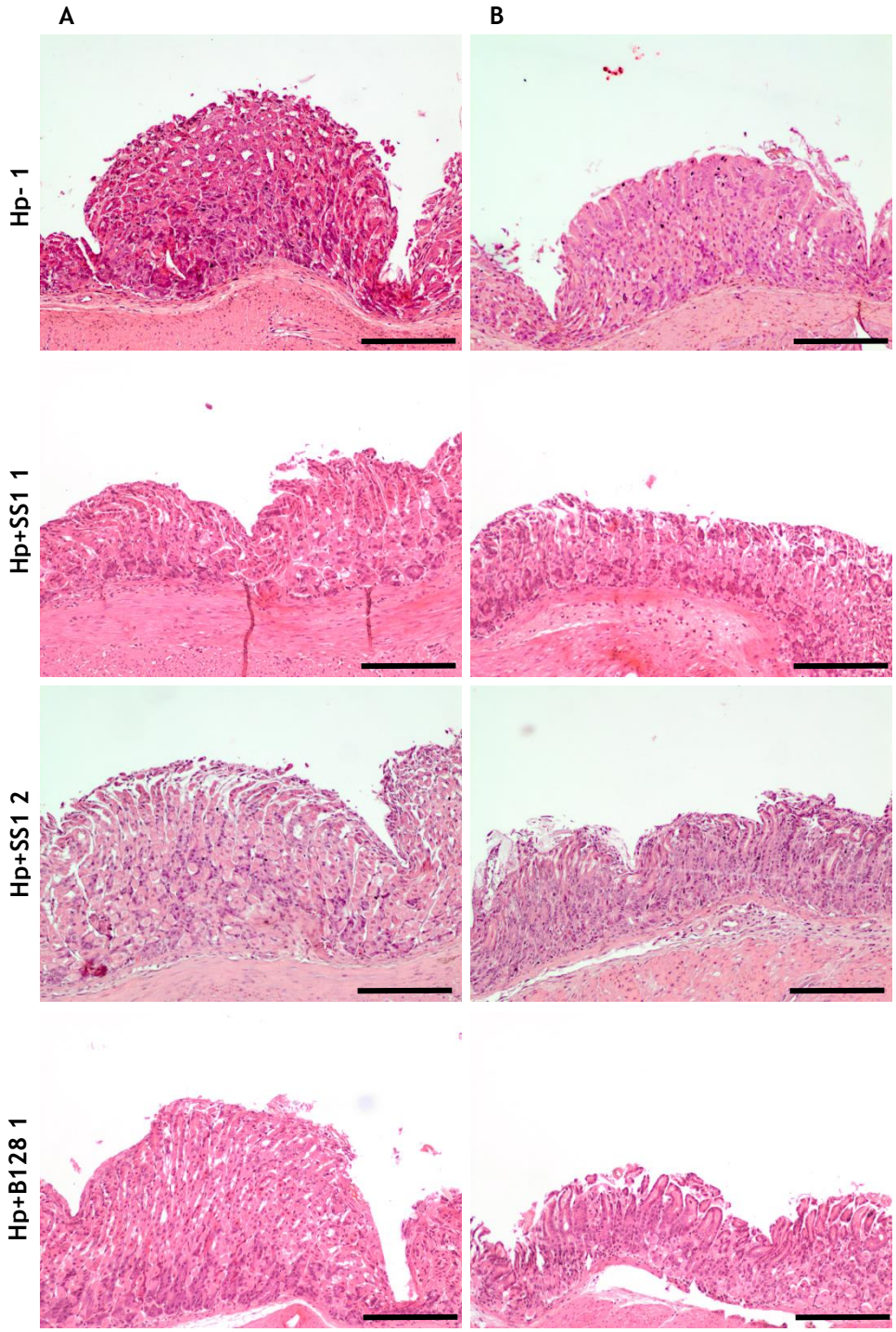
A
B
Hp- 1
Hp+SS1 1
Hp+SS1 2
Hp+B128 1

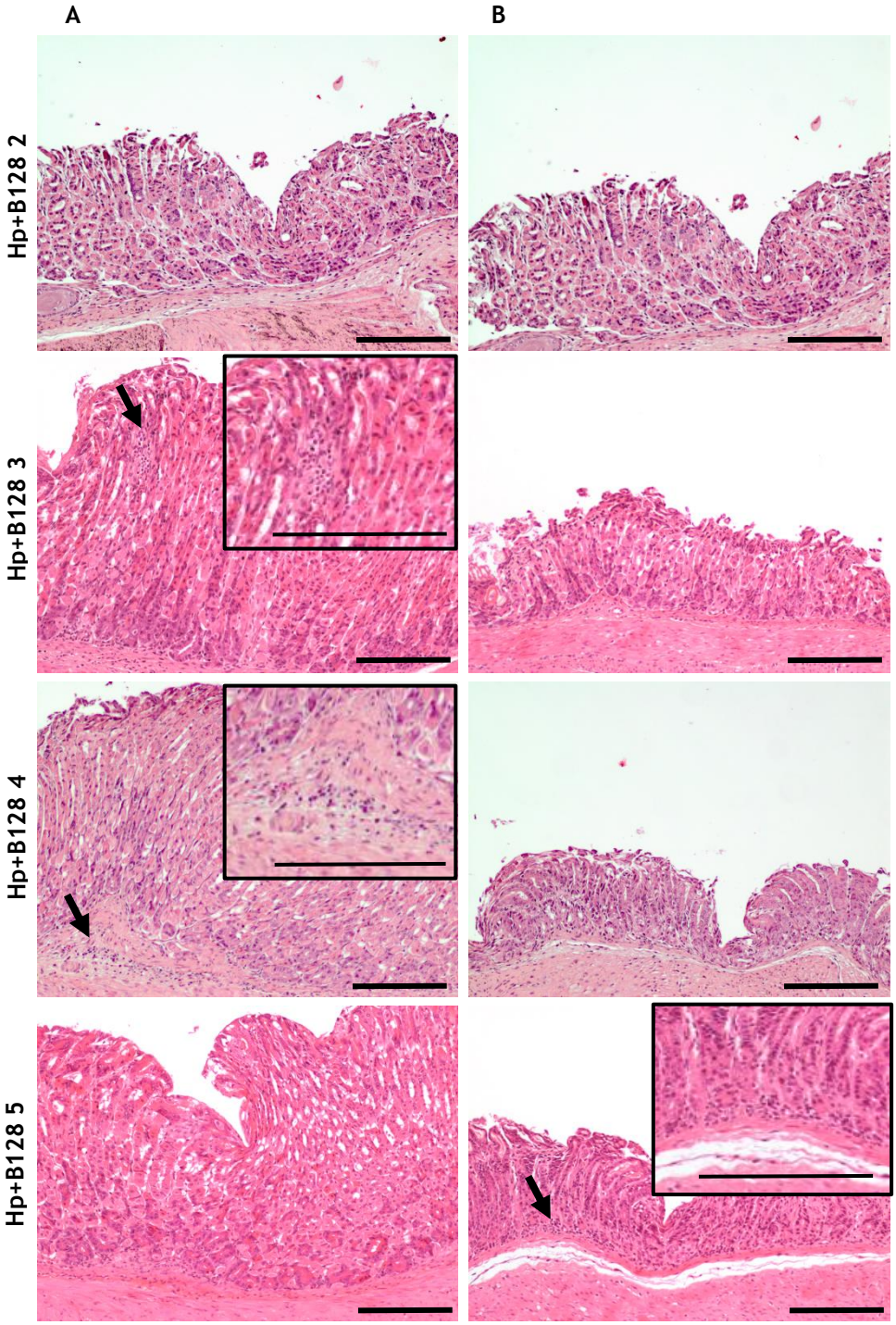
A
B
Hp+B128 2
Hp+B128 3
Hp+B128 4
Hp+B128 5

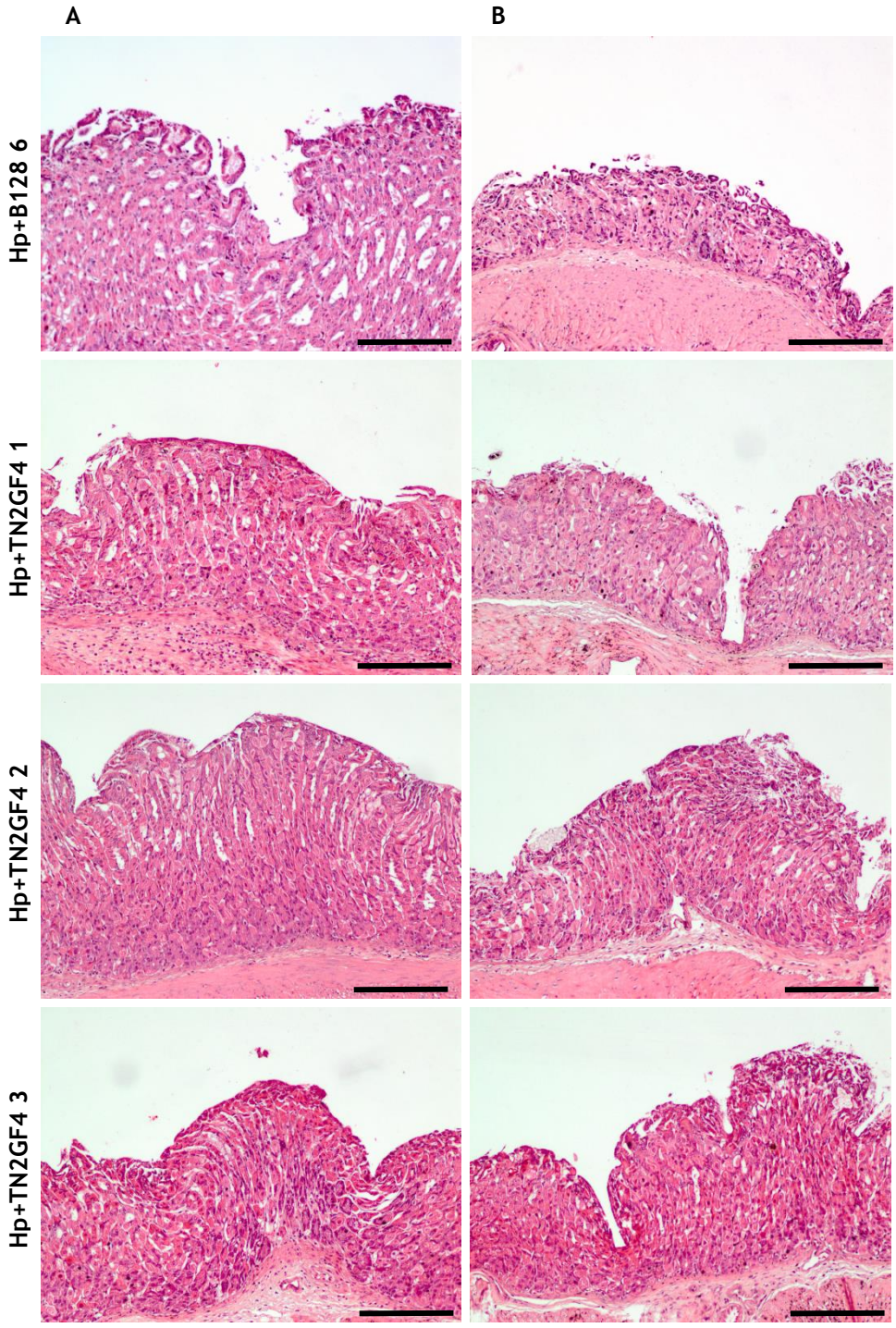
A
B
Hp+B128 6
Hp+TN2GF4 1
Hp+TN2GF4 2
Hp+TN2GF4 3

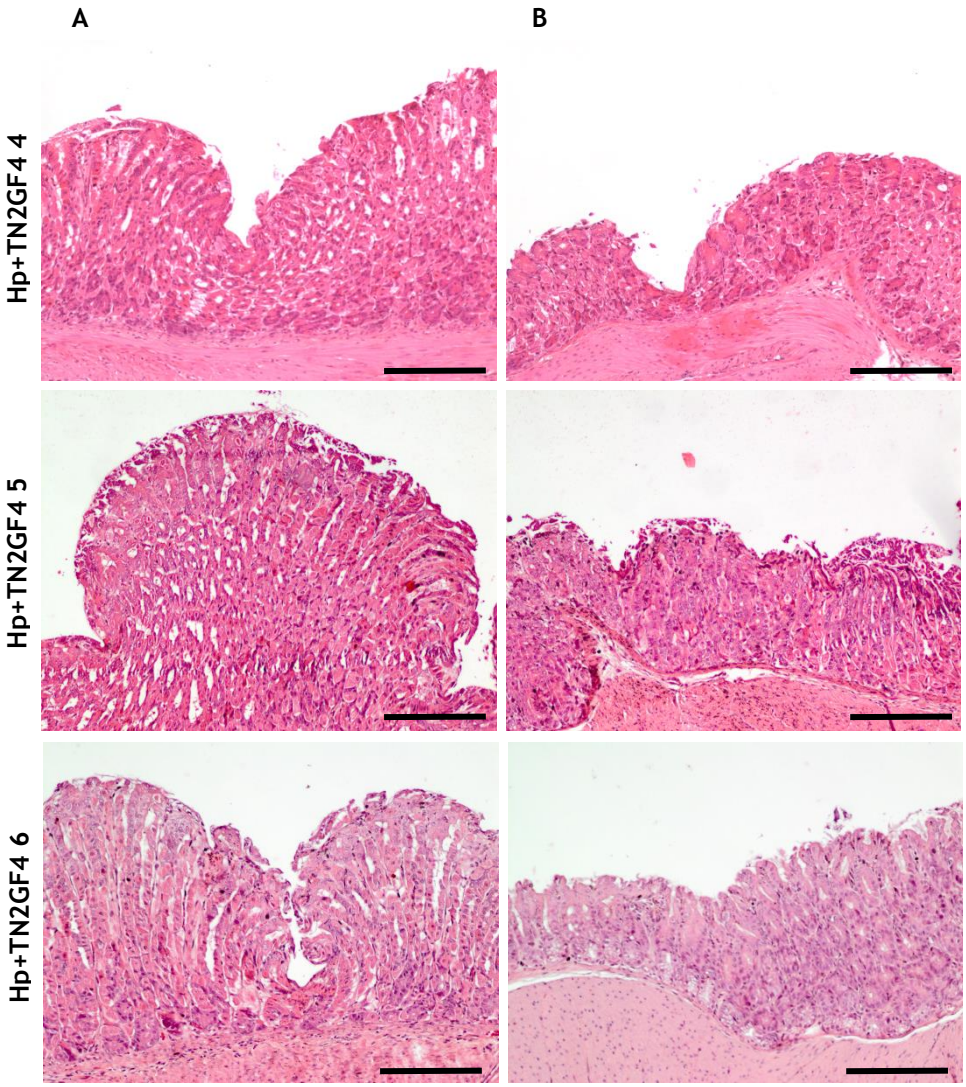

Figure 23. *H. pylori* infection - Experiment III: Histological characterization (H&E staining) of C57BL/6 mice gastric mucosa infected with *H. pylori* (*SS1, B128* and *TN2GF4* strains). Groups: **Hp-** Non-infected animals; **Hp+SS1** Animals infected with *SS1 H. pylori* strain; **Hp+B128** Animals infected with *B128 H. pylori* strain; **Hp+TN2GF4** Animals infected with *TN2GF4 H. pylori* strain. Column A – proximal portion of glandular stomach. Column B – distal portion of glandular stomach. Scalebar: 200µm.

To further explore the results found in animals infected with *B128 H. pylori* strain, stomach sections were stained with modified Giemsa, as an attempt to find bacteria. A representative illustration (Group Hp+B128, animal 4) of the results can be found in Figure 24, where it is possible to identify *H. pylori* on the surface of the gastric mucosa, confirming that the *B128* strain, isolated from an infected animal's stomach (Experiment II, Group Hp+4w, animal 6), was more prone to survive and thrive in mice stomach, being able to infect more effectively these animals. In fact, other study from *Peek, R. et al.* had already suggested that serial passages of *H. pylori* in rodents increases colonization efficiency [115], supporting the results found in this study.

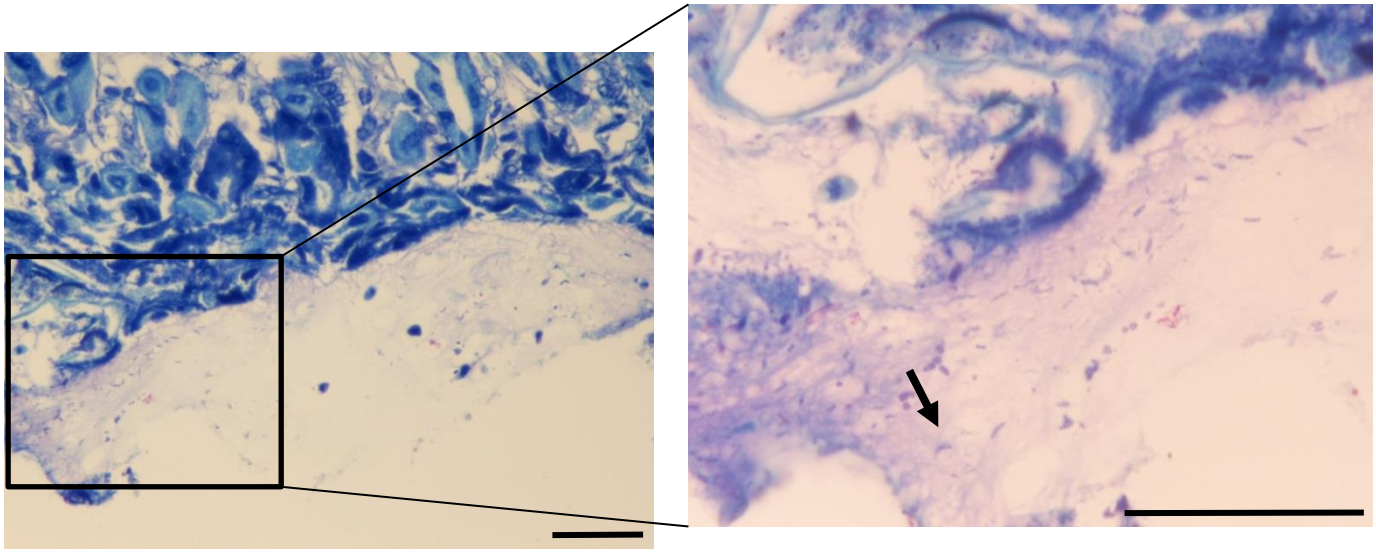

Figure 24. *H. pylori* infection – Experiment III: Histological characterization (Modified Giemsa staining) of C57BL/6 mice gastric mucosa infected with *B128 H. pylori* strain. Representative illustration of C57BL/6 mice gastric section (Group *Hp+B128*, animal 4). The arrow identifies the presence *H. pylori*. Scalebar: 50µm.

To complement the histological analysis, mice liver sections were also stained with H&E to look for possible morphological alterations. Results, presented in Figure 25, show no apparent differences between infected and non-infected animals. From all liver sections, it is possible to find hepatocytes that form hepatic cords, distributed radially around central veins, which is described as the normal structure of this organ [1]. It is to note, though, that all animals present steatosis, an hepatic fat accumulation, resultant from a diet rich in carbohydrate, which animals are subjected to.

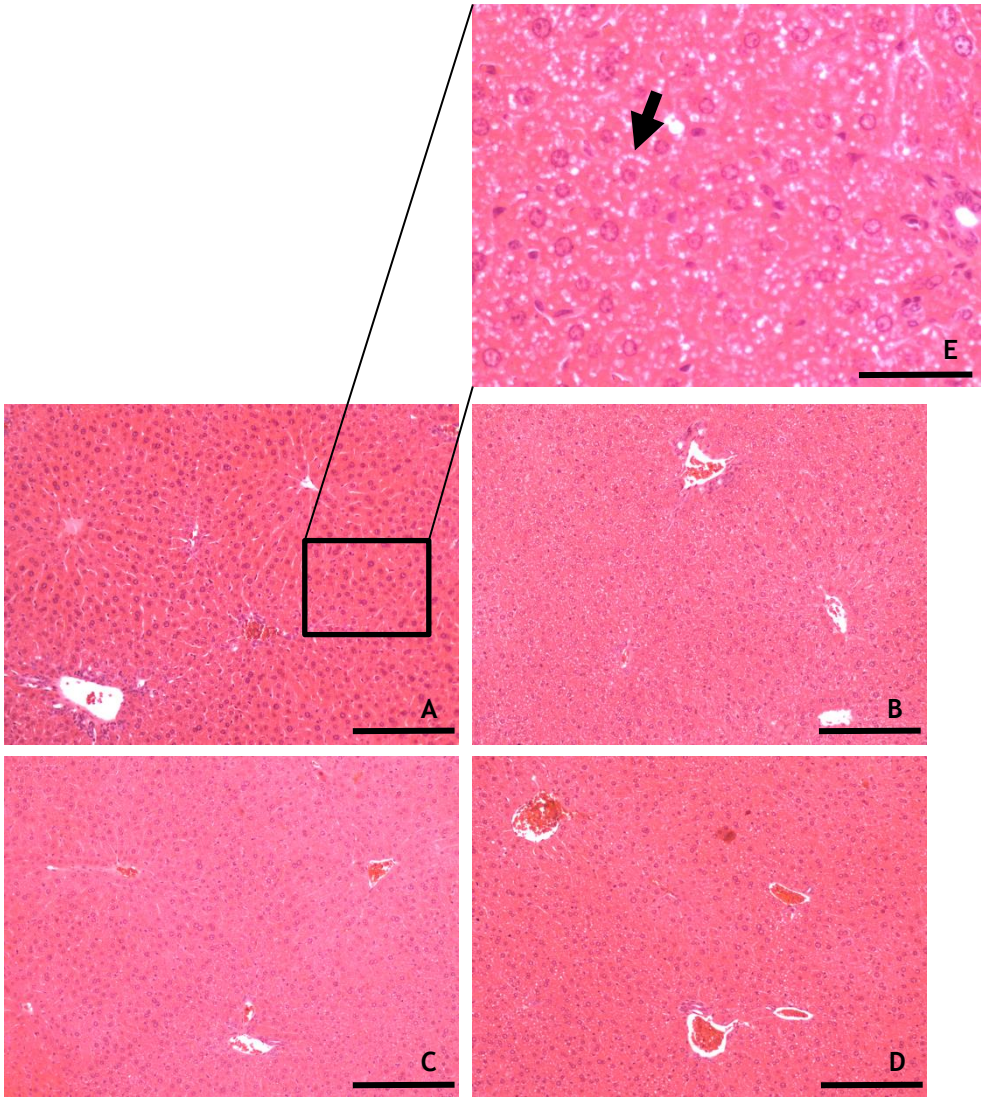

Figure 25. *H. pylori* infection – Experiment III: Histological characterization (H&E staining) of C57BL/6 mice liver. (A) Non-infected animal (Group Hp-, animal 1); (B) Animal infected with *SS1 H. pylori* strain (Group Hp+SS1, animal 2); (C) Animal infected with *B128 H. pylori* strain (Group Hp+B128, animal 4); (D) Animal infected with *TN2GF4 H. pylori* strain (Group Hp+TN2GF4, animal 10). A, B, C, D – Scalebar: 200µm; E – Scalebar: 50µm. The arrow highlights a region where it is possible to see steatosis.

4.B. Treatment of *H. pylori* infection using Ch Mics

In parallel with the establishment of *H. pylori* infection, using a *BabA* positive strain, the potential utility of chitosan microparticles as a treatment for *H. pylori* infection was also explored.

Therefore, primarily, Ch Mics were analysed morphologically and their cytotoxicity was evaluated *in vitro*, using *MKN45*, a human gastric carcinoma-derived cell line. Once this was achieved, a non-cytotoxic concentration of Ch Mics was administered to infected mice to evaluate their efficacy in the removal of *H. pylori* from C57BL/6 mice stomachs. In

this study, mice were infected with mouse-adapted *SS1* strain, a well-established model that guarantees development of infection. It is to note, though, that, since *SS1* is not *BabA* positive and as Ch Mics are not decorated with Le^b receptors, the binding of *H. pylori* did not rely on adhesin-glycans interactions, binding non-specifically to these bacteria.

4.B.1 Chitosan Microparticles

The morphology of Ch Mics was analyzed by SEM (Figure 26). Results reveal that the particles have irregular shapes and their diameters are around 40µm. Regarding their chemical composition, as expected [10], microparticles are mainly composed by carbon, having also oxygen and nitrogen in their structure.

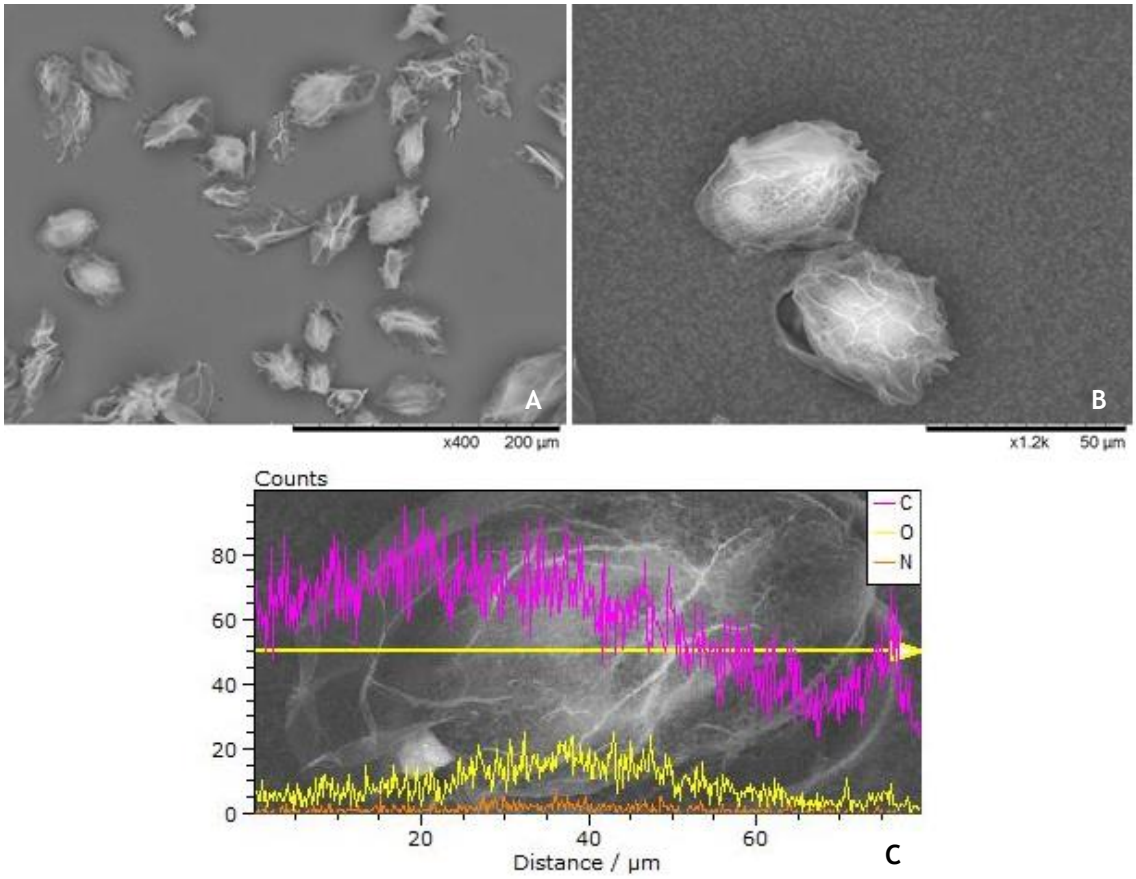

Figure 26. SEM images of Ch Mics. (A) Scalebar: 200µm; (B) Scalebar: 50µm; (C) Chemical composition and dimensions of Ch Mics.

4.B.2 Cytotoxicity of Chitosan Microparticles

In what concerns the cytotoxicity of Ch Mics, different concentrations were tested *in vitro* (1000 Mics/well, 10 000 Mics/well, 50 000 Mics/well and 100 000 Mics/well) by direct contact assay (as illustrated in Figure 27), using *MKN45* gastric cell line.

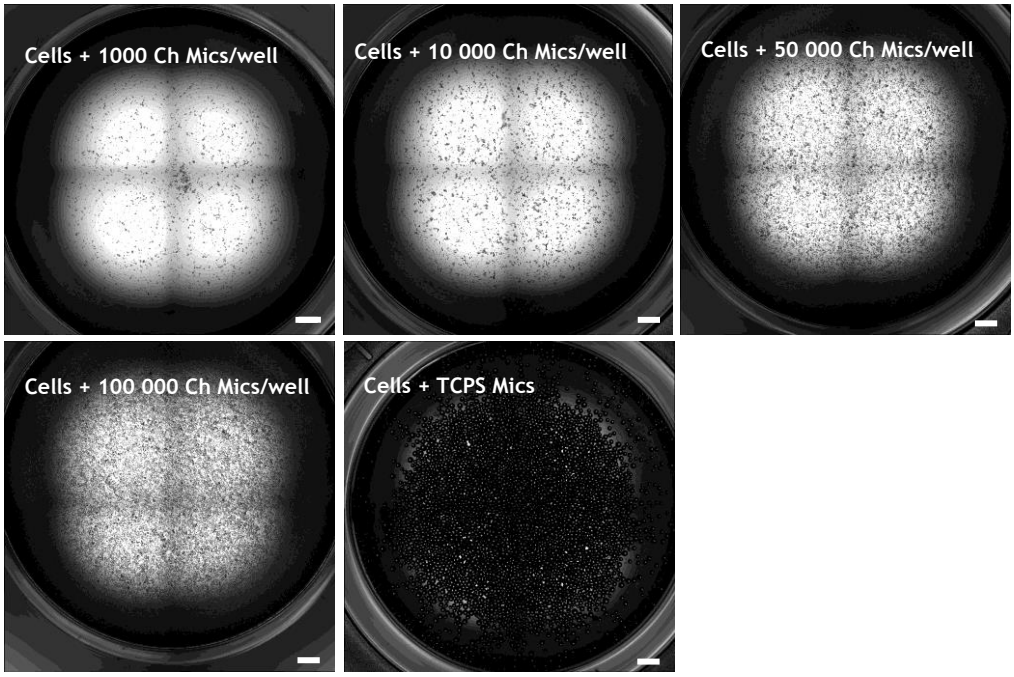

Figure 27. Optical microscopy images of a 24-well plate with increasing concentrations of Ch Mics. Scalebar: 1 mm.

Metabolic activity of cells was determined after 4h of incubation with resazurin and results are presented in Figure 28. As expected, cells cultured with H_2O_2 presented a vestigial metabolic activity of 1%, which was significantly different from the results of cells cultured in the remaining conditions. Moreover, cells cultured with TCPS Mics, although significantly different from *MKN45* cultured alone, revealed high metabolic rates, close to 90%. Analyzing, now, cells' metabolic activity when in direct contact with Ch Mics, these were all significantly different from cells cultured alone, except for a Ch Mics concentration of 1000 Mics/well. Between groups, cells cultured with 50 000 Mics/well and 100 000 Mics/well presented a significant decrease in metabolic activity, compared to wells with 1000 Mics and 10 000 Mics. Similarly, cells with 100 000 Mics/well presented significantly lower metabolic activity, in comparison with cells with TCPS Mics, suggesting that, in some extend, Ch Mics influence the behaviour of cells. In any case, metabolic activity of cells was maintained above 70%, which respects the restrictions imposed by ISO 10993-5 [114] to consider a material non-cytotoxic.

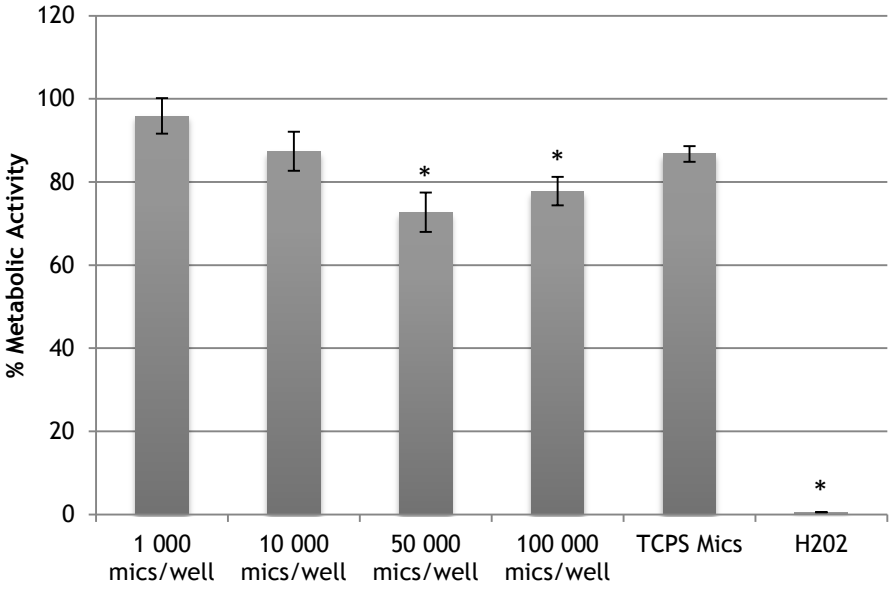

Figure 28. Metabolic activity (%) of *MKN45* cells in the presence of increasing concentrations of Ch Mics. Cells with hydrogen peroxide (H_2O_2) were used as the positive control. Cells with TCPS microspheres served as negative control and cells with 10% H_2O_2 in RPMIc were used as negative control. * Metabolic activity of cells with H_2O_2 was significantly different from all the remaining conditions ($p < 0.05$). All conditions were significantly different from cells cultured alone, except cells with 1000 Mics/well.

In parallel with this study, our group also evaluated the cytotoxicity of Ch Mics using the *AGS* human gastric adenocarcinoma cell line. For this, results revealed a metabolic activity ranging from 92.4% to 99.6%, where the highest values were found for cells cultured with 1000 Mics/well and 10 000 Mics/wells.

Cells in the different conditions were stained by immunohistochemistry and results are presented in Figure 29. Results show that, in comparison with cells alone, microparticles do not seem to alter the normal conformation and distribution of cells. The same can be verified for the cells cultured with TCPS Mics. On the other hand, H_2O_2 in culture with *MKN45* killed practically every cell.

Based on these and the results obtained for *MKN45* cell line, 10 000 Ch Mics was the value defined to administer these particles to mice.

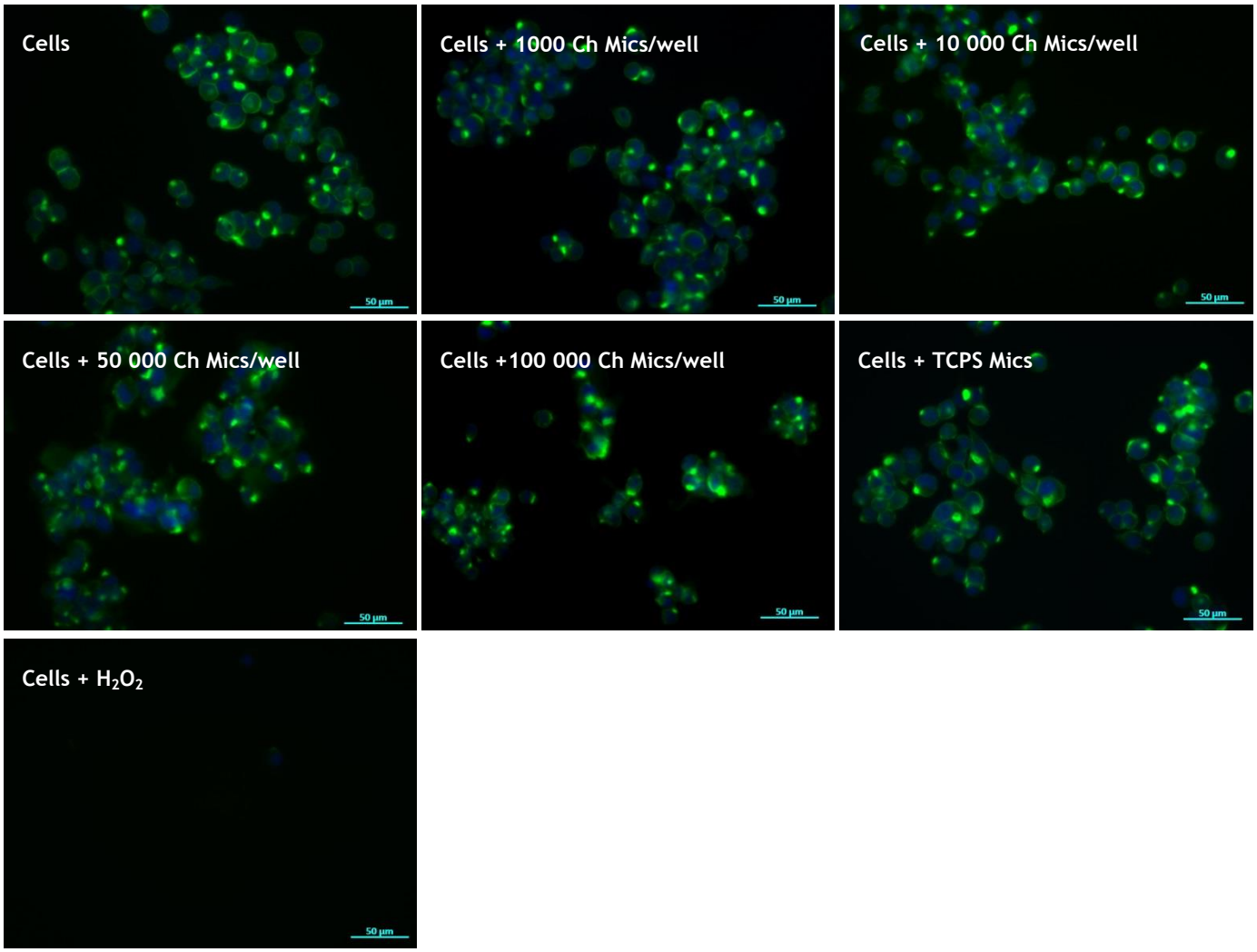

Figure 29. Immunofluorescence images of MKN45 gastric cells after 24h of incubation with increasing concentrations of Ch Mics. F-actin citoskeleton of the cells appear in green while their nuclei are coloured in blue. Scalebar: 500µm.

4.B.3 Treatment of *H. pylori* infection using Ch Mics – *In vivo* mouse model

Once tested the cytotoxicity of Ch Mics *in vitro*, the particles were administered to C57BL/6 mice (10 000 Mics/mice) to evaluate its efficiency in the treatment of *H. pylori* infection. Three weeks after bacteria inoculation (the time established to develop infection), infected mice were treated with Ch Mics for a period of 14 days. This period was defined as the treatment duration for this study since the common approach to treat *H. pylori* infection currently in clinical practice (PPI-based triple therapy) suggests treatment regimens of 14 days [116-119].

Similarly to the previous studies, animal weight variations were analyzed (Figure 30). It is possible to observe that, despite the various oral gavages and handling of animals, these maintained their good physical appearance. Besides, at the end of the experiment,

animals had the expected weight for their age (12 weeks old), as it is possible to infer from the analysis of Figure C1 *Appendix C*.

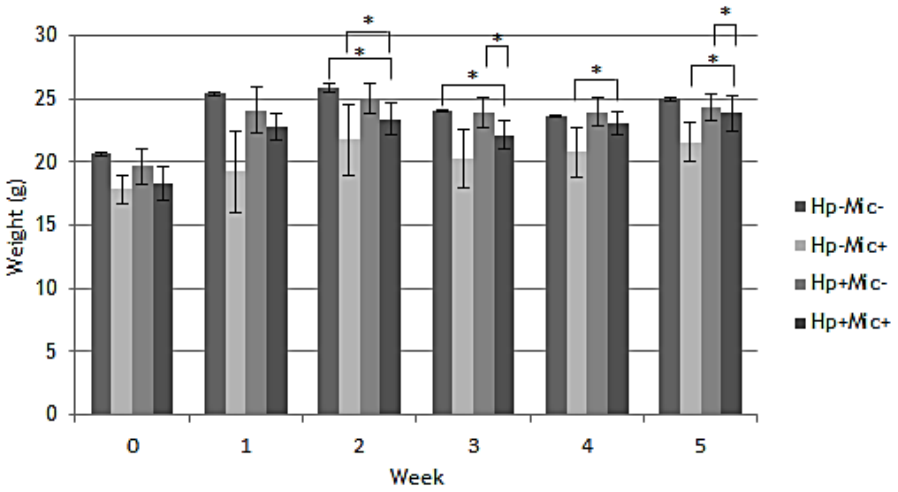

Figure 30. Efficacy of treatment against *H. pylori* infection: C57BL/6 weight variations during the development of infection with *SS1 H. pylori* strain. Groups: **Hp-Mic-** non-infected and non-treated mice; **Hp-Mic+** non-infection but treated mice; **Hp+Mic-** infected but non-treated mice; **Hp+Mic+** infected and treated mice. Values from week 0 correspond to the pre-infection weighing (the day before *H. pylori* inoculation), whereas values from weeks 1, 2 and 3 relate to post-infection weighings. * Significant differences ($p < 0.05$; *Kruskal-Wallis* non-parametric test).

To evaluate the effectiveness of this *H. pylori* infection treatment, animals' stomachs were plated and grown in blood agar plates for CFU's counting. Results obtained are illustrated in Figure 31.

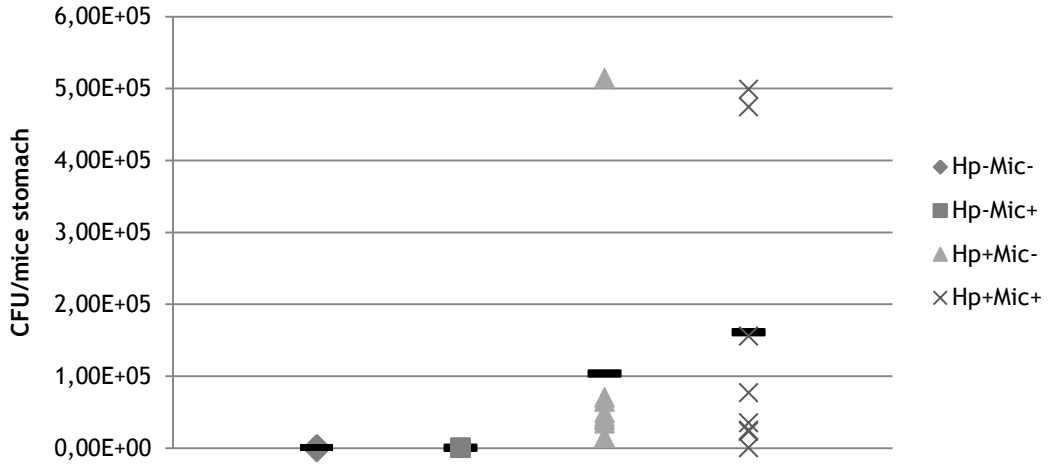

Group	Animal	CFU/mice stomach	CFU/g
Hp-Mic-	1	0	0
	2	0	0
Hp-Mic-	1	0	0
	2	0	0
Hp+Mic-	1	$3.37x10^4$	$4.93x10^2$
	2	$5,14x10^5$	$6.63x10^3$
	3	$1.45x10^4$	$1.94x10^2$
	4	$4.80x10^4$	$5.05x10^2$
	5	$3.88x10^4$	$6.57x10^2$
	6	$4.24x10^4$	$6.56x10^2$
	7	$6.98x10^4$	$1.12x10^3$
	8	$6.40x10^4$	$8.81x10^2$
Hp+Mic+	1	$2.43x10^4$	$3.53x10^2$
	2	$2.28x10^4$	$2.97x10^2$
	3	$4.98x10^5$	$8.16x10^3$
	4	$4.74x10^5$	$6.00x10^3$
	5	$3.48x10^4$	$5.61x10^2$
	6	$1.56x10^5$	$2.36x10^3$
	7	0	0
	8	$7.64x10^4$	$2.16x10^3$

Figure 31. Efficacy of treatment against *H. pylori* infection. Presence of *SS1* strain in C57BL/6 mice (CFU/mice stomach). Groups: **Hp-Mic-** non-infected and non-treated mice; **Hp-Mic+** non-infection but treated mice; **Hp+Mic-** infected but non-treated mice; **Hp+Mic+** infected and treated mice. No significant differences were found between groups.

As it is possible to observe, non-infected animals were not *H. pylori* culture positive, according to the expected. Regarding the development of infection in non-treated mice (*Hp+Mic-*), and in comparison with other published studies, the CFUs found were close to the lowest levels reported as, for this mouse strain, several authors indicate that 1 month

after infection, animals have a concentration of approximately 10^3 to 10^6 CFU/g tissue of *H. pylori* [61, 68, 77, 82].

In what concerns the comparison between treated (*Hp+Mic+*) and non-treated animals (*Hp+Mic+*), no significant differences were found. However, mice treated with Ch Mics showed higher number of CFUs per mice (with the exception of one mouse that presented no CFU). A possible explanation may be the fact that *SS1 H. pylori* infection was not homogenous, resulting in greater infection rates in some cases, when compared to others. This might have hidden possibly significant differences, translating into an unsuccessful reduction of infection. Nevertheless, the group has previously tested the use of Ch Mics (but with 170µm in diameter) and was able to reduce, although not significantly, the infection with *SS1 H. pylori* in approximately 63% (unpublished data), which might still be an indication of the potential of these particles to treat *H. pylori* infection.

Images obtained from histological analysis of stomach sections (Figure 32) reveal that, similarly to the previous experiments, non-infected animals (*Hp-Mic-* and *Hp-Mic+*) have normal gastric architecture and, particularly, the administration of Ch Mics to non-infected animals did not seem to trigger an inflammatory response, which, once again, might indicate that these Mics are non-cytotoxic.

Regarding animals infected and untreated (*Hp+Mic-*), results showed the presence of some inflammatory infiltrates. And, finally, in animals treated with Ch Mics (*Hp+Mic+*), the only animal found with no CFUs (*Hp+Mic+* 7) also presented a normal morphology, which supports once again the hypothesis of this mice being treated. For the remaining animals of this group, a more evidenced inflammatory infiltrate could be found in one of the animals with positive CFUs, which might be caused by *H. pylori*, despite the presence of Ch Mics. Furthermore, all infected animals presented atrophy in the distal portion of the stomach, which might suggest that these events are correlated.

In this study, histological sections of mice's liver were also analysed to look for morphological changes caused by the presence of Ch Mics. As it is possible to find in Figure 33 and comparing with histological sections of liver with morphological changes (Figure D2, *Appendix D*), these Mics do not seem to cause any changes in this organ suggesting, once again, no cytotoxicity.

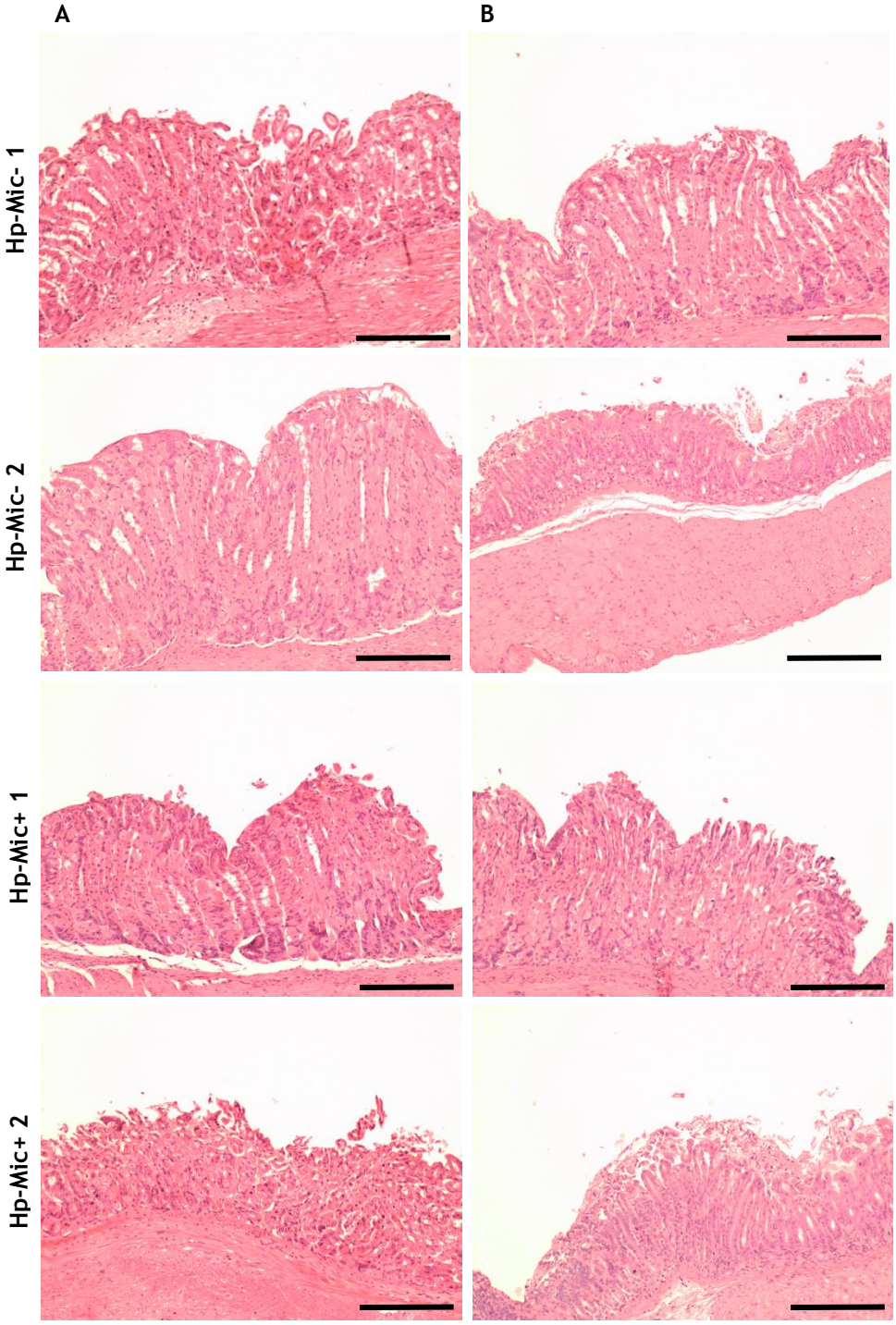
A
B
Hp-Mic- 1
Hp-Mic- 2
Hp-Mic+ 1
Hp-Mic+ 2

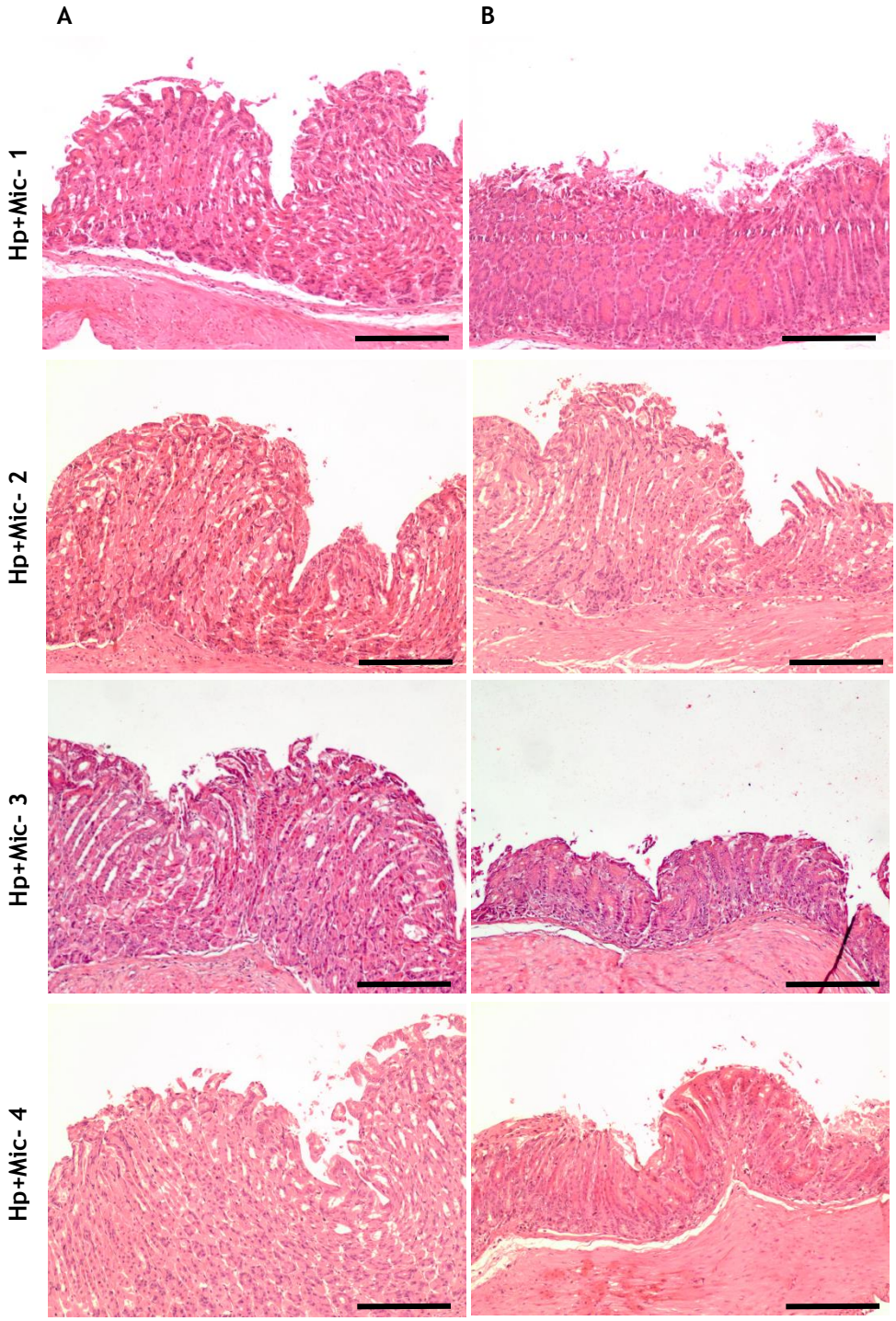
A
B
Hp+Mic- 1
Hp+Mic- 2
Hp+Mic- 3
Hp+Mic- 4

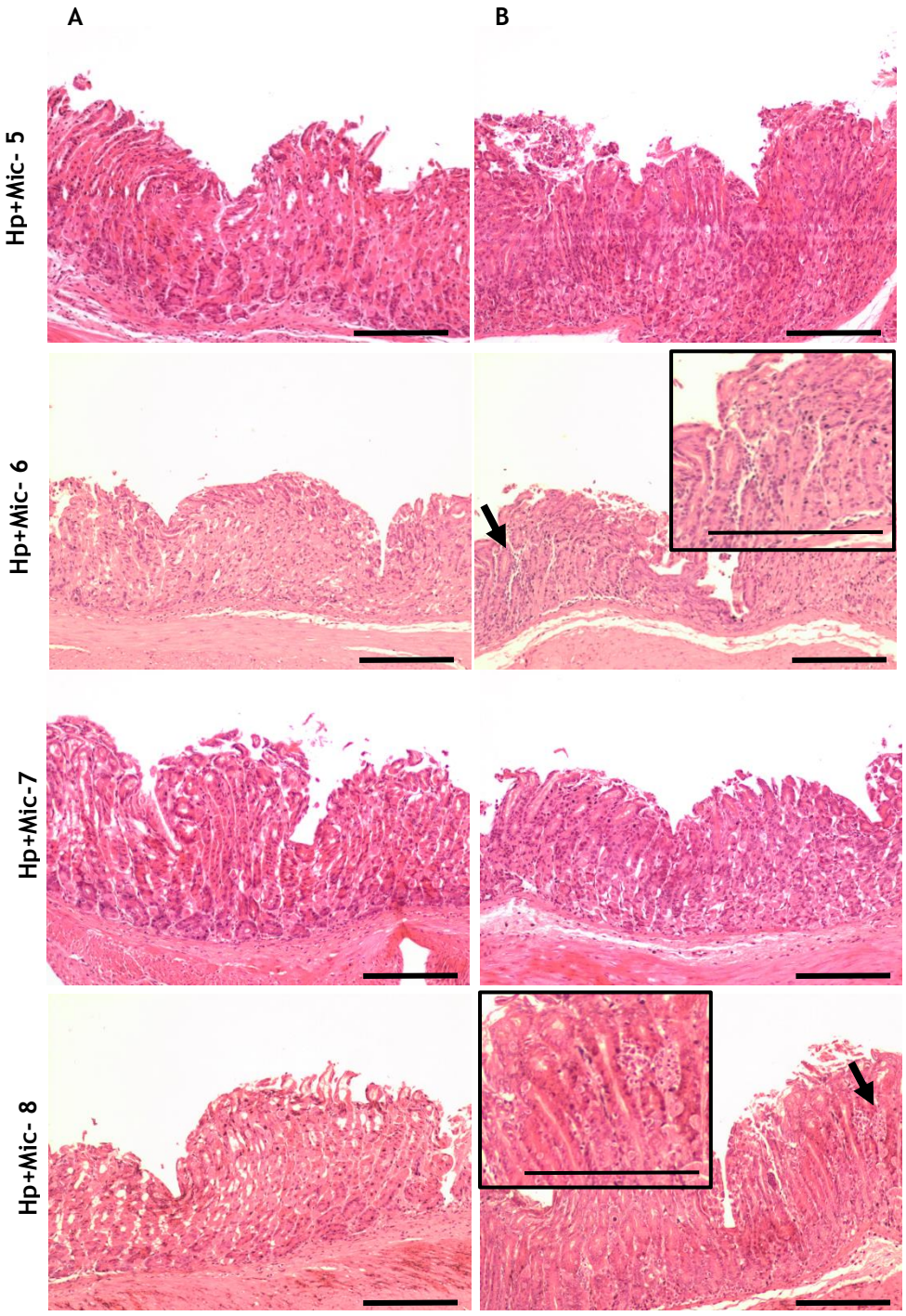
A
B
Hp+Mic- 5
Hp+Mic- 6
Hp+Mic-7
Hp+Mic- 8

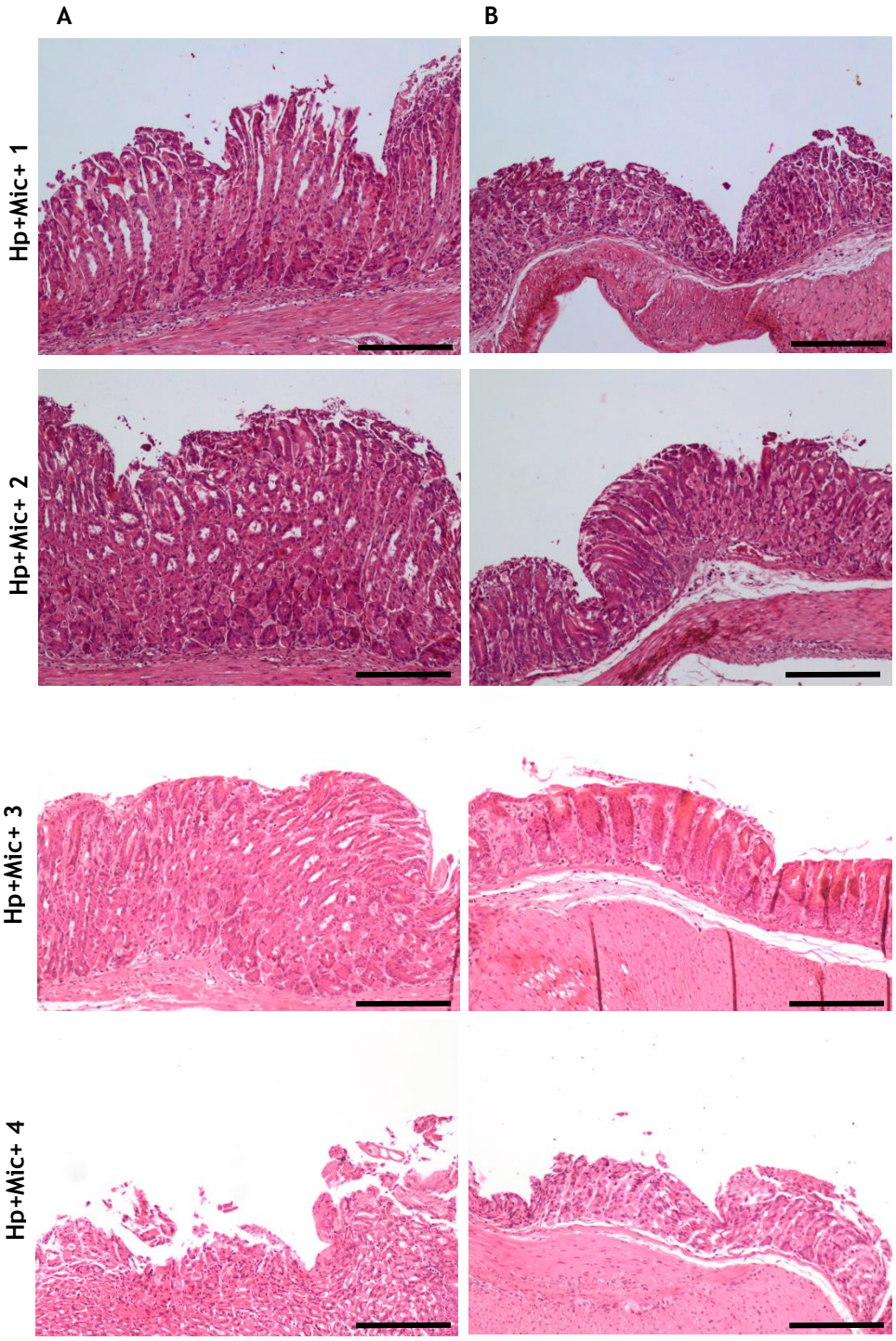
A
B
Hp+Mic+ 1
Hp+Mic+ 2
Hp+Mic+ 3
Hp+Mic+ 4

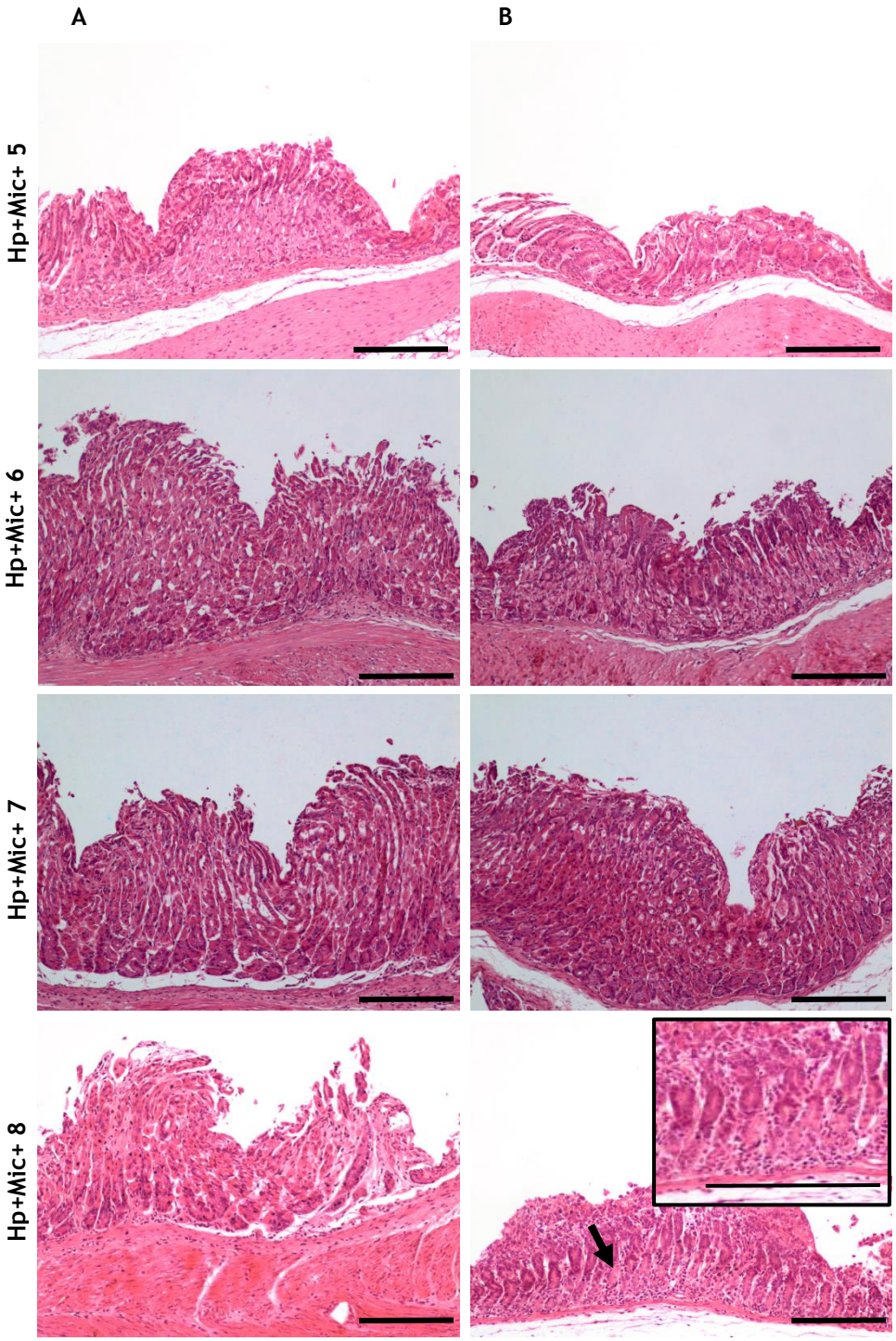

Figure 32. Efficacy of treatment against *H. pylori* infection: Histological characterization (H&E staining) of C57BL/6 mice gastric mucosa infected with *H. pylori* (*SS1* strain). Groups: **Hp-Mic-** non-infected and non-treated mice; **Hp-Mic+** non-infection but treated mice; **Hp+Mic-** infected but non-treated mice; **Hp+Mic+** infected and treated mice. Column A – proximal portion of glandular stomach. Column B –distal portion of glandular stomach. Scalebar: 200µm.

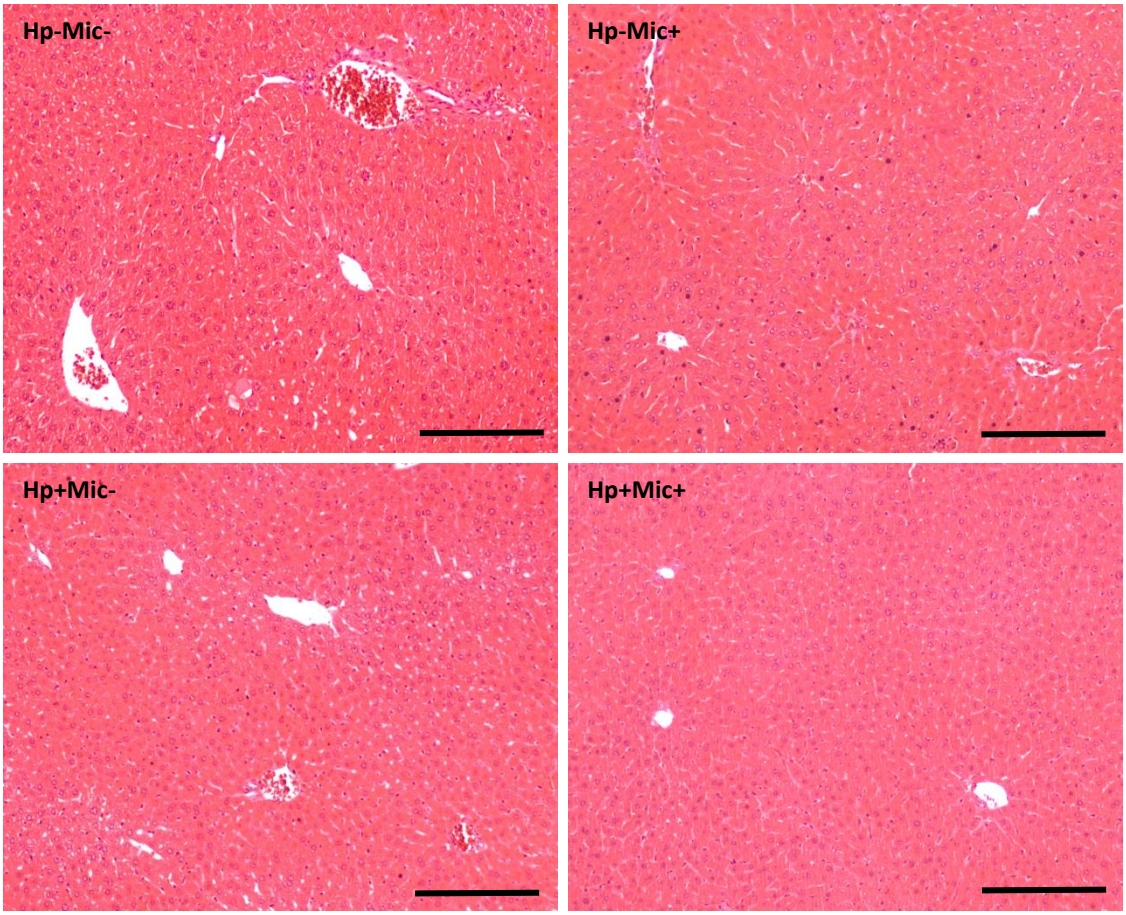

Figure 33. Efficacy of treatment against *H. pylori* infection: Histological characterization (H&E staining) of C57BL/6 mice liver. Groups: **Hp-Mic-** non-infected and non-treated mice; **Hp-Mic+** non-infection but treated mice; **Hp+Mic-** infected but non-treated mice; **Hp+Mic+** infected and treated mice. Scalebar: 200µm.

Chapter 5

Conclusion

In the present study, several strategies to establish *H. pylori* infection with a *BabA* positive strain were explored, as an attempt to enable the study of an innovative treatment based on the capacity of Le^b-coated Ch Mics to specifically bind these bacteria.

The establishment of an *H. pylori* infection model was based on the specific interactions between Le^b receptors and *BabA* adhesin. Results revealed that inoculating C57BL/6 mice with $1x10^{10}$ CFU/mL (0.2mL; 3 inoculations in one week) of *B128 BabA* positive *H. pylori* strain (isolated from infected mice) in BBL successfully infected 5 out 6 animals, with $1.55x10^4$ to $1.01x10^5$ CFU/stomach ($2.13x10^2$ to $2.36x10^3$ CFU/g).

Regarding the use of Ch Mics as a potential treatment for *H. pylori* infection, first, their cytotoxicity was evaluated *in vitro*, when in direct contact with *MKN45* gastric cells. Cells maintained high rates of metabolic activity and did not alter the morphology of cells. These results allowed the determination of an optimal concentration to administer to mice (10 000 Ch Mics/mice) to assess their *in vivo* capacity of treating *H. pylori* infection. Ch Mics did not prove to be able to reduce this infection and, so, further research needs to be performed on this topic.

5.1. Future Perspectives

Taking into consideration the results found, a new experiment using the same conditions described for experiment III is ongoing, to understand its reproducibility and to validate the infection model established.

Regarding future developments, the expression of *BabA* in *B128* strain, isolated from an infected animal, should be confirm to guarantee the utility of the infection model. PCR

could also be used as another method for the detection and/or quantification of *H. pylori* in infected animals. Finally, to better evaluate the extent of *H. pylori* infection immunohistochemistry of mice gastric sections for the proliferation index marker KI-67 could be an interesting approach. This monoclonal antibody Ki-67 is directed against a nuclear antigen present only in proliferating cells (G1, S, G2 and M phases of the cell cycle) and is helpful in the detection of infected and inflamed tissue [120, 121].

Considering the study of the cytotoxicity of Ch Mics, non-carcinoma-derived cell lines could also be tested, as suggested by *Dai, J. et al.* [122]

In what concerns the treatment of *H. pylori* infection with Ch Mics, a combination of different sized particles, and with different degrees of acetylation, could be tested, allowing, eventually, a more efficient removal of *H. pylori* from the stomach.

Additionally, and once both *H. pylori* infection and the features of Ch Mics are optimized, these particles should be decorated with Le^b receptors, to target *H. pylori* specifically and more effectively, and be evaluated using the infection model herein optimized, using a BabA positive H. pylori strain and Le^b-expressing mice.

Ideally, these experiments should evolve to human trials to better understand the real effectiveness of the proposed treatment, as it is known that, despite the undeniable value of using animal models, results obtained from these experiments cannot be fully extrapolated to humans.

References

1. Seeley, R.R., Stephans, T.D., Tate, P., *Anatomy and Physiology*. 7th Edition ed. 2006: McGraw-Hill Higher Education.
2. Margaret E. S., D.G.M., *The Digestive System: Basic Science and Clinical conditions*. 2010: Elsevier Limited.
3. American Cancer Society. Nov 2014; http://www.cancer.org/cancer/stomachcancer/.
4. Marieb, E.N. and K. Hoehn, *Human anatomy & physiology*. 2007: Pearson Education.
5. Agur A. M. R., L.M.J., Grant J. C. B., *Grant's Atlas of Anatomy*. 10th edition ed. 1999, London, UK: Lippincott Williams and Wilkins.
6. Saladin, K., *Anatomy & Physiology*. 5th edition ed. A Unity of Form and Function. 2009: McGraw-Hill Companies.
7. Britannica, E., *Human Digestive System: Stomach*. 2010.
8. Lindén, S., et al., *Strain-and blood group-dependent binding of< i> Helicobacter pylori</i> to human gastric MUC5AC glycoforms*. Gastroenterology, 2002. 123(6): p. 1923-1930.
9. Magalhaes, A. and C. Reis, *Helicobacter pylori adhesion to gastric epithelial cells is mediated by glycan receptors*. Brazilian Journal of Medical and Biological Research, 2010. 43(7): p. 611-618.
10. Inês C. Gonçalves, A.M., Ana M S Costa, José R Oliveira, Paula Gomes, Celso A Reis, M Cristina L Martins, *Bacteria-targeted biomaterials: glycan-coated microspheres to bind and remove Helicobacter pylori*. Submitted to Acta Biomaterialia.
11. Mollicone, R.B., J.; Lependu, J.; Oriol, R., *Pattern of Type-1 (Lea, Leb) and Type-2 (X, Y, H) Blood Group-Related Antigens in the Human Pyloric and Duodenal Mucosae*. Lab Invest, 1985. 53(2): p. 219-227.
12. Wang, X., *Helicobacter pylori infection in a mouse model: Development, optimization and inhibitory effects of antioxidants*. 2001: Lund University.
13. National Cancer Institute - *Stomach Cancer*. Nov 2014; http://www.cancer.gov/cancertopics/types/stomach.

14. Stolte, M. and A. Meining, *Helicobacter pylori and gastric cancer*. The oncologist, 1998. 3(2): p. 124-128.
15. Uemura, N., S. Okamoto, and S. Yamamoto, *H. pylori infection and the development of gastric cancer*. Keio J Med, 2002. 51 Suppl 2: p. 63-8.
16. Wroblewski, L.E., R.M. Peek, Jr., and K.T. Wilson, *Helicobacter pylori and gastric cancer: factors that modulate disease risk*. Clin Microbiol Rev, 2010. 23(4): p. 713-39.
17. Tomb, J.-F., et al., *The complete genome sequence of the gastric pathogen Helicobacter pylori*. Nature, 1997. 388(6642): p. 539-547.
18. Rama Bansil, J.C., *Uncovering the Secrets of Ulcer-causing Bacteria*, in *Clever biochemical strategy enables bacteria to move freely and colonize host*. 2009: National Science Foundation.
19. Kusters, J.G., A.H. van Vliet, and E.J. Kuipers, *Pathogenesis of Helicobacter pylori infection*. Clinical microbiology reviews, 2006. 19(3): p. 449-490.
20. Aspholm, M., et al., *SabA Is the H. pylori Hemagglutinin and Is Polymorphic in Binding to Sialylated Glycans*. PLoS Pathogens, 2006. 2(10): p. e110.
21. HLT, M., GL, Mendz, SL, Hazell. , *Helicobacter pylori: Physiology and Genetics*. Part II, Bacteriology. 2001, Washington (DC): ASM Press.
22. Benktander, J., et al., *Redefinition of the carbohydrate binding specificity of Helicobacter pylori BabA adhesin*. J Biol Chem, 2012. 287(38): p. 31712-24.
23. Azevedo, M., et al., *Infection by Helicobacter pylori expressing the BabA adhesin is influenced by the secretor phenotype*. The Journal of pathology, 2008. 215(3): p. 308-316.
24. Parreira, P., et al., *Bioengineered surfaces promote specific protein-glycan mediated binding of the gastric pathogen Helicobacter pylori*. Acta biomaterialia, 2013. 9(11): p. 8885-8893.
25. Dunne, C., B. Dolan, and M. Clyne, *Factors that mediate colonization of the human stomach by Helicobacter pylori*. World J Gastroenterol, 2014. 20(19): p. 5610-5624.
26. Rossez, Y., et al., *The lacdiNAc-specific adhesin LabA mediates adhesion of Helicobacter pylori to human gastric mucosa*. J Infect Dis, 2014. 210(8): p. 1286-95.
27. Alm, R.A., et al., *Genomic-sequence comparison of two unrelated isolates of the human gastric pathogen Helicobacter pylori*. Nature, 1999. 397(6715): p. 176-180.
28. Backert, S., M. Clyne, and N. Tegtmeyer, *Molecular mechanisms of gastric epithelial cell adhesion and injection of CagA by Helicobacter pylori*. Cell Commun Signal, 2011. 9(1): p. 28.

29. Saito, N., et al., *Coccoid formation as a mechanism of species-preservation in Helicobacter pylori: an ultrastructural study.* Hokkaido Igaku Zasshi, 2008. 83(5): p. 291-5.
30. Kusters, J.G., et al., *Coccoid forms of Helicobacter pylori are the morphologic manifestation of cell death.* Infect Immun, 1997. 65(9): p. 3672-9.
31. Wadström, L.A.a.T., *Basic bacteriology and culture. Helicobacter pylori: Physiology and Genetics*, ed. G.M.a.S.H. HLT Mobley. Vol. . 2001, Washington, D.C.: ASM press.
32. Enroth, H., et al., *Helicobacter pylori strain types and risk of gastric cancer: a case-control study.* Cancer Epidemiology Biomarkers & Prevention, 2000. 9(9): p. 981-985.
33. Styer, C.M., et al., *Expression of the BabA adhesin during experimental infection with Helicobacter pylori.* Infection and immunity, 2010. 78(4): p. 1593-1600.
34. Rad, R., et al., *The Helicobacter pylori blood group antigen-binding adhesin facilitates bacterial colonization and augments a nonspecific immune response.* The Journal of Immunology, 2002. 168(6): p. 3033-3041.
35. Sheu, B.-S., et al., *Development of Helicobacter pylori Infection Model in BALB/c Mice with Domestic cagA-Positive and-Negative Strains in Taiwan.* Digestive Diseases and Sciences, 1999. 44(5): p. 868-875.
36. Marie, M.A.M., *Relationship between Helicobacter pylori Virulence Genes and Clinical Outcomes in Saudi Patients.* J Korean Med Sci, 2012. 27(2): p. 190-3.
37. Yu, J., et al., *Relationship between Helicobacter pylori babA2 status with gastric epithelial cell turnover and premalignant gastric lesions.* Gut, 2002. 51(4): p. 480-484.
38. Hennig, E.E., et al., *Heterogeneity among Helicobacter pylori Strains in Expression of the Outer Membrane Protein BabA.* Infection and Immunity, 2004. 72(6): p. 3429-3435.
39. Tummuru, M., T. Cover, and M. Blaser, *Cloning and expression of a high-molecular-mass major antigen of Helicobacter pylori: evidence of linkage to cytotoxin production.* Infection and immunity, 1993. 61(5): p. 1799-1809.
40. Magalhaes, A., et al., *Fut2-null mice display an altered glycosylation profile and impaired BabA-mediated Helicobacter pylori adhesion to gastric mucosa.* Glycobiology, 2009. 19(12): p. 1525-36.
41. McClain, M., et al., *Genome sequence analysis of Helicobacter pylori strains associated with gastric ulceration and gastric cancer.* BMC Genomics, 2009. 10(1): p. 3.

42. Bindayna, K.M. and A. Al Mahmeed, *vacA genotypes in Helicobacter pylori strains isolated from patients with and without duodenal ulcer in Bahrain.* Indian Journal of Gastroenterology, 2009. 28(5): p. 175-179.

43. Malfertheiner, P., et al., *Management of Helicobacter pylori infection—the Maastricht IV/Florence consensus report.* Gut, 2012. 61(5): p. 646-664.

44. Egan, B.J., et al., *Treatment of Helicobacter pylori Infection. Helicobacter*, 2008. 13(s1): p. 35-40.

45. Papastergiou, V., S.D. Georgopoulos, and S. Karatapanis, *Treatment of Helicobacter pylori infection: Past, present and future.* World journal of gastrointestinal pathophysiology, 2014. 5(4): p. 392.

46. Perri, F., et al., *Treatment of Helicobacter pylori infection.* Helicobacter, 2003. 8(s1): p. 53-60.

47. O'Connor, A., J. Gisbert, and C. O'Morain, *Treatment of Helicobacter pylori infection.* Helicobacter, 2009. 14(s1): p. 46-51.

48. GLOBOCAN, *Stomach Cancer: Estimated Incidence, Mortality and Prevalence Worldwide in 2012.* 2012.

49. Gonçalves, I.C., et al., *The potential utility of chitosan micro/nanoparticles in the treatment of gastric infection.* Expert review of anti-infective therapy, 2014. 12(8): p. 981-992.

50. Salcedo, J.A. and F. Al-Kawas, *Treatment of Helicobacter pylori infection.* Archives of internal medicine, 1998. 158(8): p. 842-851.

51. Graham, D., et al., *Challenge model for Helicobacter pylori infection in human volunteers.* Gut, 2004. 53(9): p. 1235-1243.

52. Fernandes, M., et al., *Modulation of stability and mucoadhesive properties of chitosan microspheres for therapeutic gastric application.* International journal of pharmaceutics, 2013. 454(1): p. 116-124.

53. Gonçalves, I.C., et al., *Bacterial-binding chitosan microspheres for gastric infection treatment and prevention.* Acta biomaterialia, 2013. 9(12): p. 9370-9378.

54. Parreira, P., *Specific binding of the gastric pathogen Helicobacter pylori by bioengineered surfaces.*

55. Mitchell, H., et al., *Helicobacter pylori: Physiology and genetics.* Helicobacter pylori: Physiology and genetics, 2001.

56. Wirth, H.-P., et al., *Experimental infection of Mongolian gerbils with wild-type and mutant Helicobacter pylori strains.* Infection and immunity, 1998. 66(10): p. 4856-4866.

57. Ghoshal, N. and H. Bal, *Comparative morphology of the stomach of some laboratory mammals.* Laboratory animals, 1989. 23(1): p. 21-29.

58. Piper M. Treuting, S.M.D., *Comparative Anatomy and Histology: A Mouse and Human Atlas*. 1st ed, ed. E. Inc. 2012.
59. Gad, S.C., *Animal Models in Toxicology* Second Edition ed, ed. C. Press. 2006.
60. Fox, J.G., *The Mouse in Biomedical Research: Normative biology, husbandry, and models*. 2007: Elsevier.
61. Lee, A., et al., *A standardized mouse model of Helicobacter pylori infection: introducing the Sydney strain.* Gastroenterology, 1997. 112(4): p. 1386-97.
62. Ferrero, R. and J. Fox, *In vivo modeling of Helicobacter-associated gastrointestinal diseases*. 2001.
63. Walsh, E. and A. Moran, *Influence of medium composition on the growth and antigen expression of Helicobacter pylori.* Journal of applied microbiology, 1997. 83(1): p. 67-75.
64. Israel, D.A., et al., *Helicobacter pylori strain-specific differences in genetic content, identified by microarray, influence host inflammatory responses.* J Clin Invest, 2001. 107(5): p. 611-20.
65. Rabelo-Gonçalves, E., N.F. Nishimura, and M.R. Zeitune, *Development of a BALB/c mouse model of Helicobacter pylori infection with fresh and frozen bacteria.* Biological research, 2005. 38(1): p. 101-109.
66. Kim, D., et al., *Long-term evaluation of mice model infected with Helicobacter pylori: focus on gastric pathology including gastric cancer.* Alimentary pharmacology & therapeutics, 2003. 18(s1): p. 14-23.
67. Konturek, P.C., et al., *Mouse model of Helicobacter pylori infection: studies of gastric function and ulcer healing.* Aliment Pharmacol Ther, 1999. 13(3): p. 333-46.
68. Salama, N.R., et al., *Vacuolating cytotoxin of Helicobacter pylori plays a role during colonization in a mouse model of infection.* Infection and immunity, 2001. 69(2): p. 730-736.
69. Ding, S.-Z. and P.-Y. Zheng, *Helicobacter pylori infection induced gastric cancer; advance in gastric stem cell research and the remaining challenges.* Gut Pathog, 2012. 4(1): p. 18.
70. Watanabe, T., et al., *Helicobacter pylori infection induces gastric cancer in Mongolian gerbils.* Gastroenterology, 1998. 115(3): p. 642-648.
71. Fagerberg, D., et al., *Novel Leb-like Helicobacter pylori-binding glycosphingolipid created by the expression of human a-1, 3/4-fucosyltransferase in FVB/N mouse stomach.* Glycobiology, 2009. 19(2): p. 182-191.
72. Falk, P.G., et al., *Expression of a human alpha-1, 3/4-fucosyltransferase in the pit cell lineage of FVB/N mouse stomach results in production of Leb-containing glycoconjugates: a potential transgenic mouse model for studying Helicobacter*

pylori infection. Proceedings of the National Academy of Sciences, 1995. 92(5): p. 1515-1519.

73. Guruge, J.L., et al., *Epithelial attachment alters the outcome of Helicobacter pylori infection*. Proceedings of the National Academy of Sciences, 1998. 95(7): p. 3925-3930.
74. Pohl, M.A., et al., *Host-dependent Lewis (Le) antigen expression in Helicobacter pylori cells recovered from Leb-transgenic mice*. The Journal of experimental medicine, 2009. 206(13): p. 3061-3072.
75. Correia, M., et al., *Docosahexaenoic acid inhibits Helicobacter pylori growth in vitro and mice gastric mucosa colonization*. PloS one, 2012. 7(4): p. e35072.
76. Wang, X., et al., *RAPD-PCR, histopathological and serological analysis of four mouse strains infected with multiple strains of Helicobacter pylori*. Microbial Ecology in Health and Disease, 1999. 10(3-4): p. 148-154.
77. Ferrero, R.L., et al., *Immune responses of specific-pathogen-free mice to chronic Helicobacter pylori (strain SS1) infection*. Infection and immunity, 1998. 66(4): p. 1349-1355.
78. Lemke, L.B., et al., *Concurrent Helicobacter bilis infection in C57BL/6 mice attenuates proinflammatory H. pylori-induced gastric pathology*. Infection and immunity, 2009. 77(5): p. 2147-2158.
79. Cook, K.W., et al., *CCL20/CCR6-mediated migration of regulatory T cells to the Helicobacter pylori-infected human gastric mucosa*. Gut, 2014. 63(10): p. 1550-9.
80. Wang, G., Maier, S. E., Lo, L. F., Maier, G., Dosi, S., & Maier, R. J. , *Peptidoglycan deacetylation in Helicobacter pylori contributes to bacterial survival by mitigating host immune responses. Infection and immunity*. 2010. 78(11): p. 4660-4666.
81. Cullen, T.W., Giles, D. K., Wolf, L. N., Ecobichon, C., Boneca, I. G., & Trent, M. S. , 7(12), e1002454., *Helicobacter pylori versus the host: remodeling of the bacterial outer membrane is required for survival in the gastric mucosa*. PLoS Pathogens, 2011. 7(12).
82. Thompson, L.J., et al., *Chronic Helicobacter pylori infection with Sydney strain 1 and a newly identified mouse-adapted strain (Sydney strain 2000) in C57BL/6 and BALB/c mice*. Infection and immunity, 2004. 72(8): p. 4668-4679.
83. Machado, A.M.D., et al., *Helicobacter pylori infection induces genetic instability of nuclear and mitochondrial DNA in gastric cells*. Clinical Cancer Research, 2009. 15(9): p. 2995-3002.
84. Sozzi, M., Crosatti, M., Kim, S. K., Romero, J., & Blaser, M. J., *Heterogeneity of Helicobacter pylori cag genotypes in experimentally infected mice*. FEMS microbiology letters, 2001. 203(1): p. 109-114.

85. McGuckin, M.A., et al., *Muc1 mucin limits both Helicobacter pylori colonization of the murine gastric mucosa and associated gastritis.* Gastroenterology, 2007. 133(4): p. 1210-1218.
86. Turner, P.V., et al., *Oral gavage in rats: Animal welfare evaluation.* Journal of the American Association for Laboratory Animal Science: JAALAS, 2012. 51(1): p. 25.
87. Anon. *Mouse Husbandry, Breeding and Development*. University of Carolina, Irvine, Transgenic Mouse Facility Guidelines. [cited 2015 24 January].
88. Donnelly, T.M. *The Merk Veterinary Manual*. Gerbils 2011 [cited 2015 24 January].
89. Wang, X., et al., *Development of high-grade lymphoma in Helicobacter pylori-infected C57BL/6 mice.* Apmis, 2000. 108(7-8): p. 503-508.
90. Anonymous. *Giemsa for Helicobacter pylori*. 1997; Available from: http://www.nottingham.ac.uk/pathology/protocols/giemshel.html.
91. Schwint, O.A., et al., *A modification of the staining technique of reticular fibres for image analysis of the cardiac collagen network.* Cardiovascular Pathology, 2004. 13(4): p. 213-220.
92. Ramos-Vara, J. and M. Miller, *When Tissue Antigens and Antibodies Get Along Revisiting the Technical Aspects of Immunohistochemistry—The Red, Brown, and Blue Technique*. Veterinary Pathology Online, 2014. 51(1): p. 42-87.
93. Rotimi, O., et al., *Histological identification of Helicobacter pylori: comparison of staining methods.* J Clin Pathol, 2000. 53(10): p. 756-9.
94. Wang, X., et al., *Infection of BALB/c A mice by spiral and coccoid forms of Helicobacter pylori.* Journal of medical microbiology, 1997. 46(8): p. 657-663.
95. Hausen, H.z., *Infections Causing Human Cancer*. 2006: Wiley-VCH.
96. Ohno, T., et al., *Effects of blood group antigen-binding adhesin expression during Helicobacter pylori infection of Mongolian gerbils.* J Infect Dis, 2011. 203(5): p. 726-35.
97. Crawford, H.C., et al., *Helicobacter pylori strain-selective induction of matrix metalloproteinase-7 in vitro and within gastric mucosa.* Gastroenterology, 2003. 125(4): p. 1125-1136.
98. Leung, W.K., et al., *Effects of Helicobacter pylori eradication on methylation status of E-cadherin gene in noncancerous stomach.* Clinical cancer research, 2006. 12(10): p. 3216-3221.
99. Hitkova, I., et al., *Caveolin-1 protects B6129 mice against Helicobacter pylori gastritis.* PLoS pathogens, 2013. 9(4): p. e1003251.
100. Yamaoka, Y., D.H. Kwon, and D.Y. Graham, *A Mr 34,000 proinflammatory outer membrane protein (oipA) of Helicobacter pylori.* Proceedings of the National Academy of Sciences, 2000. 97(13): p. 7533-7538.

101. Croisier, F. and C. Jérôme, *Chitosan-based biomaterials for tissue engineering.* European Polymer Journal, 2013. 49(4): p. 780-792.
102. Sinha, V., et al., *Chitosan microspheres as a potential carrier for drugs.* International Journal of Pharmaceutics, 2004. 274(1): p. 1-33.
103. Jiang, T., et al., *Micro-and nanofabrication of chitosan structures for regenerative engineering.* Acta biomaterialia, 2014. 10(4): p. 1632-1645.
104. Patel, M.P., R.R. Patel, and J.K. Patel, *Chitosan mediated targeted drug delivery system: a review.* Journal of Pharmacy & Pharmaceutical Sciences, 2010. 13(4): p. 536-557.
105. Dhawan, S., A.K. Singla, and V.R. Sinha, *Evaluation of mucoadhesive properties of chitosan microspheres prepared by different methods.* Aaps Pharmscitech, 2004. 5(4): p. 122-128.
106. Rajput, G., et al., *Stomach-specific mucoadhesive microsphere as a controlled drug delivery system.* Systematic Reviews in Pharmacy, 2010. 1(1): p. 70.
107. Ko, J., et al., *Preparation and characterization of chitosan microparticles intended for controlled drug delivery.* International journal of pharmaceutics, 2002. 249(1): p. 165-174.
108. Dong, Y., et al., *Scalable ionic gelation synthesis of chitosan nanoparticles for drug delivery in static mixers.* Carbohydrate Polymers, 2013. 94(2): p. 940-945.
109. Mi, F.-L., et al., *Synthesis and characterization of biodegradable TPP/genipin co-crosslinked chitosan gel beads.* Polymer, 2003. 44(21): p. 6521-6530.
110. Karnchanajindanun, J., M. Srisa-ard, and Y. Baimark, *Genipin-cross-linked chitosan microspheres prepared by a water-in-oil emulsion solvent diffusion method for protein delivery.* Carbohydrate Polymers, 2011. 85(3): p. 674-680.
111. MARTINS, C., et al., *Microspheres*. 2013, Google Patents.
112. Bastos, J., et al., *Sociodemographic determinants of prevalence and incidence of Helicobacter pylori infection in Portuguese adults.* Helicobacter, 2013. 18(6): p. 413-422.
113. Parreira, P., et al., *Effect of surface chemistry on bacterial adhesion, viability, and morphology.* Journal of Biomedical Materials Research Part A, 2011. 99(3): p. 344-353.
114. *ISO 10993-5. Biological evaluation of medical devices. Tests for in vitro cytotoxicity.* 2009, Geneva: International Standards Organization.
115. Peek, R.M., *Helicobacter pylori infection and disease: from humans to animal models.* Disease models & mechanisms, 2008. 1(1): p. 50-55.
116. Chey, W.D., *Management of Helicobacter pylori Infection.* American Journal of Gastroenterology, 2007. 102: p. 1808–1825

117. Fischbach, L.A., et al., *Sources of variation of Helicobacter pylori treatment success in adults worldwide: a meta-analysis.* Int J Epidemiol, 2002. 31(1): p. 128-39.

118. Vakil, N. and J. Connor, *Helicobacter pylori eradication: equivalence trials and the optimal duration of therapy.* Am J Gastroenterol, 2005. 100(8): p. 1702-3.

119. Fuccio, L., et al., *Meta-analysis: duration of first-line proton-pump inhibitor based triple therapy for Helicobacter pylori eradication.* Ann Intern Med, 2007. 147(8): p. 553-62.

120. Sougioultzis, S., et al., *Alterations in the Proliferating Compartment of Gastric Mucosa during Helicobacter Pylori Infection: The Putative Role of Epithelial Cells Expressing p27kip1.* Mod Pathol, 0000. 16(11): p. 1076-1085.

121. Joana Gomes, A.M., Valérie Michel, Inês F. Amado, Paulo Aranha, Rikke G. Ovesen, Hans C. B. Hansen, Fátima Gärtner, Celso A. Reis, and Eliette Touati, *Pteridium aquilinum and Its Ptaquiloside Toxin Induce DNA Damage Response in Gastric Epithelial Cells, a Link With Gastric Carcinogenesis.* Toxicological Sciences, 2012. 126(1): p. 60-71.

122. Dai, J., et al., *Effects of polyunsaturated fatty acids on the growth of gastric cancer cells in vitro.* Lipids Health Dis, 2013. 12: p. 71.

123. in *Technical files of research models: C57BL/6*, C. River, Editor.

124. Fox, J. G., & Wang, T. C. (2007). Inflammation, atrophy, and gastric cancer.*Journal of Clinical Investigation*, *117*(1), 60.

125. Rangel, M., et al., *Analysis of the Toxicity and Histopathology Induced by the Oral Administration of Pseudanabaena galeata and Geitlerinema splendidum (Cyanobacteria) Extracts to Mice.* Marine drugs, 2014. 12(1): p. 508-524.

Appendix A

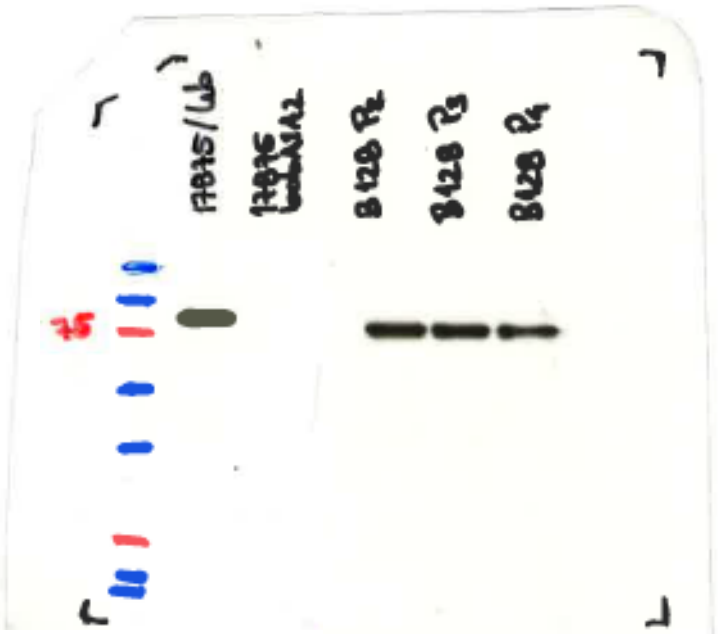

Figure A1. Preliminary results of Western Blot analysis of *H. pylori B128* strain. Results reveal the presence of *BabA* adhesin for the several passages (P2, P3 and P4). *17875/Leb* and *17876 babA1A2* served, respectively, as positive and negative controls (unpublished work).

Appendix B

The BSA calibration curve obtained for protein quantification is presented in Figure B1.

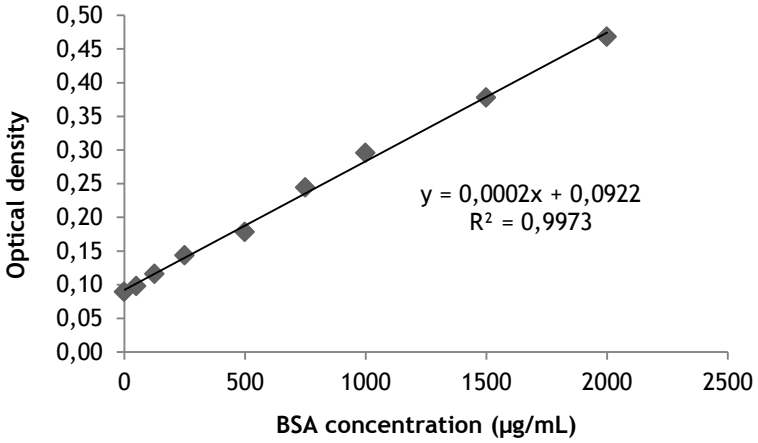

Figure B1. BSA calibration curve for total protein quantification. x corresponds to the BSA concentration (µg/mL) and y is the optical density at 750nm.

The equation obtained (presented in Figure B1) allowed the determination of the total protein concentration ($C_{protein}$) of each sample, based on equation B1.

$$C_{protein} = \frac{Optical\ density - 0.0922}{0.0002} \quad \text{(B1)}$$

Once determine the concentration of the extracts, and normalizing the amount of protein to load each lane ($m_{protein}$=25µg), the volume of protein ($V_{protein}$) was determined using equation B2.

$$V_{protein}(\mu L) = \frac{m_{protein}(\mu g)}{C_{protein}} \times 10^3 \quad \text{(B2)}$$

Appendix C

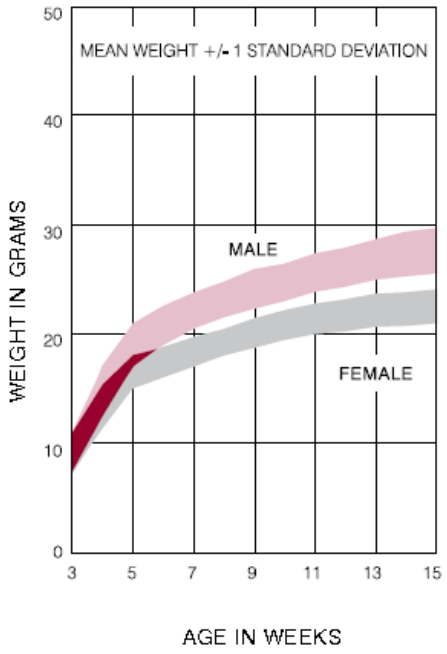

Figure C1. Normal weight variation (g) curve as a function of the age (weeks) of *C56BL/6* mice. Values indicate the mean weight of mice (male or female) and the correspondent standard deviation. Retrieved from *Charles River's Technical file for C57BL/6 mice* [123].

Appendix D

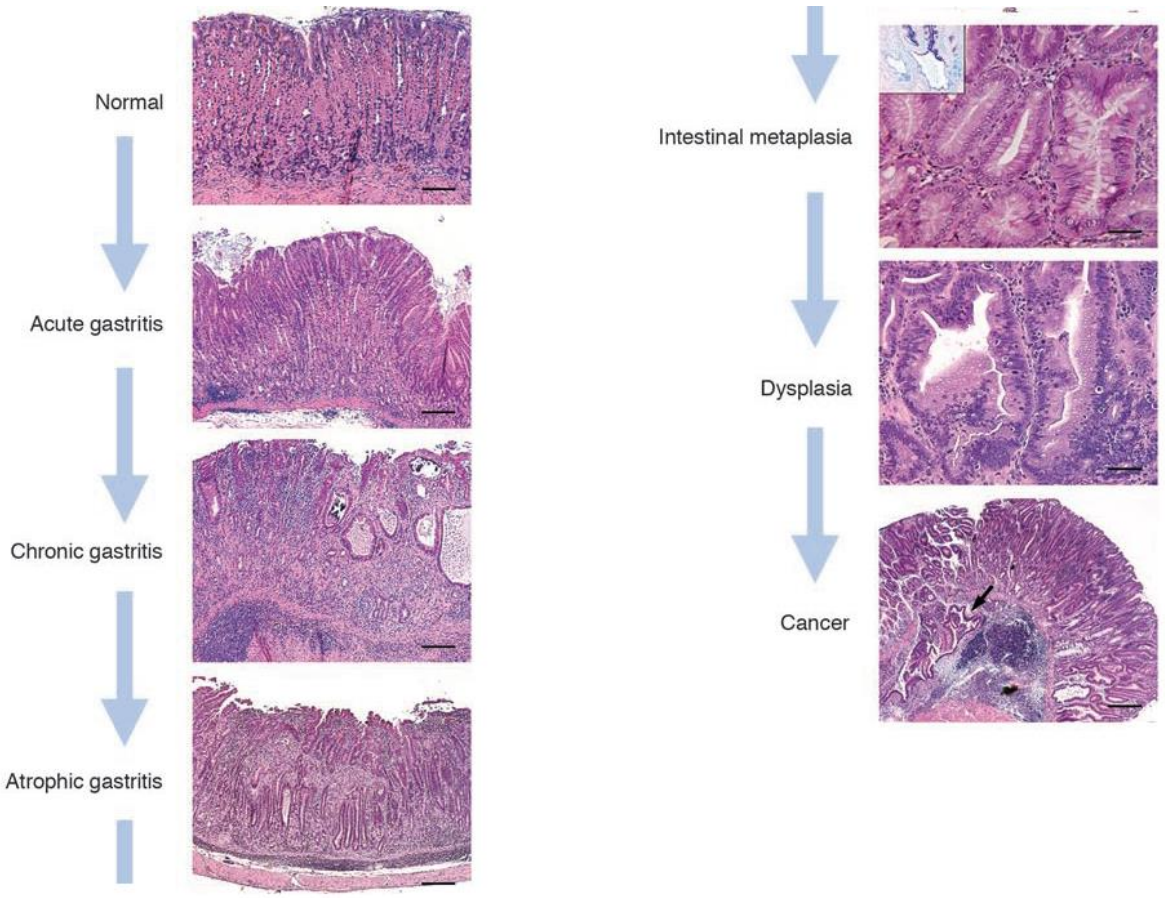

Figure D1. Histological progression of *Helicobacter*-induced gastric cancer in a mouse model. Normal: Histology of the body of the stomach. Acute gastritis: Infiltration of mucosal and submucosal lymphocytes with pockets of polymorphonuclear cells, accompanied by mild mucosal defects and edema. Chronic gastritis: Moderate to severe inflammation with marked epithelial defects including gland dilatation and mineralization. Atrophic gastritis: Chronic inflammation with focal fibrosis and complete loss of oxyntic parietal and chief cells. Intestinal metaplasia: Gastric epithelial metaplasia to an intestinal phenotype characterized by columnar elongation, mucous droplets occasionally forming goblet cells, and production of mixed acidic (blue, intestinal-type) and neutral (red, gastric-type) mucins as shown by pH 2.5 Alcian blue/PAS stain (inset). Dysplasia: High-grade glandular dysplasia characterized by irregular size and shape, infolding, branching and cell piling, and marked cellular and nuclear atypia. Cancer: Gastric intraepithelial neoplasia, here with intramucosal invasion (arrow), develops in *H. pylori*–infected wild-type B6129 mice, as well as in certain genetically engineered models (124–126). Scale bars: 160 mm (first panel); 400 mm (second through fourth panels); 80 mm (fifth panel; inset, original magnification, ×400); 40 mm (sixth panel); 800 mm (seventh panel). *Retrieved from Fox, J. et al.* [124]

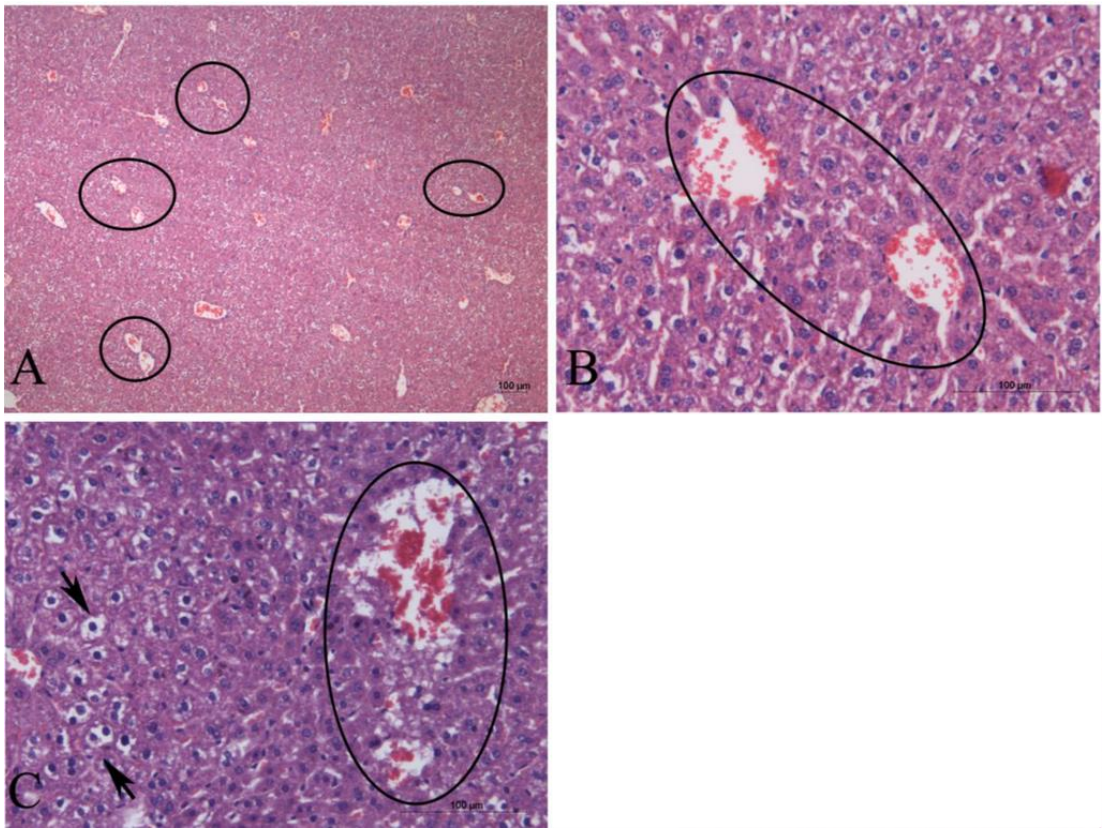

Figure D234. Histological sections of mice liver: (A) Hyperemia an proximity of the centrilobular vein (circles) and disorganization of the hepatic parenchyme; (B) Proximity of the centrilobular vein (circle) and disorganization of the hepatic parenchyme; (C) Necrosis (circle), vacuolization of liver cells (arrows), and disorganization of the hepatic parenchyme. Adapted from *Rangel, M. et al.* [124]